MODELING OF ELECTROMAGNETIC HYPERTHERMIA FOR CANCER TREATMENT

by

Selahattin NESİL

August 2007

MODELING OF ELECTROMAGNETIC HYPERTHERMIA FOR CANCER TREATMENT

by

Selahattin NESİL

A thesis submitted to

The Graduate Institute of Sciences and Engineering

of

Fatih University

in partial fulfillment of the requirements for the degree of

Master of Science

in

Electronics Engineering

August 2007
Istanbul, Turkey

I certify that this thesis satisfies all the requirements as a thesis for the degree of Master of Science.

_____
Prof. Dr. Muhammet KÖKSAL
Head of Department

This is to certify that I have read this thesis and that in my opinion it is fully adequate, in scope and quality, as a thesis for the degree of Master of Science.

_____
Assist. Prof. Dr. Erdal KORKMAZ
Supervisor

Examining Committee Members

Assist. Prof. Dr. Erdal KORKMAZ _____

Assoc. Prof. Dr. Erkan İMAL _____

Assist. Prof. Dr. Tuğrul YANIK _____

It is approved that this thesis has been written in compliance with the formatting rules laid down by the Graduate Institute of Sciences and Engineering.

_____
Assist. Prof. Dr. Nurullah ARSLAN
Director

August 2007

MODELING OF ELECTROMAGNETIC HYPERTHERMIA FOR CANCER TREATMENT

Selahattin NESİL

M. S. Thesis - Electronics Engineering
August 2007

Supervisor: Assist. Prof. Dr. Erdal KORKMAZ

ABSTRACT

In recent years, many developments in finite-difference time-domain (FDTD) computational modelling of Maxwell's equations, super computer technology, and computed tomography (CT) imagery have caused significant progress in heat delivery method, temperature monitoring, and thermal dosimetry. Electromagnetic hyperthermia method in the treatment of cancer is an application which had been revealed by these developments.

This thesis is an introductory study for electromagnetic hyperthermia in the treatment of cancer. The objective of electromagnetic hyperthermia is to destroy the tumor or cancer cells by achieving the highest possible temperature in the tumor or cancer cells without exceeding 42ºC in the surrounding healthy tissues. Many studies have shown that high temperatures can damage and kill cancer cells. Electromagnetic field is supplied to induce a temperature increase on tumor or cancer cells. In this thesis, the electromagnetic power deposition within the discretized cells is observed by solving the Maxwell's equations with FDTD. Further the thermal process is investigated by solving the Pennes' bio-heat transfer equation with finite difference method. The two dimensional (2D) specific arbsorption rate (SAR) distribution during hyperthermia treatment is presented.

Keywords: Electromagnetic Hyperthermia, Finite Difference Time Domain (FDTD) Method, Specific Absorption Rate (SAR), Bio-Heat Transfer Equation (BHTE).

KANSER TEDAVİSİ İÇİN ELEKTROMANYETİK HİPERTERMİ MODELLEMESİ

Selahattin NESİL

Yüksek Lisan Tezi – Elektronik Mühendisliği
Ağustos 2007

Tez Yöneticisi: Yrd. Doç.Dr. Erdal KORKMAZ

ÖZ

Son yıllarda, Maxwell denklemlerinin Zaman Domeninde Sonlu Farklar (FDTD) Metodu kullanılarak modellenmesinde, bilgisayar teknolojisinde ve bilgisayarlı tomografi uygulamalarında meydana gelen gelişmelerle birlikte ısı dağılımı yönteminde, sıcaklığın görüntülenebilmesinde ve sıcaklık dozunun ölçülebilmesinde önemli ilerleme kaydedilmiştir. Bu gelişmeler ile ortaya çıkmış bir uygulama da kanser tedavisinde elektromanyetik hipertermi yöntemidir.

Bu tez, kanser tedavisinde elektromanyetik hipertermi metodu için bir başlangıç çalışmasıdır. Elektromanyetik hiperterminin amacı, sağlıklı hücreler etrafında 42ºC dereceyi geçmeden, tümörlü bölgede ya da kanserli hücrelerde mümkün olan en yüksek sıcaklığın elde edilerek bu hücrelerin yok edilmesidir. Birçok çalışma yüksek sıcaklıklarda kanserli hücrelerin yok edilebildiğini göstermektedir. Tümör veya kanserli hücrelerde sıcaklık artışı, bu bölgelerde elektromanyetik alan oluşturularak sağlanmaktadır. Bu tezde, elektromanyetik gücün depolanması FDTD ile Maxwell denklemlerinin çözülmesiyle gözlemlenmiştir. Ayrıca termal sıcaklık oluşumu Sonlu Farklar (finite difference) yöntemi ile Penn's bio-ısı transferi denkleminin çözülmesiyle incelenmiştir. Hipertermi tedavisi sırasında oluşan iki boyutlu (2D) Özgül Soğurma Oranı (SAR) dağılımı sunulmuştur.

Anahtar Kelimeler: Elektromanyetik Hipertermi, Zaman Domeninde Sonlu Farklar (FDTD) Metodu, Özgül Soğurma Oranı (SAR), Bio-Isı Transfer Denklemi (BHTE).

DEDICATION

To my parents

ACKNOWLEDGEMENT

I am grateful to my adviser, Assist. Prof. Dr. Erdal KORKMAZ, for giving me the opportunity to study and conduct research for constitution of this thesis. I appreciate his patience, understanding and encouragement throughout my thesis study. As a mentor his level of commitment to research and teaching, as well as his energy, creativity, and enthusiasm are inspirational.

Next, I would like to thank all members of Fatih University Electronic Engineering Department, for their support, encouragement and the many scientific and non-scientific advices that have happened over the years.

And huge thank you to all my friends and colleagues at Fatih University, current and old, for their friendship and collaboration and companionship throughout this journey in graduate school life. To name a few: Ahmed Elajez, Ş. Eser ÖNER, Hasan Seçkin EFENDİOĞLU, Melek OKTAY, Mehmet SAĞBAŞ, M. Can BAYRAM, etc. etc.

Finally, I owe sincere thanks to my parents for their support throughout the years. I owe everything in my life to them.

TABLE OF CONTENTS

LIST OF TABLES

TABLE

LIST OF FIGURES

FIGURE

LIST OF SYMBOLS AND ABBREVIATIONS

SYMBOL/ABBREVIATION

σ	Conductivity
ε	Permittivity
μ	Permeability
η	Intrinsic Impedance
Γ	Reflection Coefficient
ω	Radian frequency
∇	Laplacian Operator
k	Thermal Conductivity (W/m/°C)
C_b	Heat Capacity of Blood (4000 J/kg/°C);
C_t	Heat Capacity of Tissue (4000 J/kg/°C);
ρ_b	Density of Blood (1000 kg/m^3);
ρ_t	Density of Tissue (1000 kg/m^3);
T	Temperature of the Tissue (°C)
w	Blood Perfusion Rate ($kg/s\text{-}m^3$)
ABC	Absorbing Boundary Conditions
ASTRO	The American Society For Therapeutic Radiology And Oncology
BHTE	Bio Heat Transfer Equation
CCS	Canadian Cancer Society
CRT	Conformal Radiation Therapy
FDTD	Finite Difference Time Domain
IMRT	Intensity Modulated Radiation Therapy
NCI	National Cancer Institute
PAMF	Palo Alto Medical Foundation
PML	Perfectly Matched Layer

SAR	Specific Absorption Rate
TM	Transverse Magnetic
TE	Transverse Electric

CHAPTER 1

INTRODUCTION

Cancer has been a scary word to hear for human being. Almost everyone knows someone who has been seriously ill or died from cancer. It is one of the leading causes of the death. Unfortunately, every year over a few millions of people at any ages get cancer and some of them are dying. Today, millions of people are living with cancer or have been cured of the disease. Cancer affects and changes the lifestyle of patients and their families at the same time. In this respect, many countries are establishing and funding the clinicals that conduct research to cure cancer.

The complexity of the cancer disease makes it hard to find the real causes of the disease and to find a proper cure therapy. In a human body, the basic units of life are cells. Normal cells grow, divide, and die in an order. If the cells in a part of the body begin to grow out of control, then cancer develops there. Cancer is a group of diseases in which abnormal cells divide uncontrollably. Unlike normal cells, cancer cells just continue to grow and divide out of control and don't die. Cancerous cells can invade and destroy healthy tissues. They can also spread to other parts of the body. Cancer can occur in any cell type and can therefore affect any of the body's tissues or organs. There are many types of cancer. Most cancers are named for the type of cells or the organ in which they begin. Cancer usually forms as a solid tumor but some cancers do not form. However not all tumors are cancerous.

Different types of cancer can behave very differently. The reason of some cancer types is known or is estimated however, it is still uncertain what causes most of cancer types. For example, smoking is known to cause a type of lung cancer. And skin cancer results from strong sunlight. Some other things that are thought to cause cancer are genetics, irregular nutrition, drinking alcohol and a polluted environment. Many risk

factors that increase the chance of having cancer has identified as mentioned above. It can be said that some cancers are often caused by not a single factor but a variety factors.

Since cancer was discovered as a disease, there have been many treatments to cure it. Unfortunately today, there is no certain cure for many types of cancer. That is why, some of these treatments are used to defeat cancer and others are used to reduce the side effects of cancer. The most common types of cancer treatment are surgery, chemotherapy and radiotherapy. These treatments are aimed at removing the cancer cells or destroying them in the body. All of these treatments can be applied alone or in combination according to type of cancer.

Surgery is the oldest form of cancer treatment. Cancerous tumor or tissue is physically removed from the body by surgery with an operation. There are many factors that cause the side effects after surgery. These side effects take shape by depending on the size and location of the tumor, the type of operation, and the patient's general health (NCI Fact Sheet 6.7, 2005). Some pain may become after surgery, but this pain is controllable with some medical approaches. Surgery can be the greatest way for cure for some types of cancer. But it has a lot of risk factor. Because the removing cancer cells from the body without damaging is very difficult. Surgery needs an expert who must be very competent of this operation to achieve the best outcome.

The most common treatment type of cancer is chemotherapy. In chemotherapy, cancer cells throughout the body are killed with helping of drugs. One drug or a combination of drugs may be used within chemotherapy. These drugs can affect cancer cells anywhere in the body. Thus, chemotherapy can be referred as a systemic treatment (Cukier, 2005). Chemotherapy is applied alone or with other treatments. Although chemotherapy is effective method in cancer treatment, it has the side effects by depending mainly on the drugs and the doses. The disadvantage of chemotherapy is that healthy cells can also be harmed by anticancer drugs. Chemotherapy can also have several neurological side effects, such as fuzzy thinking and difficulty concentrating.

Radiation is one of the major forms of treatment in cancer therapy besides chemotherapy and surgery. Radiation therapy is one of the cornerstones of cancer treatment. The goal of radiation therapy is to kill the cancer cells with as little risk as

possible to normal cells. The radiation therapy treatment plan, which is determined by finding directions of beams, beam intensities and a realization of optimal intensities on the equipment, is a complex task (Ehrgott and Burjony, 2001). High-energy x-rays are used to treat cancer in radiation therapy. Increasingly, radiotherapy is used in combination with surgery and chemotherapy (Peters and Kenney, 2002). Radiation therapy can be used to treat many kinds of cancer in almost any part of the body. Normal cells are also affected by radiation but, unlike cancer cells, most of them recover from the effects of radiation. The dose of radiation is limited or decreased to protect normal cells.

Scientists are constantly working to find and improve new treatment techniques. These techniques are aimed to be more precise and much less invasive then current techniques. Recently, the new radiation techniques are started to get more importance in the treatment of cancer. Hyperthermia is the most important one of these techniques. In this respect, this study is covered by electromagnetic hyperthermia and its application.

Hyperthermia is a type of cancer treatment and also called thermal therapy or thermotherapy. The goal of electromagnetic hyperthermia is to increase the temprature of cancer tissues by exposing them to electromagnetic radiation. In cancer tissues high temperatures up to 45 ºC is desirable (NCI Fact Sheet 7.3, 2004), (Deufhard et al.,1997). Research has shown that high temperatures can damage and kill cancer cells, usually with minimal injury to normal tissues. Moreover, hyperthermia increases the effect of radiotherapy or chemotherapy.

In this thesis we make a computational electromagnetic model in order to calculate the electromagnetic behavior in human tissues. When we obtain the electromagnetic behavior in tissues then we can calculate the change in temperature in exposed tissues.

The chapters are arranged to give general information about cancer, radiation therapy, hyperthermia, and bioheat transfer and to study the results that are occurred by electromagnetic hyperthermia.

CHAPTER 2

RADIATION THERAPY FOR CANCER TREATMENT

This chapter is designed to present radiation therapy with its all applications. The contents are based on all details about radiation therapy. All parts of this chapter describe respectively what radiation therapy is and, how radiation therapy is used to treat cancer. The treatment plannig of radiation is proposed in detail. It explains the two most common types of radiation therapy, external radiation and internal radiation therapy. Other applications about radiation therapy are mentioned briefly.

2.1 HISTORY OF RADIATION THERAPY

Radiation therapy has been used to cure cancer or other diseases for more than hundred years (Haas et al., 1998). Radiographic images have been used as a vital component in planning radiation treatment since the first therapeutic use of x-rays almost 100 years ago (Kalet and Austin-Seymour, 1997). The first use of radiation as a treatment of cancer effectively had started after the discovery of the x-ray by German physicist Wilhelm Conrad Roentgen in 1895, radioactivity by Becquerel and radium by Marie and Pierre Curie (Imaginis, 2006). In fact, the first successful radiation treatment for cancer was reported in 1899. The investigation of x-rays radiation for treatment of diseases moved into clinical routine in the early 1920s.

Radiation was given in single with large doses in its first years. However, there many problems or complications that occurred due to the destruction of normal tissues (Calvagna, 2007). Because the radiation dosage could not be calculated. Because of this, the relationship betweeen the radiation dosage and the biological effects had been

started to study by scientists. The use of fractioned doses of radiation rather than single dose was comprehended. The late 1920's saw the identification of a dosage unit of radiation. The total dose of radiation had been divided into several small doses.

Radiation therapy was an insufficient method for cancer treatment with little or no curative effects between 1920 and 1940 years (Coosa Valley Technical College (CVTC), 2007). The radiation therapy of this era involved a massive exposure of radiation to a large area of the body with the hope that the tumor would be destroyed with a single treatment. Radiation was applied as level of kilovoltage during this period. High energies, which are higher than 200 kV, had been obtained after the discovery of the vacum x-ray tube. Some surface cancers could be cured with this advance.

The use of mega-voltages to treat cancer had started in between 1940-1960. This period witnessed the development and the widespread use of radioactive cobalt. In addition, electrical devices such as linear accelerator that produces high energy were discovered in the same time. These machines produced x-rays capable of deep penetration, making it possible to treat tumors located below the skin surface. Mega-voltage machines offered many advantages. The greater penetration of the x-rays was one of them.

The mega-voltage radiation machines, radiobiology, the computer and controlled clinical trials, had been further developed and refined from 1960 to today (Coosa Valley Technical College (CVTC), 2007). Now, there are machines that are capable of delivering adequate doses of radiation to tumors located in all areas of the body. These machines are also known as accelerators.

During the first century of radiation therapy many dramatic advances have taken place. The improvements of treatment outcome have mainly been linked to developments in the areas of molecular and clinical oncology, radiation biology and radiation physics (Brahme, 2000). For some decades, radiation therapy has been largely successful in cancer treatment. Today, it can be said that radiation ranks among the most thoroughly investigated causes of disease and radiation therapy is considered to be a major treatment modality for cancer.

2.2 BASIC PRINCIPLES OF RADIATION THERAPY

2.2.1 Definition of Radiation Therapy

Technical improvements in the application of x-rays, computed tomography scans, magnetic resonance imaging with and without spectroscopy, ultrasound, positron emission tomography scans, and electronic portal imaging (and our understanding of their limitations) have greatly improved the ability to identify tumors (Bucci, et al., 2005). Radiation therapy has become one of the cornerstones of cancer treatment becuse of this.

Radiation therapy is also called radiotherapy, x-ray therapy, or irradiation (NCI Fact Sheet 7.1, 2004), (The NCI booklet, 1998). The basic objective of radiotherapy cancer treatment is to apply ionizing radiation (typically x-rays) to destroy cancerous tumor cells while protecting healthy tissue surrounding the tumor (Stewart and Davison, 2006), (Enderling et al., 2005), (Kalet and Austin-Seymour, 1997), (Artacho Terrer et al., 2007). The radiation therapy problem (RTP) is the use of particle beams to treat tumors. Beams of particles, usually photons or electrons, are oriented at various angles and with varying intensities to deposit dose (energy/unit mass) to the tumor (Lodwick and Neumaier, 2001). The main idea is to deposit as much dose as possible to the tumor while sparing normal tissue. The effects of radiation as a therapy on tissues and their cells are very complex. Radiation therapy destroys cells in the area being treated by damaging their genetic features. When these damaged cancer cells die, the human body naturally eliminates them.

Radiation therapy is given through different methods, depending on the type of disease, its location and patient's general health. Radiation therapy may be used alone or in combination with other therapies (Peters and Kenny, 2002). For example, larynx and prostate cancer are generally treated with radiation alone, but breast cancer can be treated with surgery, radiation therapy and chemotherapy (ASTRO, 2004). A radiation therapy may be chosen by an oncologist in a number of different ways. It is very important to determine the goal of treatment to get best results. Radiation therapy may be used to remove tumors that have not spread to other parts of body and reduce the risk that cancer cells replace.

In some cases, the goal of radiation treatment is the complete destruction of an entire tumor (NCI Fact Sheet 7.1, 2004). In other cases, the aim is to shrink a tumor and relieve symptoms. In either case, doctors plan treatment to spare as much healthy tissue as possible.

There may be little or no side effects after radiation therapy (ASTRO, 2004). Many of the side effects of radiation therapy are related to the area that is being treated. These side effects are usually temporary and can be treated by the doctor or other members of the treatment team.

Radiation dose or application time may be decreased or arranged according to status of patient to minimize the negative effects of radiation for normal tissues. This process is called as fractionation of the dose (Calvagna, 2007). This is very vital application to help oncologists. Because it allows destroying cancer cells in the same time that normal tissues repair themselves. The radiation beam is shaped by a device as called a collimator to reduce healthy tissue irradiation (Stewart and Davison, 2006).

There may be some symptoms during radiation therapy. These symptoms include pain, uncontrolled bleeding, tumor obstruction around major blood vessels and organs, and spinal cord compression. Radiation treatments do not involve pain or any other sensation. Radiation therapy can also be given to help reduce symptoms such as pain from cancer that has spread to the bones or other parts of the body. This is called palliative radiation therapy (NCI Fact Sheet 7.1, 2004). Although patients are afraid they will feel intense heat, there is no heat, light, or sound associated with the treatment.

Before radiation treatment begins, firstly tests have to be obtained. These are used to determine what type of cancer exists. Once the diagnosis has been made, the patient probably talks with several oncology specialists, such as a surgeon, a medical oncologist and a radiation oncologist, to discuss his or her treatment choices. These specialists usually work together to help recommend the best treatment for the patient.

The most elegant aspect of radiation therapy as compared with other forms of cancer treatment is that precisely aimed the radiation beams to maximize the radiation dose deposited in the target, relative to the dose received by other parts of the body (Kalet and Austin-Seymour, 1997).

2.2.2 Physical and Mathematical Aspects of Radiation

In this part of thesis, radiation is dealt with physical and mathematical point of view to enlighten the way for understanding its electromagnetic behavior as a cancer therapy. The following sections cover the basic physics of radiation and its application for the cure of tumor or cancerous area. And it deals with radiation therapy where beams of penetrating radiation are directed in the cancerous area from an external source. This section will help to understand radiation therapy best.

2.2.2.1 Basic Radiation Physics

There are two main categories for radiation. These are known as non-ionizing radiation and ionizing radiation which are shown in Fig. 2.1. Although ionizing radiation can ionize matter but non-ionizing radiation can not ionize matter. This is the difference between them.

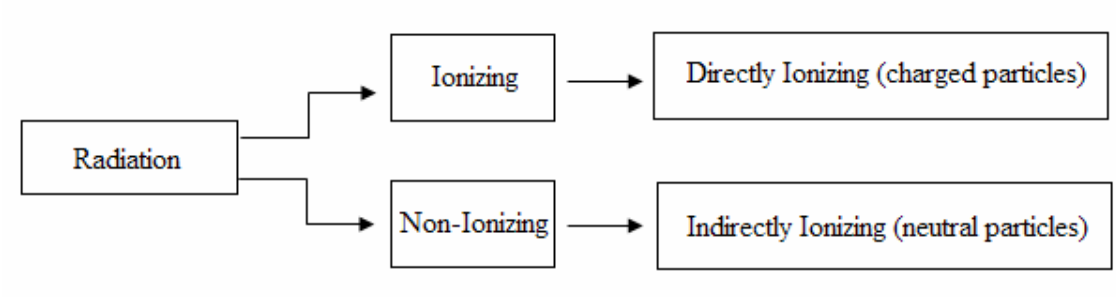

Figure 2.1 Classification of Radiation

There are two ways to apply ionizing radiation. These are directly and indirectly ionizing radiation. Directly ionizing radiation uses charged particles such as electron, proton, alpha particle, heavy ion. Indirectly ionizing radiation uses neutral particles such as photon (x rays, gamma rays), neutron. This is the most common type of the use of radiation (NDT Resource Center, 2007).

Both X-rays and gamma rays can be formed by frequency, wavelength, and velocity. However, they act somewhat like a particle at times in that they occur as small "packets" of energy and are referred to as "**photons."**

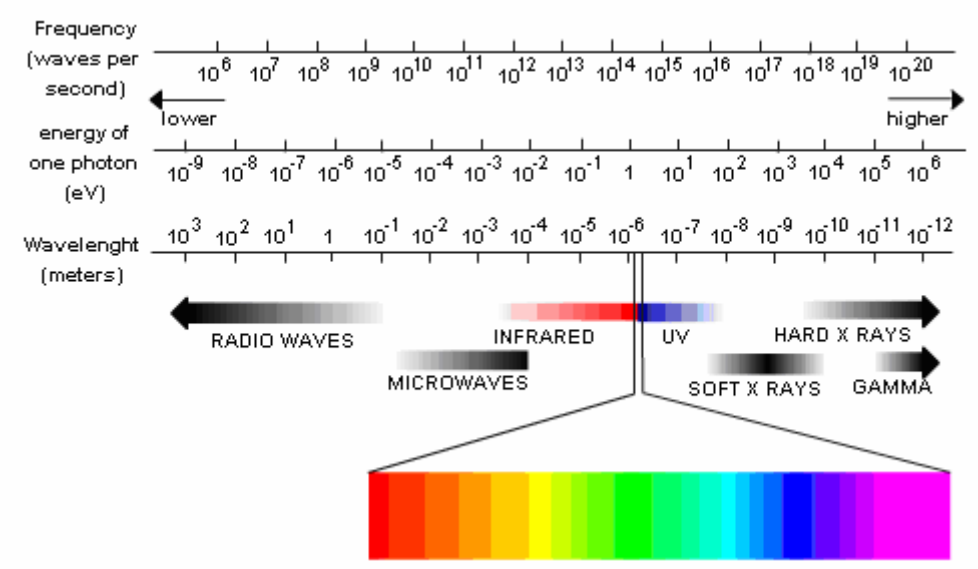

Figure 2.2 Electromagnetic Spectrum (NDT Resource Center, 2007).

As penetrating radiation moves from point to point in matter, it loses its energy through various interactions with the atoms it encounters. The rate at which this energy loss occurs depends upon the type and energy of the radiation and the density and atomic composition of the matter through which it is passing (NDT Resource Center, 2007).

The term "ionization" refers to the complete removal of an electron from an atom following the transfer of energy from a passing charged particle. In describing the intensity of ionization, the term "specific ionization" is often used. This is defined as the number of ion pairs formed per unit path length for a given type of radiation.

Because of their double charge and relatively slow velocity, alpha particles have a high specific ionization and a relatively short range in matter (a few centimeters in air and only fractions of a millimeter in tissue). Beta particles have a much lower specific ionization than alpha particles and, generally, a greater range. For example, the relatively energetic beta particles from P32 have a maximum range of 7 meters in air and 8 millimeters in tissue. The low energy betas from H3, on the other hand, are stopped by only 6 millimeters of air or 6 micrometers of tissue.

Gamma-rays, x-rays, and neutrons are referred to as indirectly ionizing radiation since, having no charge, they do not directly apply impulses to orbital electrons as do alpha and beta particles (NDT Resource Center, 2007).

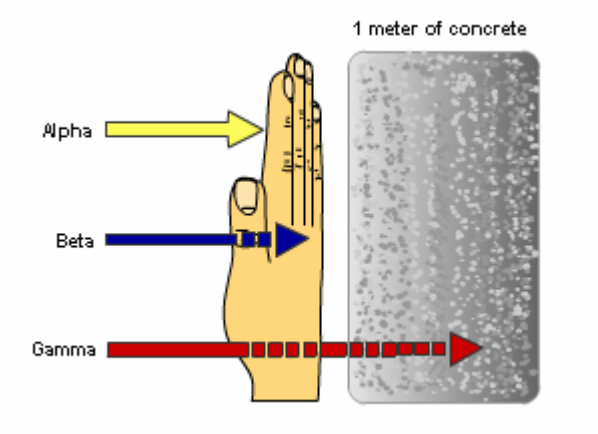

Figure 2.3 The penetrating power of radiation (NDT Resource Center, 2007).

Electromagnetic radiation proceeds through matter until there is a chance of interaction with a particle. If the particle is an electron, it may receive enough energy to be ionized, whereupon it causes further ionization by direct interactions with other electrons. As a result, indirectly ionizing radiation (e.g. gamma, x-rays, and neutrons) can cause the liberation of directly ionizing particles (electrons) deep inside a medium. Because these neutral radiations undergo only chance encounters with matter, they do not have finite ranges, but rather are attenuated in an exponential manner. In other words, a given gamma ray has a definite probability of passing through any medium of any depth.

2.2.2.2 X-rays

X-rays are just like any other kind of electromagnetic radiation. They can be produced in parcels of energy called photons, just like light. There are two different atomic processes that can produce X-ray photons (NDT Resource Center, 2007). One is called Bremsstrahlung and is a German term meaning "braking radiation." The other is called K-shell emission. They can both occur in the heavy atoms of tungsten. Tungsten is often the material chosen for the target or anode of the x-ray tube.

Both ways of making X-rays involve a change in the state of electrons. However, Bremsstrahlung is easier to understand using the classical idea that radiation is emitted when the velocity of the electron shot at the tungsten changes (Prutchi et al., 1999). The negatively charged electron slows down after swinging around the nucleus of a positively charged tungsten atom. This energy loss produces X-radiation. After emitting the spectrum of X-ray radiation, the original electron is slowed down or stopped.

2.2.2.3 Gamma Rays

Gamma radiation is one of the three types of natural radioactivity. Gamma rays are electromagnetic radiation, like X-rays (NDT Resource Center, 2007). The other two types of natural radioactivity are alpha and beta radiation, which are in the form of particles. Gamma rays are the most energetic form of electromagnetic radiation, with a very short wavelength of less than one-tenth of a nanometer.

Gamma radiation is the product of radioactive atoms. Depending upon the ratio of neutrons to protons within its nucleus, an isotope of a particular element may be stable or unstable (Prutchi et al., 1999).

2.2.2.4 Properties of X-Rays and Gamma Rays

X-rays are produced by an x-ray generator and radioactive atoms supply gamma radiation. They are both part of the electromagnetic spectrum (NDT Resource Center, 2007). They are waveforms, as are light rays, microwaves, and radio waves. X-rays and gamma rays cannot been seen, felt, or heard (Prutchi et al., 1999). They have no charge and no mass and, therefore, are not influenced by electrical and magnetic fields and will generally travel in straight lines.

They are not detected by human senses (cannot be seen, heard, felt, etc.). They travel in straight lines at the speed of light. Their paths cannot be changed by electrical or magnetic fields. They can be diffracted to a small degree at interfaces between two different materials. They pass through matter until they have a chance encounter with an atomic particle. Their degree of penetration depends on their energy and the matter they are traveling through. They have enough energy to ionize matter and can damage or destroy living cells.

2.2.2.5 Radiation Dose control and calculations in Radiation Therapy

In the early days of radiotherapy, ‘dose’ was used in a pharmacological sense quantifying the amount of radiation given rather than its physical impact on the irradiated matter (Ahnesjö and Aspradakis, 1999). Today, absorbed dose is strictly defined as mean energy imparted (by ionizing radiation) per mass, i.e. dose is decoupled from the radiation used to deliver it. Therefore, absorbed dose is the fundamental physical quantity of interest for relating radiation treatment to its outcome. The energy

deposited per unit mass of tissue is referred to as absorbed dose and is the source of the biological response exhibited by irradiated tissues (Holder and Salter, 2005). Radiation dose to each site depends on a number of factors, including the type of cancer and whether there are tissues and organs nearby that may be damaged by radiation (NCI Fact Sheet 7.1, 2004).

One of the most important considerations in radiation therapy is the precision with which the radiation dose can be delivered to the tumor (Entine et al., 1992). This is due to the well documented fact that a variation in dose of 5% can make a large difference in the tumor control probability and in the likelihood of serious complications.

In dose calculation, termed dosimetry, the relevant physical and biological characteristics of the irradiated object and the relevant information about the radiation source (geometry, physical nature, intensity, etc.) serve as input data. The result (output) of the calculation is a dose function whose values are the dose absorbed as a function of location inside the irradiated body.

Units of absorbed dose are typically expressed as Gy (pronounced Gray) or centiGray (cGy). One Gy is equal to one Joule (J) of energy deposited in one kilogram (kg) of matter. The potential benefit radiation therapy must be weighted against the potential risk of complications predominately to dose (Abitbol et al., 1988).

A total dose of 60 Gy, for example, might be delivered in 2 Gy daily fractions over 30 treatment days. Two Gy represents a daily dose of radiation that is typically tolerated by healthy cells but not by tumor cells. The difference between the tolerable dose of tumor and healthy cells is often referred to as a therapeutic advantage, and radiotherapy exploits the fact that tumor cells are so focused on reproducing that they lack a well-functioning repair mechanism possessed by healthy cells.

The doses of radiation used to destroy cancer cells can also harm normal cells. For this reason, the safety of radiation therapy has been the origin of some fears for patients. But radiation therapy has been used successfully to treat patients. In that time, many advances have been made to ensure that radiation therapy is safe and effective. Cancer cells are more sensitive to radiation than normal cells.

2.3 RADIATION THERAPY TREATMENT PLANNING

The identification of a set of beam angles and weights that provide a lethal dose to the tumor cells while sparing healty tissue with a resulting dose distribution acceptable and approved by the oncologists is called a treatment plan (Lodwick and Neumaier, 2001). When designing a patient's treatment plan, the goal is to provide the highest probability of tumor control while maintaining an acceptable probability of radiation induced complications. Unfortunately, it is very difficult to quantify optimality in radiation therapy (Shepard et al., 1999). The automation of radiotherapy treatment planning has become possible with the development of fast computers (Haas et al., 1998).

The basic requirements of an radiation therapy plan system are as follows (Kalet and Austin-Seymour, 1997); First, It has to model the patient's body, including the soft tissue volume (enclosed by skin), internal organs relevant to the region being irradiated, the target (tumor plus allowance for other factor). Second, It has to model the geometry and dosimetric properties of the various radiation beams in use in radiation therapy, high-energy x-rays, high-energy electron beams (and in our case at the University of Washington, fast neutron beams as well). And finally, It has to display the anatomic and radiation beam information in cross-sectional views or projected views (called ''beam's eye views''), and in the crosssectional views also display a contour map or other rendition of the levels of radiation dose throughout the area.

Radiation therapy planning has to find a precarious balance between ineffective underdosing of the tumour (the target volume) and dangerous overdosing of surrounding tissue (organs at risk).

Treatment plans are commonly based on desired dose levels, which are specified for the tumour and each organ at risk. These desired dose levels are chosen so that a high tumour control probability is realised (lower bound on dose levels in tumour cells), but also that probability of complications in any organ at risk is low (upper bound on dose level in healthy tissue). Beams are focused on the centre of the tumour (isocentric geometry). This is illustrated in Fig. 2.4.

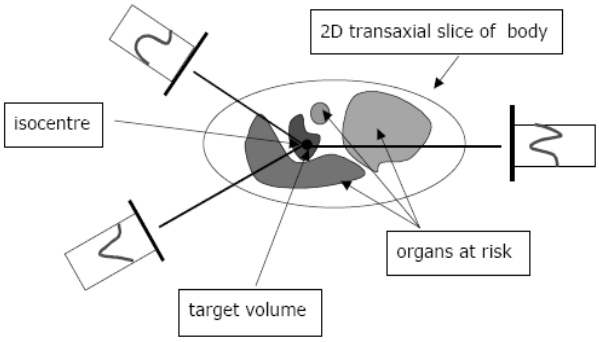

Figure 2.4 Illustration of radiation treatment planning problem (Ehrgott and Burjony, 2001).

There are two principal aspects of radiation therapy that call for mathematical modelling (Cencor, 1999). The first is the calculation of the radiation dose which is a measure of the actual energy absorbed per unit mass (Shepard et al., 1999) everywhere in the irradiated tissue. The second aspect is the mathematical inverse problem of the first. Much of current radiation therapy treatment planning (RTTP) is still done in two dimensions where only a single plane through the center of the target is considered. RTTP is also still done mostly in a trial-and-error fashion by picking a machine setup that gives rise to a certain external radiation intensity field (function) and then using a forward-problem-solver software package to determine the resulting dose function, which is shown in Fig. 2.5.

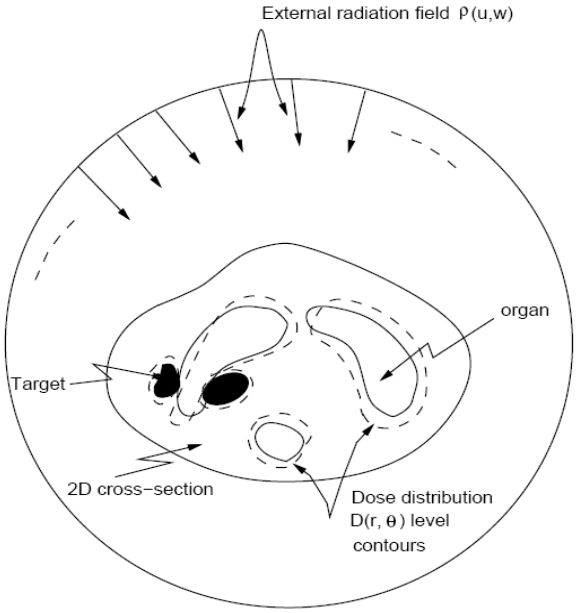

Figure 2.5 *2D RTTP*, an ext. radiation fields result in a dose distribution (Cencor, 1999).

Automated solution of the inverse problem of RTTP should be useful in handling difficult planning cases, particularly in 3D{RTTP, which is shown in Fig. 2.6.

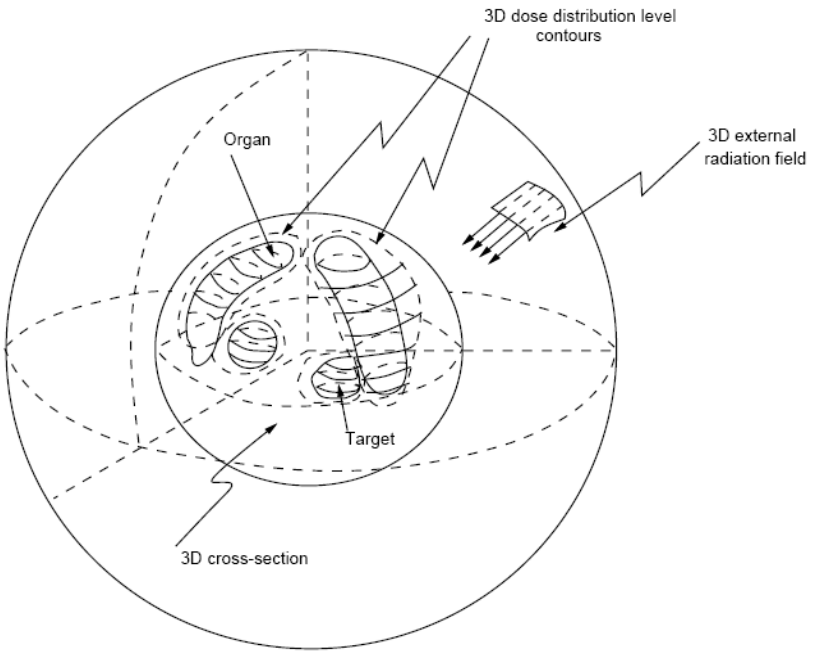

Figure 2.6 *3D RTTP*, fully 3D cross section, external radiation field and dose distribution (Cencor, 1999).

There, it would be much more difficult to reach an acceptable plan by trial-and-error because of the multitude of potential directions from which the 3D object can be irradiated.

Before radiation treatment begin, a very precise type of treatment planning called simulation has to be done in order to pinpoint the exact area of the body to be treated. The x-rays, scans and other information obtained during this simulation process are used to determine how the treatments can be given, the amount of radiation and the number of treatments that are needed. This is done with an x-ray machine called a 'simulator'. It is called a simulator because it is built to simulate (or be like) a radiotherapy machine, but without giving the treatment. The pictures it produces are used, along with any scans, to line up the area to be treated.

Modern advances in computers have fueled parallel advances in imaging technologies. The improvements in imaging have in turn allowed a higher level of complexity to be incorporated into radiotherapy treatment planning systems (Bucci, et

al., 2005). As a result of these changes, the delivery of radiotherapy evolved from therapy designed based primarily on plain (two dimensional) x-ray images and hand calculations to three-dimensional x-ray based images incorporating increasingly complex computer algorithms.

It is important to be able to derive from the image data sharp boundaries defining organs. This process is called image segmentation (Kalet and Austin-Seymour, 1997). The contoured volume models are also useful in the calculation of radiation dose from each beam, since it is easy to determine the path taken through such objects, by a radiation beam and thus compute the effect of density differences in the tissue.

Two kinds of accuracy requirements guide the use of images in radiation therapy: spatial accuracy and dose accuracy. They are related because the accurate computation of dose depends on accurate spatial information about the patient's tissues, as well as their density and composition. The International Commission on Radiation Units (ICRU) has recommended that the dose in the volumes of interest should be known to an accuracy of 5%.

Any technologic improvements must be backed by clinical data showing an actual benefit to patients. The expected benefit from advanced treatment planning such as 3D CRT and IMRT and improved patient localization methods introduced in tandem with these techniques is two-fold: (1) improvement in tumor control and (2) decrease in side effects and toxicities (Bucci, et al., 2005).

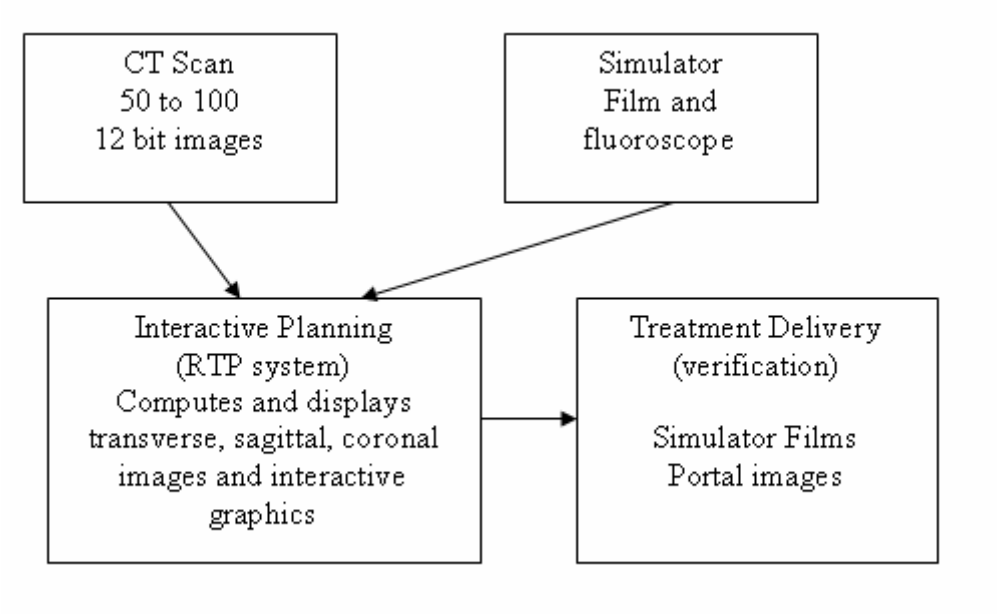

Figure 2.7 The radiation treatment planning process (Kalet and Austin-Seymour, 1997).

Fig. 2.7 shows the planning process, indicating the kinds of images generated or used in each of the steps for radiation therapy treatmet planning.

When the treatment is being planned, measurements will be taken, for example from the treatment couch to the tattoos. This is because the distance between the source of radiation (the machine) and the target (the cancer) is very important in working out the radiotherapy dose. The further away from the source, the lower the radiation dose.

When all this information is put together, the planning computer can work out the best positioning of the radiotherapy beams to treat all the cancer but give as little radiotherapy to healthy body organs in the area as possible. Simulation may take anywhere from 30 minutes to 2 hours depending on the type and location of the tumor.

Over years of practice, physicians develop insights into what is “optimal” for a particular type of cancer in a particular location. The physician must also consider the patient’s medical history and the institution’s capabilities. Thus, it is important that the optimization approach provides the physician with sufficient flexibility so that he or she can always produce an acceptable treatment plan.

Radiation therapy is applied by a medical team who are highly trained professionals in radiation oncology. The diagram of radiation therapy team is shown in Fig. 2.8.

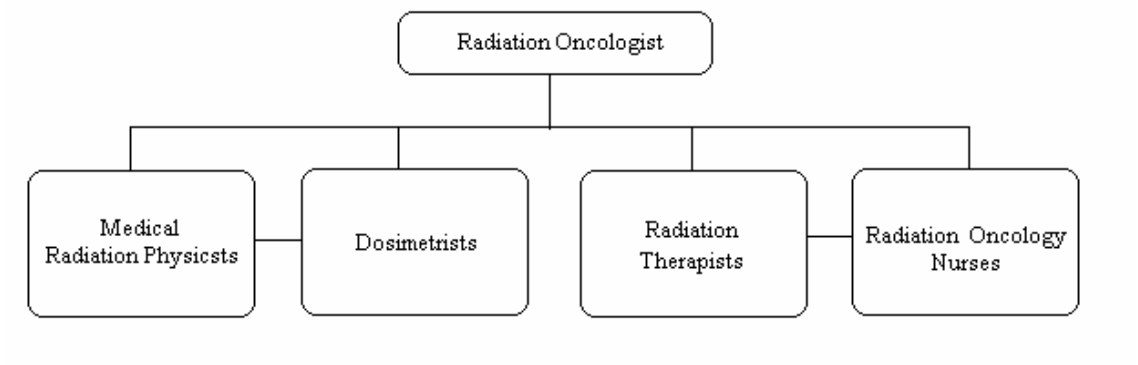

Figure 2.8 Radiation Therapy Team Diagram

Radiation oncolgists are the doctors who manage the radiation therapy. They work with the other members of the radiation therapy team to develop and prescribe the treatment plan. The radiation oncologist oversees the progress and adjusts the treatment. Radiation oncologists identify and treat the side effects that may occur due to radiation therapy. They work closely with other physicians, including medical oncologists and surgeons, and all members of the radiation oncology team.

Qualified medical physicists work directly with the radiation oncologist during treatment planning and delivery. They oversee the work of the dosimetrist and help ensure that complex treatments are properly tailored for each patient (ASTRO, 2004). Medical physicists are responsible for developing and directing quality control programs for equipment and procedures. Their responsibility also includes making sure the equipment works properly by taking precise measurements of the radiation beam and performing other safety tests on a regular basis.

Dosimetrists work with the radiation oncologist and medical physicist to carefully calculate the dose of radiation to make sure the tumor gets enough radiation. Using computers, they develop a number of treatment plans that can best destroy the tumor while sparing the normal tissues.

Radiation therapists work with radiation oncologists to administer the daily radiation treatment under the doctor's prescription and supervision. They maintain daily records and regularly check the treatment machines to make sure they are working properly.

Radiation oncology nurses work with radiation oncologists and radiation therapists to care for the patients and their family at the time of consultation, while they are receiving treatment.

2.4 TYPES OF RADIATION THERAPY

The goal of radiation therapy is to get high dose of radiation into the body to destroy the cancer cells. Several different radiation techniques have been developed and applied to accomplish this aim. One or a combination of these techniques can be applied.

The type of radiation to be given depends on the type of cancer, its location, how far into the body the radiation will need to go, the patient's general health and medical history, whether the patient will have other types of cancer treatment, and other factors. Treatment team and patient determine which type of tecniques or how much radiation is best to cure of cancer. There are two main ways in radiation therapy. These are external and internal applications. These applications are presented in detail in the following sections.

2.4.1 External Beam radiation therapy

External radiation therapy is the most common type of radiotherapy. There are many types of cancer, which are cancer of the brain, breast, bladder, cervix, larynx, lung, prostate, and vagina, can be treated by external therapy (NCI Fact Sheet 7.1, 2004). External therapy is applied by using a machine outside of body. Different types of machines are used The most common type of machine used to deliver external beam radiation therapy is called a linear accelerator (ASTRO, 2004), (NCI Fact Sheet 7.1, 2004), sometimes called a "linac" shown in Fig. 2.9. A linear accelerator (linac) generates high energy electrons and photons (typically 5-25 MeV). The device is

capable of rotating about a single axis of rotation so that beams may be delivered from essentially 360 degrees about the patient. Additionally, the treatment couch, on which the patient lies, can also be rotated through, typically, 180 degrees (Holder and Salter, 2005). A beam of radiation is directed through the skin to a tumor and the immediate surrounding area in order to destroy the main tumor or any nearby cancer cells during external beam radiation therapy. The area affected by the tumour is divided in small cubes called voxels, usually tens of thousands, in order to obtain an accurate representation of the volume (Artacho Terrer et al., 2007). The radiation dose can be calculated by the experts. The total dose of radiation and number of treatments depend on the size, location and type of cancer.

Figure 2.9 A Linear Accelerator (Holder and Salter, 2005).

There is no pain or blood when external radiation therapy is given into body. On the contrary, external radiation may be used to relieve pain or other problems that are occurred during other treatment options (NCI Fact Sheet 7.1, 2004). The treatments are typically given to minimize side effects every day for a number of weeks Actual treatment time ranges from 2 to 5 minutes (Mayo Clinic, 2007).

External beam radiation therapy can be loosely subdivided into the general categories of conventional radiation therapy and, more recently, conformal radiation therapy techniques. External beam therapy has several special types. Most common used types of these are discussed in the following sections.

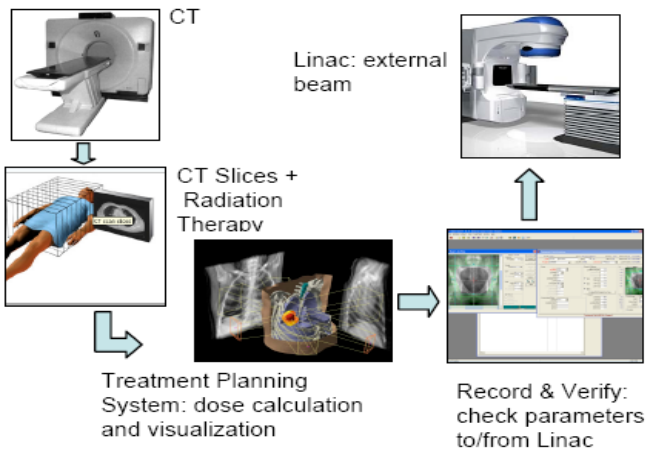

Figure 2.10 General flow of external radiation therapy treatments (Hamza-Lup et al., 2006).

2.4.1.1 Three-Dimensional Conformal Radiation Therapy (3D-CRT)

3D (3D-CRT) Conformal Radiation Therapy is used to treat tumors that in the past might have been considered too close to vital organs and structures for radiation therapy (PAMF, 2004). It is a technique that uses computers and computer assisted tomography scans (CT or CAT scans) and/or magnetic resonance imaging scans (MR or MRI scans) to obtain 3D images of the tumor and surrounding organs (ASTRO, 2004). The radiation beams can exactly be shaped to the size and shape of patient's tumor.

2.4.1.2 Intensity Modulated Radiation Therapy (IMRT)

Motivated by medical and computing advances, interest in *intensity-modulated* radiotherapy (IMRT) has grown in the radiotherapy community over the past decade (Stewart and Davison, 2006). A relevant development in the last decade is the intensity modulated radiotherapy (IMRT) system, where the distribution of the dose can be controlled with spatial accuracy using multileaf collimators (Artacho Terrer et al., 2007). Optimal dose distributions in intensity-modulated radiotherapy (IMRT) are commonly obtained through an iterative optimization method that typically requires a large number of dose calculations to converge (Wu et al., 2003). In IMRT, the collimator leaves are dynamically positioned during a fraction so the resulting post-fraction delivered radiation dose has a non-uniform intensity. In IMRT planning, linear or quadratic objective functions are the most usual choices.

IMRT creates a shaped radiation beam, delivering high doses of radiation to the tumor and significantly smaller doses of radiation to the surrounding normal tissues. The radiation beam can be seperated into many parts. These are called as “beamlets”. And the intensity of each beamlet can be adjusted individually. This may increase the success of the cure and result higher cancer-control rate and a lower rate of side effects.

The IMRT technology allows precisely delivering the radiation to the tumor cells. An IMRT treatment plan specifies how much radiation will be delivered from each beamlets at which angles in each treatment session so that the target volume can be radiated uniformly at the maximum capacity without exceeding the healthy tissue constraints (Arangarasan et al., 2005). This treatment planning requires an iterative work between a physician and an IMRT technician that is a time consuming process. Current state-of-the-art method is to determine an IMRT treatment plan at the beginning and use it with no changes during the course of the treatment. A conventional IMRT treatment plan is show in Fig. 2.11.

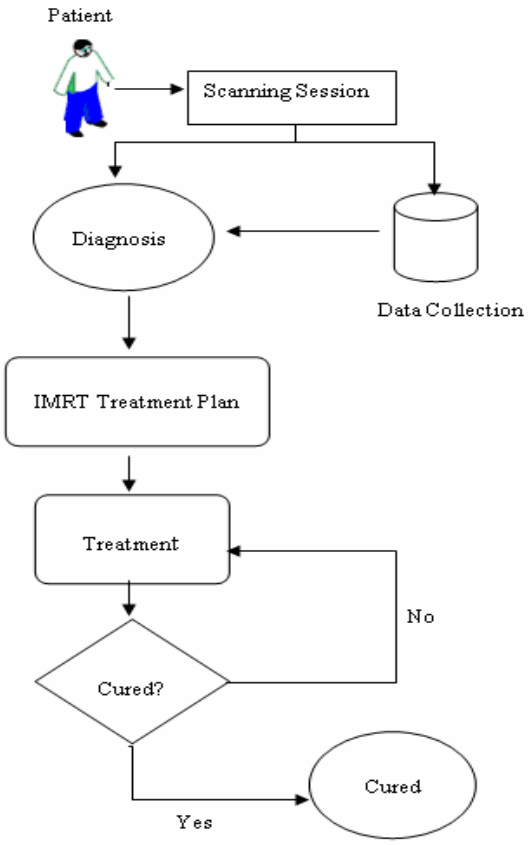

Figure 2.11 Conventional IMRT Treatment Plan (Arangarasan et al., 2005).

2.4.1.3 Stereotactic Radiotherapy

Stereotactic radiotherapy is a radiation technique that precisely generates radiation beams to destroy certain types of tumors. It is the most commonly used technique to treat brain tumors (Clark and Mckenzie, 1999) (ASTRO, 2004). This technique may be successfull to treat cancer rather than other parts of the body. Multiple small fractions of radiation are used in stereotactic radiotherapy. This means small dose radiation can be applied. This may improve outcomes and minimize the negative effects of therapy. More normal tissue can be protected with this application. Radiotherapy may be the only treatment if a very small area is affected.

2.4.1.4 Proton Beam Therapy

This is one of the most precise and sophisticated forms of external beam radiation therapy available. The advantage of proton radiation therapy over x-rays is its ability to deliver higher doses of shaped beams of radiation directly into the tumor while minimizing the dose to normal tissues .

2.4.1.5 Neutron Beam Therapy

Neutron beam therapy is a type of radiation therapy. Neutron therapy treats certain tumors that cannot be removed with surgery

2.4.2 Internal Radiation Therapy (Brachytherapy)

Also known as internal radiation, brachytherapy uses the radiation that is placed very close to the tumor or cancereous cells. High dose radiation can be delivered directly to the cancer cells with minimal harm to normal tissue. The radioactive sources used in brachytherapy, such as thin wires, ribbons, capsules or seeds, come in small sealed containers (ASTRO, 2004). Some sources are applied permanently. These sources are kept in a small holders. These are called as implants (NCI Fact Sheet 7.1, 2004). Other sources are placed temporarily inside the body, and the radioactive sources are removed after the prescribed dose of radiation has been delivered.

2.4.3 Other Radiation Therapies

2.4.3.1 Systemic Radiation Therapy

Systemic radiation therapy is the use of radioactive isotopes to treat certain cancers is called (ASTRO, 2006). In systemic radiation therapy, the radiation source is given as a liquid. The radiation source spreads throughout the body (CCS, 2006).

2.4.3.2 Radio immunotherapy

Recent research has focused on the use of radioactive monoclonal antibodies, also called radiolabeled antibodies, to deliver doses of radiation directly to a tumor. This process is known as radioimmunotherapy.

2.4.3.3 Radiosensitizers and Radioprotectors

Two types of drugs are being studied for their effect on cells undergoing radiation. One type includes drugs designed to make tumors more sensitive to radiation. It is hoped that these radiosensitizers will help radiation better destroy tumors. Other types of drugs are being evaluated to better protect the normal tissues near the area being treated. These are called radioprotectors. An example of a radioprotector is a drug designed for head and neck cancer patients that helps decrease soreness some patients may feel during treatment and the dryness some patients may experience after treatment is completed.

2.4.3.4 Intraoperative Radiation Therapy

Radiation therapy given during surgery is called intraoperative radiation therapy. The goal of intraoperative radiation therapy is to deliver a boost of radiation to a localized volume in carefully selected situations where there is a high risk of local recurrence of the tumor after surgical resection. Intraoperative radiation therapy is helpful when vital normal organs are dangerously close to the tumor. During an operation, a surgeon temporarily moves the normal organs out of the way so radiation can be applied directly to the tumor. This allows your radiation oncologist to avoid exposing those organs to radiation. Intraoperative radiation can be given as external beam therapy or as brachytherapy.

CHAPTER 3

HYPERTHERMIA IN CANCER TREATMENT

For most of the cancer patients, chemotherapy and radiotherapy are two of the most popular and effective methods in the treatment of cancer. Cancer could be a very violent and sometimes an incurable disease. However, both chemotherapy and radiotherapy would damage the normal and abnormal tissues. Patients also have to suffer from great pain during these treatments. Alternatively, there are many promising cancer therapy techniques developed in last years. Hyperthermia cancer therapy is one of the promising approaches. This chapter describes all detailed applications about hyperthermia. And the following sections deal with the physical and biological basis of hyperthermia.

3.1 BASIC PRINCIPLES OF HYPERTHERMIA

Historically, the treatment of cancer with hyperthermia can be traced back to 3000 B.C. (Chou, 1988). The current interest in hyperthermia came into the limelight in the early 1970s, where strong research activities were begun addressing both the biological and clinical usefulness of this modality (Nielsen et al., 2001). It was initiated by the first international congress on hyperthermic oncology in Washington in 1975. This interest has followed a course that is usual for a new type of treatment. Although hyperthermia was first employed as a treatment for malignant disease in the last century, it is only relatively recently that its mode of action and clinical application have been subjected to serious scientific research (Dunscombe et al., 1989).

3.1.1 Definition of Hyperthermia

A dictionary explanation of the word “hyperthermia” is “overheating of the body”. However, hyperthermia is an alternative cancer treatment as a therapy in which body tissue is revealed to high temperatures (Yang et al., 2005). The objective of hyperthermia treatment of cancer is to increase the temperature in the tumor volume above 42ºC - 43ºC for a sufficient period of time (Jordan et al., 1999). This process must protect normal physiological temperatures (well below 42 ºC) in the surrounding tissues (Converse et al., 2006). Researches had shown that high temperatures can damage and kill cancer cells. This approach usually causes minimal injury to normal tissues. Hyperthermia may shrink tumor or cancer cells by killing them or damaging their proteins and structures (Hildebrandt et al., 2002).

Hyperthermia can be applied as an supplement therapy with different established cancer treatments such as radiotherapy and chemotherapy (Wust et al., 2002). Hyperthermia may make some cancer cells more sensitive to radiation or harm other cancer cells that radiation cannot damage.

Hyperthermia and radiation therapy are often given within an hour of each other when they are combined. The effects of certain anticancer drugs may be enhanced by hyperthermia. Hyperthermia has been dealt with numerous clinical trials in combination with radiation therapy and/or chemotherapy. These studies have focused on the treatment of many types of cancer, including sarcoma, melanoma, and cancers of the head and neck, brain, lung, esophagus, breast, bladder, rectum, liver, appendix, cervix, and peritoneal lining (NCI Fact Sheet 7.3, 2004). Many of these studies, but not all, have shown a significant progress in the treatment of tumor or cancer cells when hyperthermia is applied with other treatments.

The combination of radiation therapy and hyperthermia may make the radio resistant tumor cells more sensitive to radiation (Abitbol et al., 1988). This is demonstrated by comprehensive laboratory datas. In addition, tumor cells in the synthetic phase of the reproductive cycle which are typically resistant to radiation may be more responsive to radiation with the addition of hyperthermia.

A high rate of complete response in the patients who are treated with radiation and hyperthermia is indicated by many clinical trials (Abitbol et al., 1988). The compared rates of this response are shown in Table 3.1.

Table 3.1 The rate of complete response with irradiation or hyperthermia alone.

Author	Criteria of Response	Radiation Therapy and Hyperthermia	Radiation Alone
Kim, Y. (1985)	Complete	33 %	----
Kim, J. (1982)	Complete	80 %	33 %
Scott, N.L. (1983)	Complete	87 %	39 %

The results outlined above indicate the potential usefulness of radiation therapy and hyperthermia to superficial tumors.

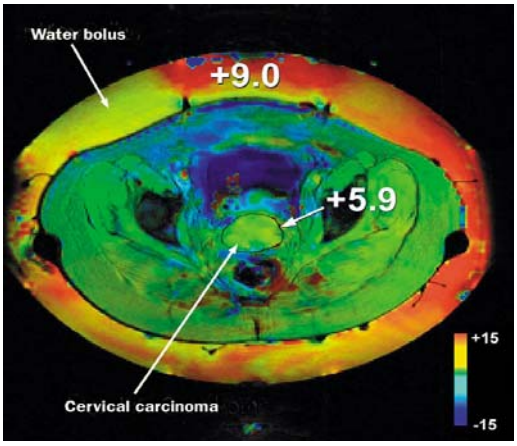

Figure 3.1 Non-invasive measurement of temperature distribution in the hybrid hyperthermia applicator (Wust et al., 2002).

The properties of hyperthermia are not only limited to its interaction with conventional treatment types (Babincová et al., 1999). There are a number of exciting areas. It may have a new area to apply, such as gene therapy. One of the major challenges in the current development of gene therapy strategies is the ability to regulate the expression of therapeutic genes to suitable levels (Wust et al., 2002). The use of heat inducible promoters can obtain controllable gene expression. This has been shown by several preclinical studies.

More recent studies have now shown that the antitumour activity of such vascular targeting therapies can be significantly enhanced by combination with hyperthermia. Other hyperthermia combination approaches, such as with chemotherapy, are not necessarily new, but there are clearly new drugs/combinations that may have potential in this regard.

Most normal tissues are not damaged during hyperthermia if the temperature remains under 42°C. However, higher temperatures may occur in various spots (NCI Fact Sheet 7.3, 2004). This changes due to regional differences in tissue characteristics. This can cause in burns, blisters, discomfort, or pain. Perfusion techniques can cause tissue swelling, blood clots, bleeding, and other damage to the normal tissues in the perfused area; however, most of these side effects are temporary.

3.1.2 Methods to Increase Temperature

The heating patterns of a particular modality is needed before the treatment. Numerical modeling is used to predict the heating patterns. The next step is to use the heat transfer equation to calculate the temperature distribution after the pattern is obtained (Chou, 1988). Numerous papers have been published on mathematical modeling of this process. Numerical techniques, such as finite differences, finite element, moment, and finite-difference time-domain methods, have been used for numerical modeling.

Radiobiologists carefully studied the effects of hyperthermia on normal and tumor cells during the last two decades (Strohbehn and Douple, 1984). The results of these cell survival studies in the 1970s showed that cessation of cell division, defined as mitotic death or cell killing, was attained if cells were exposed to temperatures in excess of approximately 40ºC for time periods of 30 min or more. In Fig.3.2, the surviving fraction of the heated cells is plotted on the ordinate as a function of the time the cells were held at a specific temperature.

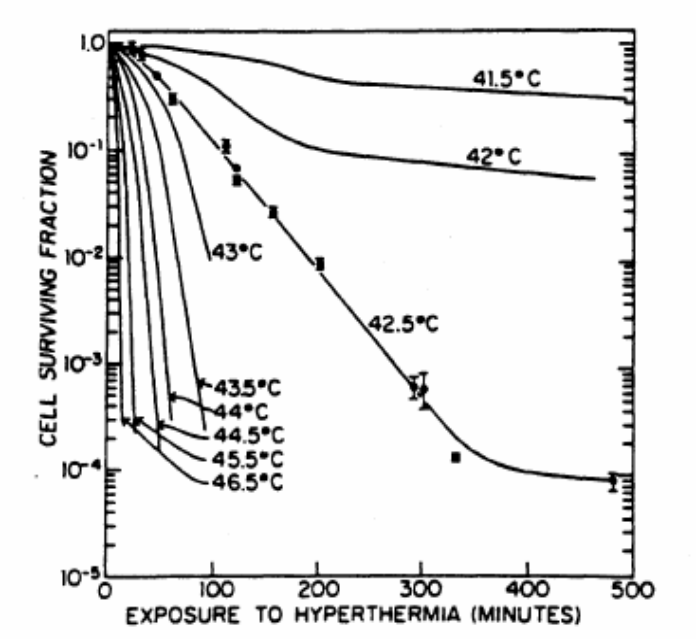

Figure 3.2 Cell survival curves (Dewey et al., 1977).

Heat is applied by increasing temperature in tissue. There are different heating techniques to achieve this. These are such as ultra sound, hot water tubes, ferromagnetic seeds and electromagnetic radiation (Yang et al., 2005). Infrared radiation can be used to heat the whole body. More deeply located tumours can be treated by applying radiation in the radiofrequency range. Small and easily accessible tumours can be heated by inserting electrodes into the tumor. These electrodes behave as small antennas.

Electromagnetic or ultrasound energy is directed at the treatment volume. The energy distribution in the tissues strongly depends on tissue characteristics and is thereby inhomogeneous. The heated part depends on the physical characteristics of the energy source and on the type of applicator. The temperature distribution is not simply a result of the energy distribution. But it also depends on thermal tissue characteristics and blood flow.

The systemic temperature of human body is 37.5ºC. To reach temperatures clearly above this temperature in a defined target volume is a technical challenge and still under development. The temperature increase is induced by applying a power-density specific absorption rate (SAR; measured in W/kg) (Wust et al., 2002). Human basal metabolic

rate (basal metabolism) is above 1 W/kg. Perfusion is against the temperature rise. It counteracts it. Perfusion rates in human tumours are around 515 mL per 100 g per min, but they vary widely. To reach therapeutic temperatures of about 42 ºC at least in some parts of such tumours necessitates power density of about 20-40 W/kg at the target region.

The convenient temperature distribution for clinical purposes is still unknown. The achieved temperature distributions have limited absolute values (minimum temperatures typically lie between 39.5 ºC and 40.5 ºC). Its reason is physical and physiological characteristics such as electrical tissue boundaries, local perfusion variations, and perfusion regulations. Only about 50 % of deeply located tumours reach at least 42ºC at one particular measurement point.

The temperature distributions should be achieved as high and homogeneous as possible, although the tumour temperatures for clinical efficacy are still unclear. Monitoring and control of temperature distribution has not yet been intensively scrutinized.

3.2 TREATMENT PLANNING OF HYPERTHERMIA

If it is accepted that hyperthermia may be a useful therapeutic modality for cancer, then there is still the question of how hyperthermia should be applied clinically. Hyperthermia treatment planning is needed to design, control, document and evaluate a treatment and thus to provide the data for treatment optimization and to provide the insight to design better heating equipment. The subject of this section, treatment planning for hypertyhermia, may be resolved into three components which are introduced below.

3.2.1 Specific Absorption Rate (SAR) and its Distribution

In this part, the rate of energy absorption per unit mass is determined. Two or three dimension modelling is under specified conditions in standard phantoms or in a patient from a given treatment machine.

The heating technique is characterized under the specific conditions by the collected data during this procedure. And general identification of those sites and target volumes is allowed by this (Dunscombe et al., 1989). In addition, one group of input parameters, which is essential for the calculation of the temperature distribution, is formed by the distribution of the Specific Absorption Rate (SAR).

The objective of fulfilling Specific Absorption Rate (SAR) measurements is to describe the energy delivery equipment by determining the pattern of energy deposition.

3.2.3 Temperature and its Distribution

In a patient throughout the course of a clinical treatment, the distribution of temperature is determined in two or three dimensions. The temperature data accumulated during the clinical treatment constitute the most precious record of that treatment and are the ultimate source of data characterizing the heating session. In practice, and with currently available invasive thermometry, complete temperature distributions in vivo cannot be determined (Dunscombe et al., 1989). The state of the art is presently limited to recommending minimum procedures which could probably indicate when an appropriate hyperthermic treatment had been delivered. It remains a topic of considerable research interest to devise methods of deducing complete temperature distributions from the limited measurements possible in the clinic.

3.2.3 Treatment Planning

The selection of the optimal treatment technique is called as treatment planning. Treatment planning is fraught with difficulty. The content of available treatment machines and on the computation of the expected three dimensional temperature distribution in a patient (Dunscombe et al., 1989).

3.3 HYPERTHERMIA APPLICATION METHODS

Several methods of hyperthermia are currently under study. But three methods can be distinguished in the clinical application of hyperthermia. These are known as local, regional and whole body hyperthermia (Wust et al., 2002). In the sections that follow each of the these methods is discussed in some detail.

3.2.1 Local hyperthermia

Local hyperthermia is applied to heat a small area, such as a tumor. Different types of energy may be used to apply heat. These are including microwave, radiofrequency, and ultrasound (NCI Fact Sheet 7.3, 2004). Heating of small volumes of tumors usually up to 50 cm^2 in area and up to 4 cm in depth located near the surface of the body can be achieved quite easily today. The clinical experience is by Perez and Meyer with localized hyperthermia and irradiation. The majority of studies include the use of microwaves, usually at 915 MHz.

Antennas or applicators heat superficial tumours. Microwaves or radiowaves are placed on that surfaces with a contacting medium. Several types of applicators have been used clinically. These are waveguide applicators, horn, spiral, current sheet, and compact applicators, etc. (Wust et al., 2002). The main components of such a hyperthermia system are shown in Fig. 3.3. The electromagnetic coupling of the applicator to the tissue is made certain by using a water bolus. The output of the power generator controls intratumoral temperature.

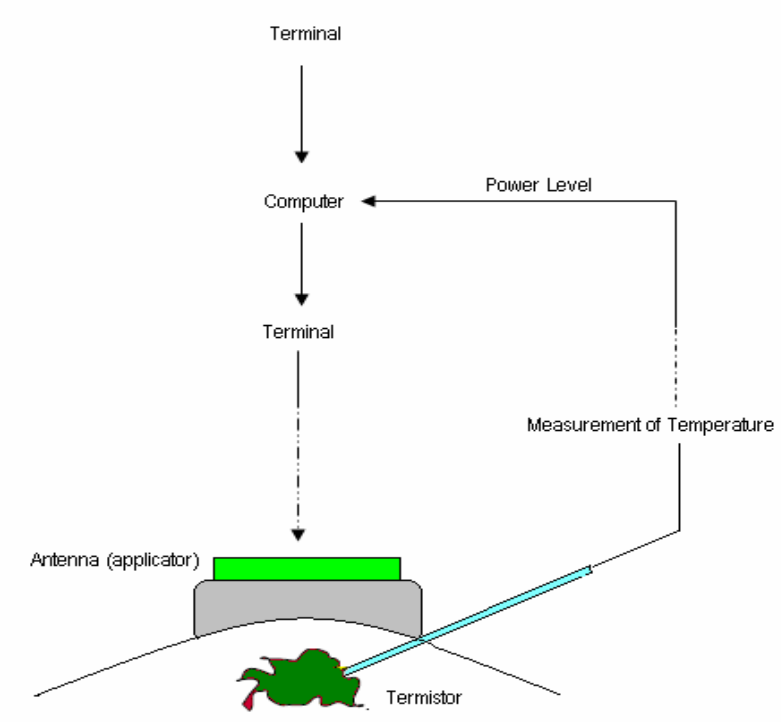

Figure 3.3 Scheme of a system for local hyperthermia (Wust et al., 2002).

The resulting SAR distribution is subject to strong physical curtailment resulting in a therapeutic depth of only a few centimetres and is even further limited in regions with an irregular surface, such as the head and neck area, the supraclavicular region, or the axilla. Quality-assurance guidelines have been developed for local hyperthermia. Commercially available electromagnetic applicators (Fig. 3.4) have a typical emitting diameter of 15 cm at a frequency of 150 - 430 MHz with therapeutic depths not more than 3 cm (Wust et al., 2002).

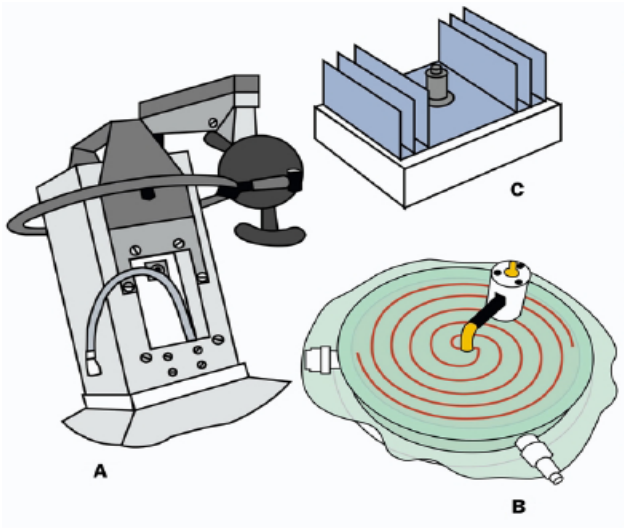

Figure 3.4 Applicator types for local hyperthermia, such as (a) waveguide applicator; (b) spiral applicator; and (c) current sheet applicator (Wust et al., 2002).

There are several approaches to local hyperthermia. They depend on the tumor location, Local hyperthermia can be applied by external, intraluminal or interstitial methods (Yang et al., 2005), (NCI Fact Sheet 7.3, 2004).

Some tumors are in or just below the skin. External approaches are used to treat them. External applicators are positioned around or near the suitable region. And the tumor is exposed to energy to raise its temperature. Deep tumors within the body can be treated by using interstitial techniques, such as brain tumors. This technique is more useful than external techniques to heat tumor at high temperatures. To do this, probes or needles are used in the tumor. The probe should be properly positioned within the tumor. Imaging techniques, such as ultrasound, may be used to control it.

Local hyperthermia causes to increase the systemic temperature and absolute temperature (Yang et al., 2005). The absolute temperature increase depends on both the

treatment volume to which energy is applied and the measures taken to help the patient lose energy. During hyperthermia, the tumor temperatures are increased as high as possible. And these high rates are applied as long as the tolerance limits of the surrounding normal tissues are not exceeded.

3.3.2 Regional hyperthermia

Regional hyperthermia is a rather recent promising modality of cancer therapy based on the local heating of tumor tissue to about 44 ºC usually applied in combination with radiotherapy or chemotherapy. The aim is to optimize the generated temperature distribution within the patient's body such that essentially the tumor is heated, but preferably not any sane tissue (Deufhard et al.,1997) (Strohbehn and Douple, 1984). For this reason, patient-specific treatment planning is necessary, which involves the segmentation of medical image data, the generation of geometrical patient models, and the solution of partial differential equations.

Regional hyperthermia can be applied by Deep tissue. Deep-seated tumours - eg, of the pelvis or abdomen - can be heated by arrays of antennas (Yang et al., 2005). To heat deep-seated tumors noninvasively is difficult. RF energy can be deposited into the center of the body but a large region is affected (Chou, 1988). Differential increases of blood flow in the normal and tumor tissues may result in higher temperature in tumors than normal organs. However, this temperature differential cannot be assured.

The concept behind regional hyperthermia is based on the fact that it is difficult to precisely define a tumor margin, and that the tumor may be disseminated throughout normal tissue in given region (Strohbehn and Douple, 1984). Therefore, it is reasonable to try to heat a substantial region surrounding the known tumor volume.

The Sigma-60 applicator is a widely spread applicator (shown in Fig. 3.5), which consists of four dipole antenna pairs arranged in a ring around the patient (Wust et al., 2002). Dipole antennas are schematically shown in Fig. 3.5a. These external applicators are positioned around the body cavity or organ to be treated, and microwave or radiofrequency energy is focused on the area to raise its temperature. Each antenna pair can be controlled in phase and amplitude, there are restrictions in terms of the generated SAR distribution.

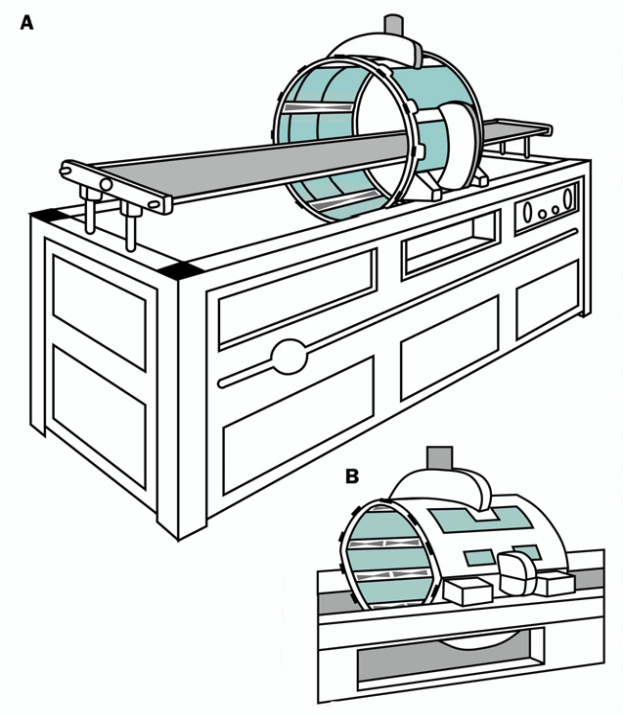

Figure 3.5 (a) Sigma-60 applicators (four dipole pairs) with treatment couch of the BSD-2000 system for regional hyperthermia. (b) A novel multiantenna applicator Sigma-Eye (12 dipole pairs) mounted on the same treatment unit as shown in (a) **(**Wust et al., 2002).

The major problem when using external methods such as electromagnetic applicators is that the designer only has control over the energy radiated into the tissue (Strohbehn and Douple, 1984). However, the actual temperature distribution is a function of the absorption properties of anatomical structures, thermal conductivity, and blood flow.

Regional hyperthermia is applied by perfusion of a limb, organ or body cavity with heated fluids. Deep tissue approaches may be used to treat cancers within the body, such as cervical or bladder cancer. Regional perfusion techniques can be used to treat cancers in the arms and legs, such as melanoma, or cancer in some organs, such as the liver or lung. In this procedure, some of the patient's blood is removed, heated, and then pumped (perfused) back into the limb or organ. Anticancer drugs are commonly given during this treatment.

3.3.3 Whole-body hyperthermia

The main expression for whole body hyperthermia is that cancer is a systemic disease and that cancer cells have in many cases metastasized throughout the body (NCI Fact Sheet 7.3, 2004) (Strohbehn and Douple, 1984). Whole body hyperthermia is one of the most efficient possibilities to treat systemic malignant diseases (Babincová et al., 1999).

For whole-body hyperthermia, several methods have been used. In whole-body hyperthermia, energy is supplied into the body, while at the same time energy losses are minimized (Yang et al, 2005).

In recent years, only radiant systems are in clinical use, with typical preheating times of 60-90 min (from 37.5°C upwards). The Aquatherm system (Fig. 3.6) is an isolated moisture-saturated chamber equipped with waterstreamed tubes (50 - 60 °C) on the inner sides, in which the patient is positioned. Long-wavelength infrared waves are emitted. A substantial increase in the skin blood circulation is induced (subcutaneous venous plexus), and energy absorbed superficially is transported into the systemic circulation. Since energy release through perspiration is blocked, the heating time is quite short (60-90 min).

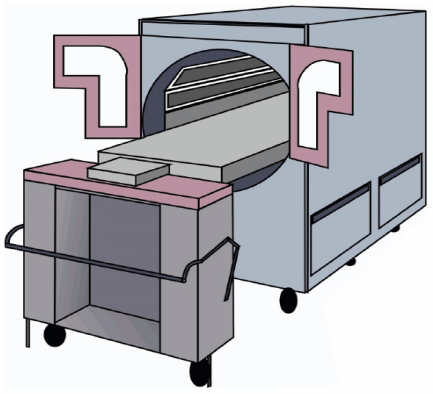

Figure 3.6 Schematic drawing of the Aquatherm system for whole-body hyperthermia (Wust et al., 2002).

The patient is positioned in a moisture-saturated cabin with hot water tubes (60ºC) inside. After a systemic temperature of 41.8 ºC has been achieved, the patient is thermally isolated with blankets.

Figure 3.7 Schematic drawing of the Iratherm system for whole-body hyperthermia (Wust et al., 2002).

The Iratherm-2000 system (Fig. 3.7) uses special water-filtered infrared radiators, resulting in an infrared spectrum with a maximum near to visible light. The penetration depth in this frequency range is slightly higher (about 2 mm), but every system for whole-body hyperthermia can cause superficial overheating, resulting in thermal lesions. Water-filtered infrared radiators emit their energy from top and bottom. Thermal isolation is ensured by various transport foils. After a systemic temperature of 41.8 - 42.0 ºC has been achieved, power is reduced and a steady state is adjusted.

CHAPTER 4

NUMERICAL RESULTS AND THEIR INTERPRETATIONS

4.1. INTRODUCTION

As mentioned in the previous chapter, the basic objective of hyperthermia is to raise the temperature in the tumor volume above the treatment temperature without overheating area, and to avoid damaging the surrounding healty tissue. To achieve this process, the calculation of electromagnetic fields in the tumor volume or cancerous cells and the analysis of temperature distribution in that area are needed.

This chapter presents the main study of this thesis. In this chapter, the hyperthermia application is studied in three main approaches. First, a methodology is constituted for hypethermia technique. This means that the required system for patient-specific modelling has to be obtained before the treatment. After the system which is the best for the patient is determined, the electromagnetic field distribution is obtained. The Finite Difference Time Domain (FDTD) method is used to calculate the electromagnetic field distribution throughout the tissues. And finally, the temperature distribution is observed. The bioheat equation has to be solved to calculate the temperature increase in the tumor tissue. Finite Difference Method (FDM) is used to realize this process. The numerical results and simulations of all these applied methods are covered and discussed in the following sections.

4.2. THE FORMATION OF TREATMENT PLANNING SYSTEM

Before the treatment begins, a treatment planning system needs to be illustrated to follow as a treatment plan of electromagnetic hyperthermia. A simple treatment which is formed for this study is shown in Fig. 4.1 as a block diagram.

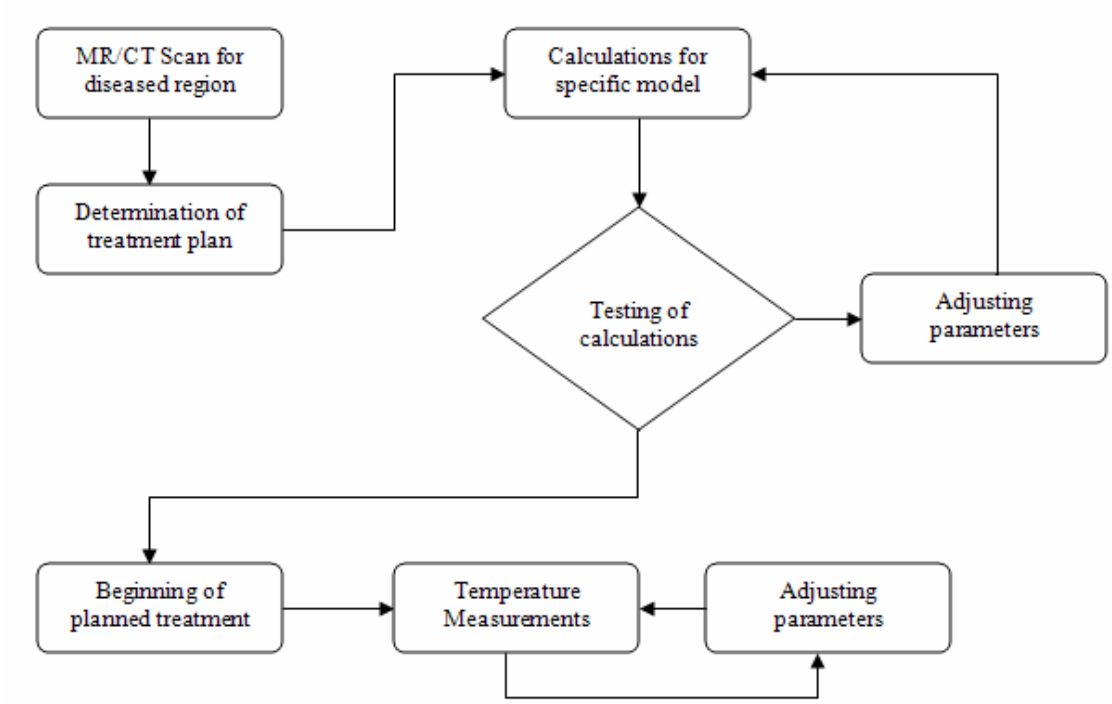

Figure 4.1 Block Diagram for Hyperthermia Treatment Plan.

The mathematical model of the patient is first generated. This is accomplished by generating (MRI) or X-ray CT images of the patient. The next step is to define a treatment plan. The required calculations are computed according to illustrated mathematical model. In the next step, these calculations are controlled and compared with theoretical ones. If they are convenient, then we can pass onto the next step. This step is the beginning of our treatment plan. The next step includes the temperature measurements due to adjusted parameters. Measurements of the temperature field are periodically made and the performance of the system is evaluated. If results are not required, the control algorithm decides automatically what changes are needed to the input parameters and implements them.

4.3. THE FDTD ANALYSIS IN HYPERTHERMIA SYSTEM

The Finite-Difference Time-Domain (FDTD) method provides a direct time-domain solution of Maxwell's equations in differential form by discretizing both the physical region and time interval using a uniform grid. The FDTD method is a powerful computational electromagnetic technique for modelling the electromagnetic space. It is very successfully and widely used to the modeling of electromagnetic phenomena.

In the following sections, firstly Maxwell's equations and Yee's FDTD algorithm will be introduced. Secondly, Implementation of one dimensional and two dimensional FDTD methods, which we have applied, will be reported with all calculations and simulations.

4.3.1 Maxwell's Equations and Yee's Algorithm for FDTD

The simulation of electromagnetic waves generated by an electromagnetic source is discussed. The equations for these waves are given by the time-dependent Maxwell's equations in free space.

The time-dependent Maxwell's curl equations in free space are

$$\frac{\partial \mathbf{E}}{\partial t} = \frac{1}{\varepsilon_0} \nabla \times \mathbf{H} \tag{4.3.1}$$

$$\frac{\partial \mathbf{H}}{\partial t} = -\frac{1}{\mu_0} \nabla \times \mathbf{E} \tag{4.3.2}$$

Both **E** and **H** are vectors in three dimensions which represent the electric field and magnetic field respectively.

Maxwell's equations are discretized using a Yee cell (Yee, 1966). The basic idea of Yee's algorithm is to discretize both the physical region and the time interval of the differential form of three dimensional Maxwell's equations. Then the space and time models are established so the algorithm can update electromagnetic field values time step by time step from two parts: Field values calculated in previous time steps and field values in the adjacent space cells. The geometrical representation of Yee Cell in three dimensions is depicted in Fig. 4.2. This model made it possible for the utilization of

modern computation resources on Maxwell's equations, and created a new area of electromagnetic scientific research.

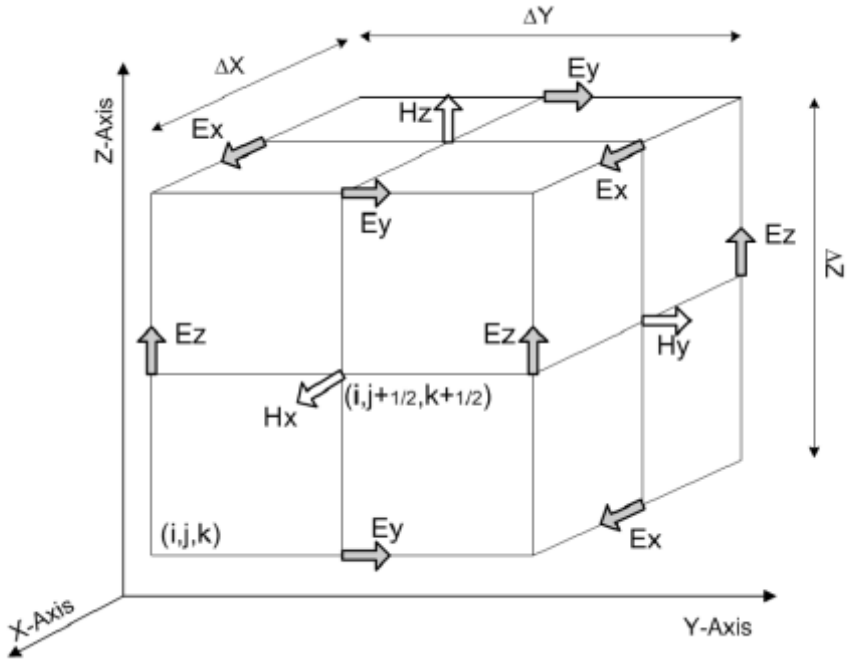

Figure 4.2 The geometrical representation of Yee Cell in three dimensions.

Δx, Δy, Δz are the three dimensions of this cube. We use (i; j; k) to denote the point whose real coordinate is $(i\Delta x, j\Delta y, k\Delta z)$ in the model space. Instead of placing **E** and **H** components in the center of each cell, **E** and **H** field components here are interlaced so that every **E** component is surrounded by four circulating **H** components, and every **H** components is surrounded by four circulating **E** components.

4.3.2 One-Dimensional FDTD Analysis in Free Space

To gain insight into the algorithm, we start by reducing Maxwell's equations to one dimension. First, we can write equations (4.3.1) and (4.3.2) in vector form. The vector differential operator, “del” or “nabla”, is defined

$$\nabla = \mathrm{i}\frac{\partial}{\partial x} + \mathrm{j}\frac{\partial}{\partial y} + \mathrm{k}\frac{\partial}{\partial z} \tag{4.3.3}$$

We start to analyze the electromagnetic field calculations of hyperthermia with one dimensional FDTD approach. If we assume that the propagation of the wave is in *z*-direction then we have only E_x and H_y components for the electric and magnetic field in one dimensional simulation.

Let $\mathbf{E} = (E_X, E_y, E_Z)$. The cross product of ∇ and **E** is given by

$$\nabla \times \mathbf{E} = \begin{vmatrix} \mathrm{i} & \mathrm{j} & \mathrm{k} \\ \frac{\partial}{\partial x} & \frac{\partial}{\partial y} & \frac{\partial}{\partial z} \\ E_X & E_y & E_Z \end{vmatrix} \tag{4.3.4}$$

Using the above expressions we rewrite

$$\begin{pmatrix} \frac{\partial E_X}{\partial t} \\ \frac{\partial E_y}{\partial t} \\ \frac{\partial E_Z}{\partial t} \end{pmatrix} = \frac{1}{\varepsilon_0} \begin{vmatrix} \mathrm{i} & \mathrm{j} & \mathrm{k} \\ \frac{\partial}{\partial x} & \frac{\partial}{\partial y} & \frac{\partial}{\partial z} \\ H_X & H_y & H_Z \end{vmatrix} = \frac{1}{\varepsilon_0} \begin{bmatrix} \frac{\partial H_Z}{\partial y} - \frac{\partial H_y}{\partial z} \\ \frac{\partial H_X}{\partial z} - \frac{\partial H_Z}{\partial x} \\ \frac{\partial H_y}{\partial x} - \frac{\partial H_X}{\partial y} \end{bmatrix} \tag{4.3.5}$$

$$\begin{pmatrix} \frac{\partial H_X}{\partial t} \\ \frac{\partial H_y}{\partial t} \\ \frac{\partial H_Z}{\partial t} \end{pmatrix} = \frac{1}{\mu_0} \begin{vmatrix} \mathrm{i} & \mathrm{j} & \mathrm{k} \\ \frac{\partial}{\partial x} & \frac{\partial}{\partial y} & \frac{\partial}{\partial z} \\ E_X & E_y & E_Z \end{vmatrix} = \frac{1}{\mu_0} \begin{bmatrix} \frac{\partial E_Z}{\partial y} - \frac{\partial E_y}{\partial z} \\ \frac{\partial E_X}{\partial z} - \frac{\partial E_Z}{\partial x} \\ \frac{\partial E_y}{\partial x} - \frac{\partial E_X}{\partial y} \end{bmatrix} \tag{4.3.6}$$

To continue our simplification to the one-dimensional problem we must make the assumption that the electric field oscillates only in the xz plane and that it travels in the z direction. Then $E_y = 0$. Since electromagnetic waves are transverse waves, they oscillate perpendicularly to the direction of propagation z: Thus $E_z = H_z = 0$; and hence $\mathbf{E} = (E_X, 0, 0)$.

We also know that the electric field and magnetic field travel perpendicular to one another. Thus their dot product must be zero, or

$$\mathbf{E}\cdot\mathbf{H} = (E_x,0,0)\cdot(H_x,H_y,0) = E_xH_x = 0 \tag{4.3.7}$$

Knowing that $E_x \neq 0$ and using the zero factor property we see that $H_y = 0$. Thus, since $H_z = 0$; we see that $\mathrm{H} = (0,H_y,0)$. Hence equations become

$$\begin{pmatrix} \dfrac{\partial E_x}{\partial t} \\ 0 \\ 0 \end{pmatrix} = \frac{1}{\varepsilon_0}\begin{bmatrix} \dfrac{\partial H_y}{\partial z} \\ 0 \\ 0 \end{bmatrix} \tag{4.3.8}$$

$$\begin{pmatrix} 0 \\ \dfrac{\partial H_y}{\partial t} \\ 0 \end{pmatrix} = -\frac{1}{\mu_0}\begin{bmatrix} 0 \\ \dfrac{\partial E_x}{\partial z} \\ 0 \end{bmatrix} \tag{4.3.9}$$

or equvalently,

$$\frac{\partial E_x}{\partial t} = -\frac{1}{\varepsilon_0}\frac{\partial H_y}{\partial z} \tag{4.3.10}$$

$$\frac{\partial H_y}{\partial t} = -\frac{1}{\mu_0}\frac{\partial E_x}{\partial z} \tag{4.3.11}$$

In these equations, the electric field is directed in the x direction, the magnetic field is directed in the y direction, and they are traveling in the z direction.

Taking the central difference approximations for both the temporal and spatial derivatives gives

$$\frac{E_x^{n+1/2}(k) - E_x^{n-1/2}(k)}{\Delta t} = -\frac{1}{\varepsilon_0}\frac{H_y^n(k+1/2) - H_y^n(k+1/2)}{\Delta x} \tag{4.3.12}$$

$$\frac{H_y^{n+1}(k+1/2) - H_y^n(k+1/2)}{\Delta t} = -\frac{1}{\mu_0}\frac{E_x^{n+1/2}(k+1) - E_x^{n+1/2}(k)}{\Delta x} \tag{4.3.13}$$

In these two equations, time is specified by the superscripts, $t = \Delta t \cdot n$. The term "$n+1$" means one time step later. The terms in parentheses represent distance, "k" means the distance $z = \Delta x \cdot k$.

$$E_x^{n+1/2}(k) = E_x^{n-1/2}(k) - \frac{\Delta t}{\varepsilon_0 \Delta x}\left[H_y^n(k+1/2) - H_y^n(k-1/2) \right] \tag{4.3.14}$$

$$H_y^{n+1}(k+1/2) = H_y^n(k+1/2) - \frac{\Delta t}{\mu_0 \Delta x}\left[E_x^{n+1/2}(k+1) - E_x^{n+1/2}(k) \right] \tag{4.3.15}$$

Since ε_0 and μ_0 differ by several orders of magnitude we normalize the field values by introducing

$$\widetilde{E} = \sqrt{\frac{\varepsilon_0}{\mu_0}} E \tag{4.3.16}$$

Substituting this into Eqs. (4.3.14) and (4.3.16) gives

$$\widetilde{E}_x^{n+1/2}(k) = \widetilde{E}_x^{n-1/2}(k) - \frac{1}{\sqrt{\varepsilon_0 \mu_0}} \frac{\Delta t}{\Delta x}\left[H_y^n(k+1/2) - H_y^n(k-1/2) \right] \tag{4.3.17}$$

$$H_y^{n+1}(k+1/2) = H_y^n(k+1/2) - \frac{1}{\sqrt{\varepsilon_0 \mu_0}} \frac{\Delta t}{\Delta x}\left[\widetilde{E}_x^{n+1/2}(k+1) - \widetilde{E}_x^{n+1/2}(k) \right]. \tag{4.3.18}$$

The cell size Δx is chosen, and then the time step Δt is determined by

$$\Delta t = \frac{\Delta x}{2 c_0}, \tag{4.3.19}$$

where c_0 is the speed of the light in free space. Therefore,

$$\frac{1}{\sqrt{\varepsilon_0 \mu_0}} \frac{\Delta t}{\Delta x} = c_0 \frac{\Delta x/(2c_0)}{\Delta x} = \frac{1}{2} \tag{4.3.20}$$

For different time steps, free space FDTD simulations are shown in Fig. 4.3. Gaussian pulse is used to generate source. The pulse is originated in the center of FDTD

medium. As we see, the pulse is spreading outward to the limits. And the E_x field has always positive amplitude in both directions.

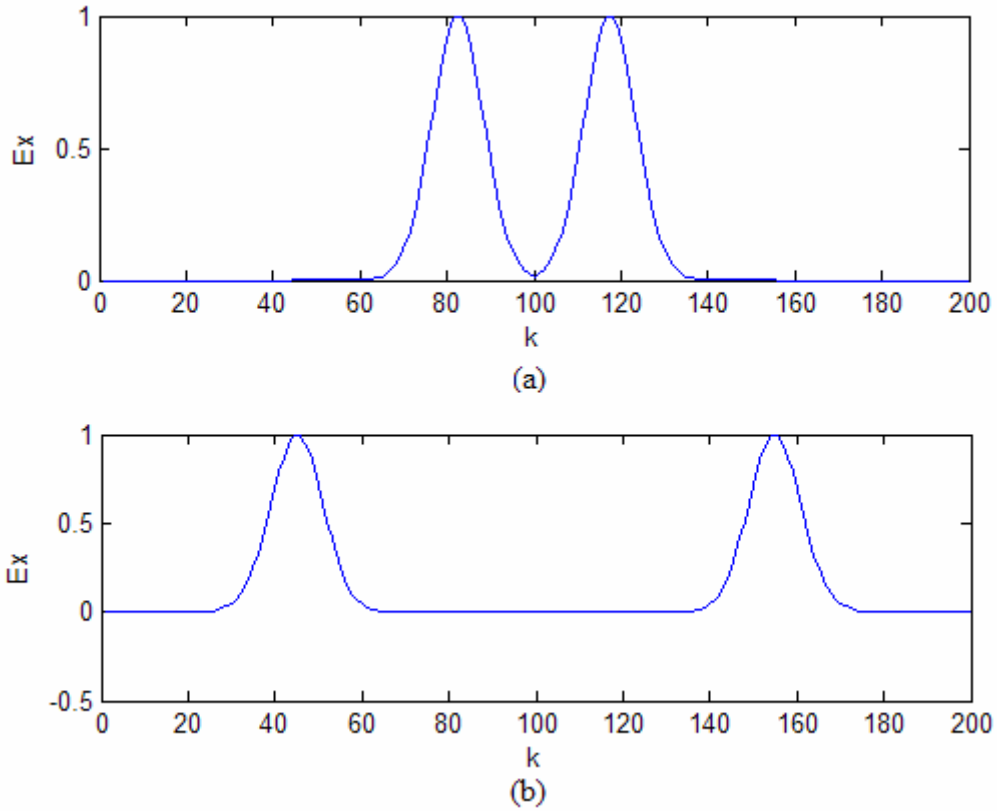

Figure 4.3 FDTD Simulation in free space after (a) 75 time steps and (b) 150 time steps with Gaussian pulse. The pulse is placed in the center of medium.

4.3.3 Stability Condition and the Absorbing Boundary Conditions

The determination of the time step is an important issue. The electromagnetic waves propagate in free space with the speed of light c_0 and in dielectrics it propagates slower than c_0 depending on the dielectric properties. So in free space to propagate a distance of one cell requires a minimum time of $\Delta t = \Delta x / c_0$. When we go to the two-dimensional computation the wave will also propagate in the diagonal direction, which brings the time requirement to $\Delta t = \Delta x / \sqrt{2} c_0$. Obviously, three-dimensional simulation requires $\Delta t = \Delta x / \sqrt{3} c_0$. This condition is know as the 'Courant Condition' (Sullivan, 1996). For the stability of the compuational schem we will use

$$\Delta t = \frac{\Delta x}{2c_0} \tag{4.3.21}$$

In FDTD modeling the boundary of the created computational space can reflect the fields back into our computational space. It will then be very hard to distinguish which fields are the real fields. To avoid that problem all the fields at the boundary of the problem space must be absorbed. Absorbing Boundary Conditions (ABC) are used to keep outgoing **E** and **H** fields without reflection.

In Fig. 4.4, FDTD simulation is generated for different time steps with absorbing boundary conditions. Again the pulse is placed at the center in this simultion. Gaussian pulse is generated in the center and goes outward. And notice that the pulse is absorbed at the limits of medium. At more than 250 time steps, the pulse will be completely absorbed.

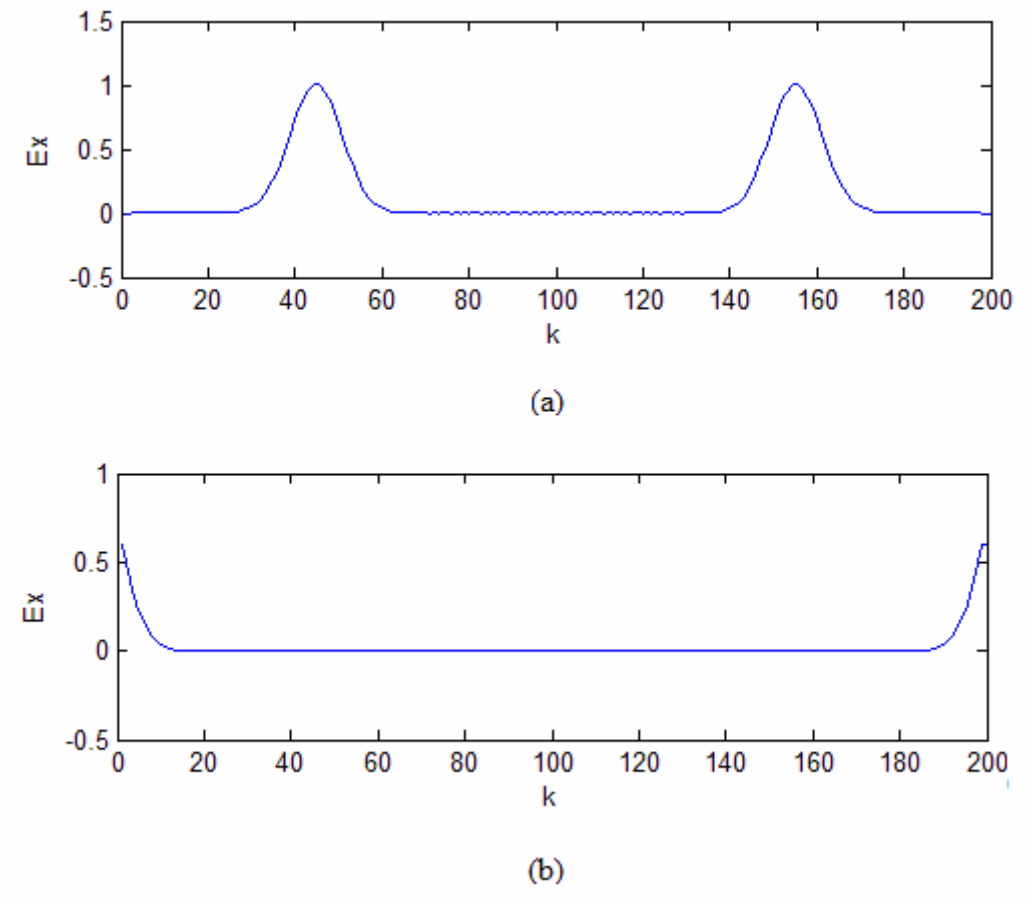

Figure 4.4 FDTD simulations with absorbing boundary conditions for (a) 150 time steps and (b) 250 time steps.

In FDTD calculation scheme to calculate the **E** field, we need to know the surrounding **H** values. At the boundary of the problem space we do not have the value behind boundary. Since we do not have other sources outside the problem space the fields at the edge must be propagated outward. So if a wave is traveling toward a boundary in free space with the speed of light c_0, in one time step of the FDTD algorithm, it travels

$$\text{distance} = \mathrm{c}_0 \Delta t = \mathrm{c}_0 (\frac{\Delta x}{2\mathrm{c}_0}) = \Delta x/2 . \tag{4.3.22}$$

That means it takes two time steps for a wave front to cross one cell. So the boundary condition might be

$$E_x^n(0) = E_x^{n-2}(1) . \tag{4.3.23}$$

4.3.4 One-Dimensional FDTD Analysis in a Dielectric Medium

In dielectric medium, we have to add the relative dielectric constant ε_r to Maxwell's equations.

$$\frac{\partial \mathbf{E}}{\partial t} = \frac{1}{\varepsilon_r \varepsilon_0} \nabla \times \mathbf{H} \tag{4.3.24}$$

$$\frac{\partial \mathbf{H}}{\partial t} = -\frac{1}{\mu_0} \nabla \times \mathbf{E} \tag{4.3.25}$$

As the same approach in Eq. (4.3.16), some changes are made;

$$\frac{\partial E_x(t)}{\partial t} = \frac{1}{\varepsilon_r \sqrt{\varepsilon_0 \mu_0}} \frac{\partial H_y(t)}{\partial z} \tag{4.3.26}$$

$$\frac{\partial H_y(t)}{\partial t} = -\frac{1}{\sqrt{\varepsilon_0 \mu_0}} \frac{\partial E_x(t)}{\partial z} \tag{4.3.27}$$

and finite difference approximations applied;

$$E_x^{n+1/2}(k) = E_x^{n-1/2}(k) + \frac{1}{\sqrt{\varepsilon_0 \mu_0}} \frac{\Delta t}{\Delta x}\left[H_y^n(k+1/2) - H_y^n(k-1/2) \right] \tag{4.3.28}$$

$$H_y^{n+1}(k+1/2) = H_y^n(k+1/2) + \frac{1}{\sqrt{\varepsilon_0 \mu_0}} \frac{\Delta t}{\Delta x}\left[E_x^{n+1/2}(k+1) - E_x^{n+1/2}(k) \right], \tag{4.3.29}$$

by using the Eq.(4.3.20) into these formulas, thus equations become

$$E_x^{n+1/2}(k) = E_x^{n-1/2}(k) + 0.5\left[H_y^n(k+1/2) - H_y^n(k-1/2) \right] \tag{4.3.30}$$

$$H_y^{n+1}(k+1/2) = H_y^n(k+1/2) + 0.5\left[E_x^{n+1/2}(k+1) - E_x^{n+1/2}(k) \right] \tag{4.3.31}$$

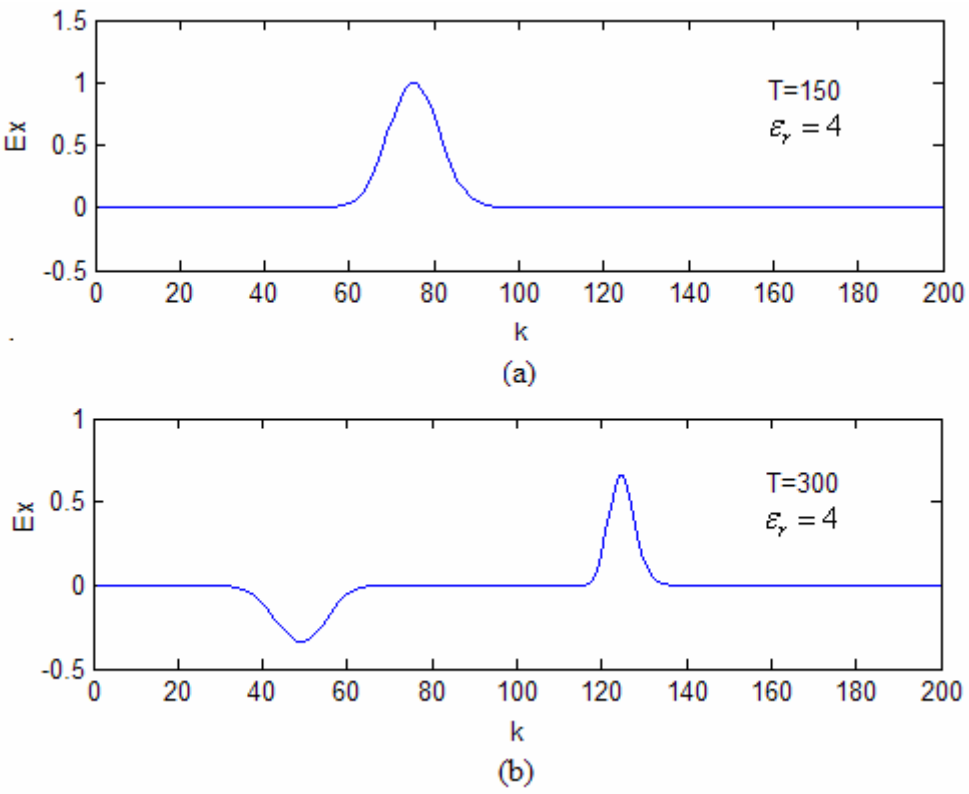

Figure 4.5 FDTD simulations in a dielectric medium for (a) 150 time steps (b) 200 time steps.

Fig. 4.5 presents the simulation of electromagnetic field distribution in a dielectric medium with dielectric constant $\varepsilon_r = 4$. Gaussian pulse is used as source. The pulse is given at the twentieth cell.

4.3.5 One-Dimensional FDTD Analysis in a Lossy Dielectric Medium

In this thesis we want to model human tissues which are lossy dielectric mediums. Maxwell's curl equations

$$\varepsilon \frac{\partial \mathbf{E}}{\partial t} = \nabla \times \mathbf{H} - \mathbf{J} \tag{4.3.32}$$

$$\frac{\partial \mathbf{H}}{\partial t} = -\frac{1}{\mu_0} \nabla \times \mathbf{E} \tag{4.3.33}$$

J is the current density, which is $\mathbf{J} = \sigma \mathbf{E}$.

When we apply the change of variable in Eq. (4.3.16), which yields

$$\frac{\partial E_x(t)}{\partial t} = -\frac{1}{\varepsilon_r \sqrt{\varepsilon_0 \mu_0}} \frac{\partial H_y(t)}{\partial z} - \frac{\sigma}{\varepsilon_r \varepsilon_0} E_x(t) \tag{4.3.34}$$

$$\frac{\partial H_y(t)}{\partial t} = -\frac{1}{\sqrt{\varepsilon_0 \mu_0}} \frac{\partial E_x(t)}{\partial z} \,. \tag{4.3.35}$$

When we take the finite difference approximations for both the temporal and spatial derivatives,

$$\begin{aligned} \frac{E_x^{n+1/2}(k) - E_x^{n-1/2}(k)}{\Delta t} = & -\frac{1}{\varepsilon_r \sqrt{\varepsilon_0 \mu_0}} \frac{H_y^n(k+1/2) - H_y^n(k-1/2)}{\Delta x} \\ & - \frac{\sigma}{\varepsilon_r \varepsilon_0} \frac{E_x^{n+1/2}(k) - E_x^{n-1/2}(k)}{2} \end{aligned} \tag{4.3.36}$$

by replacing the Eq. (4.3.20) into Eq.(4.3.33), Thus Eq. becomes,

$$\begin{aligned} E_x^{n+1/2}(k)\left[1 + \frac{\sigma \Delta t}{2\varepsilon_0 \varepsilon_r}\right] = & E_x^{n-1/2}(k)\left[1 - \frac{\sigma \Delta t}{2\varepsilon_0 \varepsilon_r}\right] \\ & - \frac{1/2}{\varepsilon_r}\left[H_y^n(k+1/2) - H_y^n(k-1/2)\right] \end{aligned} \tag{4.3.37}$$

or

$$E_x^{n+1/2}(k) = E_x^{n-1/2}(k) \frac{\left[1 - \frac{\sigma \Delta t}{2\varepsilon_0 \varepsilon_r}\right]}{\left[1 + \frac{\sigma \Delta t}{2\varepsilon_0 \varepsilon_r}\right]} - \left[H_y^n(k+1/2) - H_y^n(k-1/2)\right] \frac{1/2}{\varepsilon_r \left[1 + \frac{\Delta t \sigma}{2\varepsilon_r \varepsilon_0}\right]} \,. \tag{4.3.38}$$

Table 4.1 The dielectric properties of some body tissues at different frequencies.

Tissue name	at 700 MHz		at 900 MHz		at 1250 MHz		at 1500 MHz	
	σ[S/m]	ε_r	σ[S/m]	ε_r	σ[S/m]	ε_r	σ[S/m]	ε_r
Bladder	0.3584	19.149	0.3831	18.936	0.43419	18.667	0.4769	18.511
Blood	1.4559	62.103	1.5379	61.36	1.7076	60.448	1.8499	59.929
Fat	0.04659	5.4966	0.05104	5.462	0.06031	5.4136	0.06803	5.3833
Muscle	0.8789	55.587	0.94294	55.032	1.0761	54.35	1.1881	53.963
Prostate	1.1306	61.296	1.2096	60.553	1.3719	59.65	1.5074	59.143
Skin Dry	0.79996	42.698	0.86674	41.405	0.98369	40.057	1.0716	39.433
Skin Wet	0.77354	47.051	0.84465	46.08	0.98063	44.979	1.0889	44.412

The dielectric properties of some body tissues at different frequencies are shown in Table 4.1. First we simulate the one dimensional FDTD of a sinusoidal pulse at 1.5 GHz originates at cell number 20 and travels into the lossy dielectric which is human fat tissue at cell number 100 with $\varepsilon_r = 5.3833$ and $\sigma = 0.068028$. The simulation results for different time steps are shown in Fig. 4.6. As a second work, we applied a Gausian pulse for the same conditions and the same tissue properties. Since the characteristics impedance of the dielectric is lower than the free space a part of the incident wave reflect back and the remaining part continue with traveling in the lossy dielectric as can be seen in Fig. 4.7.

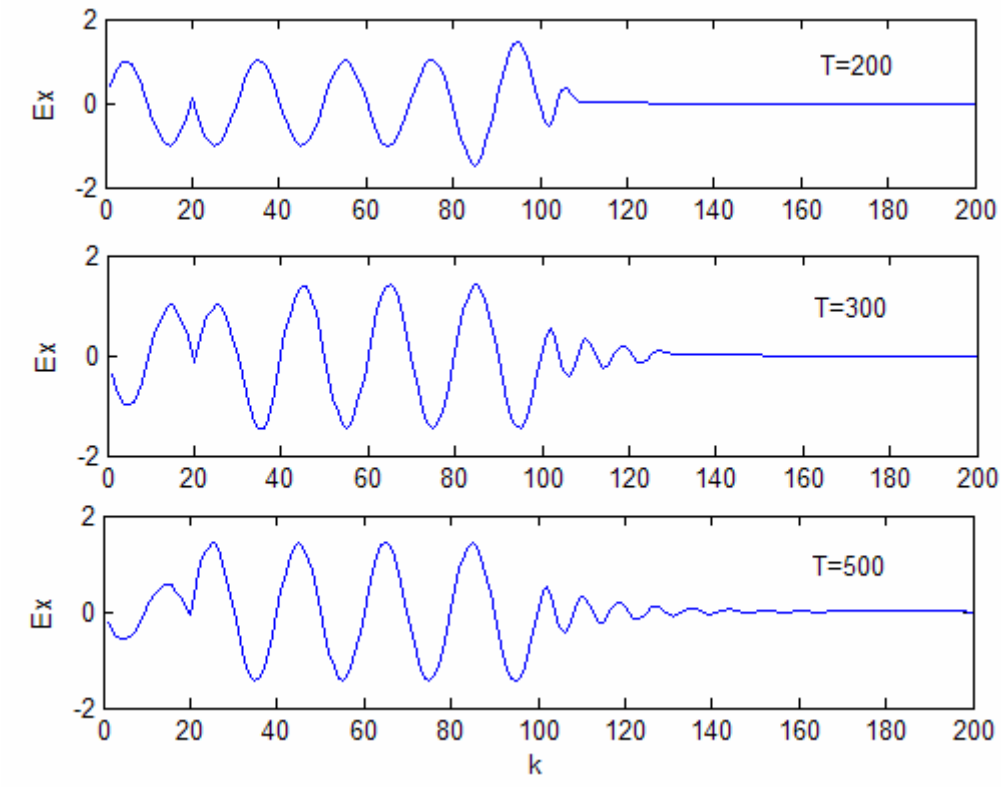

Figure 4.6 Simulations of sinusoidal wave of 1.5 GHz at different time steps for human fat tissue which starts at cell number 100 with $\varepsilon_r = 5.3833$ and $\sigma = 0.068028$.

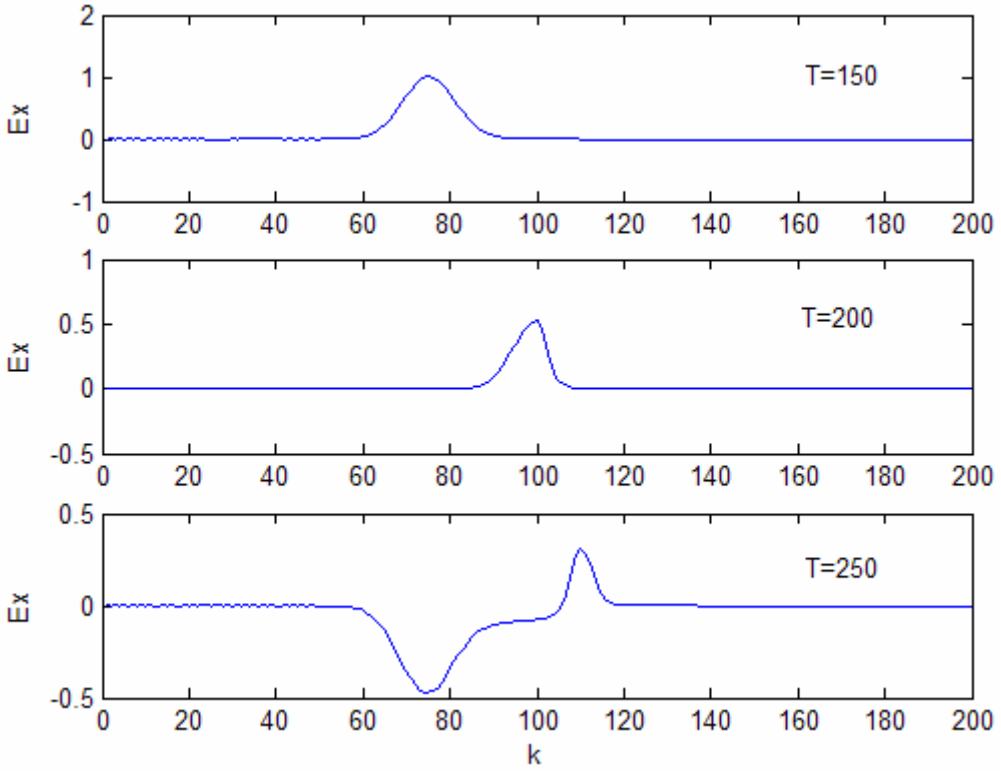

Figure 4.7 Simulations of Gaussian wave of 1.5 GHz at different time steps for human fat tissue which starts at cell number 100 with $\varepsilon_r = 5.3833$ and $\sigma = 0.068028$.

4.3.6 Two-Dimensional FDTD Analysis

In this section two dimensional FDTD simulation is presented. Firstly the basics of two dimensional FDTD formulations is described. The absorbing boundary conditions are described. And finally, two-dimensional FDTD is applied in hyperthermia conditions.

First examine the normalized Maxwell's equations

$$\frac{\partial \widetilde{\mathbf{D}}}{\partial t} = \frac{1}{\sqrt{\varepsilon_0 \mu_0}} \nabla \times \mathbf{H} \tag{4.3.39}$$

$$\widetilde{\mathbf{D}}(\omega) = \varepsilon_r^*(\omega)\, \widetilde{\mathbf{E}}(\omega) \tag{4.3.40}$$

$$\frac{\partial \mathbf{H}}{\partial t} = -\frac{1}{\sqrt{\varepsilon_0 \mu_0}} \nabla \times \widetilde{\mathbf{E}}\,. \tag{4.3.41}$$

in which $\varepsilon_r^*(\omega)$ is frequency depending relative permittivity for lossy medium.

In two-dimensional simulation, there are two groups for three vectors (x, y, z). One of them is the transverse magnetic (TM) mode, which is composed of $\widetilde{E}_z$, H_x and H_y. And the other one is transverse electric (TE) mode, which is composed of $\widetilde{E}x, \widetilde{E}y$ and H_z. Now we will investigate the TM mode. The normalized Maxwell's equations are reduced to

$$\frac{\partial D_z}{\partial t} = \frac{1}{\sqrt{\varepsilon_0 \mu_0}} \left(\frac{\partial H_y}{\partial x} - \frac{\partial H_x}{\partial y} \right) \tag{4.3.42}$$

$$D_z(\omega) = \varepsilon_r^*(\omega) E_z(\omega) \tag{4.3.43}$$

$$\frac{\partial H_x}{\partial t} = -\frac{1}{\sqrt{\varepsilon_0 \mu_0}} \frac{\partial E_z}{\partial y} \tag{4.3.44}$$

$$\frac{\partial H_y}{\partial t} = \frac{1}{\sqrt{\varepsilon_0 \mu_0}} \frac{\partial E_z}{\partial x}\,. \tag{4.3.45}$$

It is that there is a systematic interleaving of the fields to be calculated. This graphical representation is shown in Fig. 4.8.

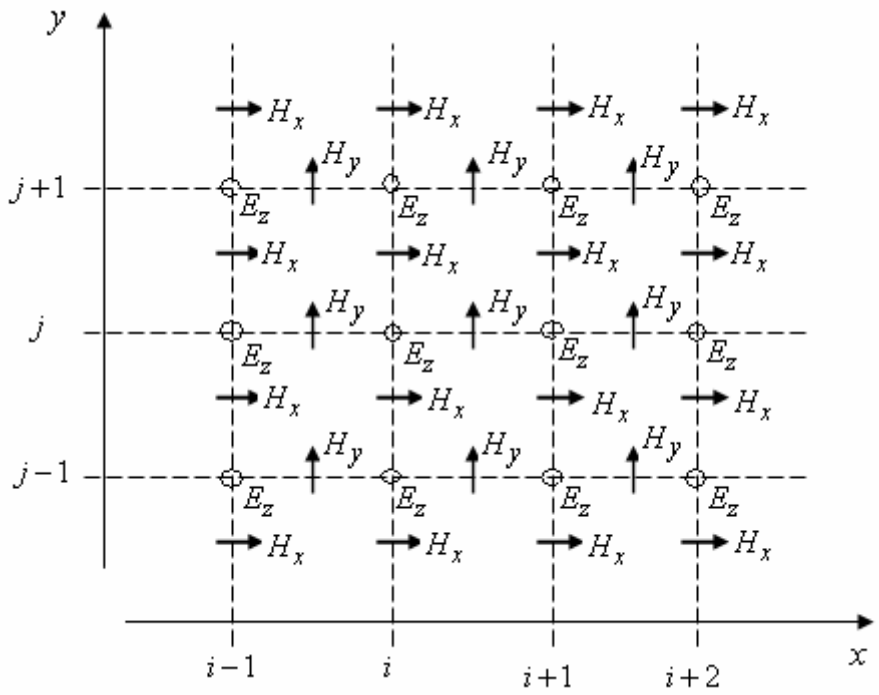

Figure 4.8 The graphical representation of the E and field in 2D TM formulation.

The reduced TM mode Maxwell's equations are added into the finite differencing scheme results in the following difference equations (Berenger, 1994):

$$\frac{D_z^{n+1/2}(i,j)-D_z^{n-1/2}(i,j)}{\Delta t}=\frac{1}{\sqrt{\varepsilon_0\mu_0}}\left(\frac{H_y^n(i+1/2,j)-H_y^n(i-1/2,j)}{\Delta x}\right)-\frac{1}{\sqrt{\varepsilon_0\mu_0}}\left(\frac{H_x^n(i,j+1/2)-H_x^n(i,j-1/2)}{\Delta x}\right) \tag{4.3.46}$$

$$\frac{H_x^{n+1}(i,j+1/2)-H_x^n(i,j+1/2)}{\Delta t}=-\frac{1}{\sqrt{\varepsilon_0\mu_0}}\left(\frac{E_z^{n+1/2}(i,j+1)-E_z^{n+1/2}(i,j)}{\Delta x}\right) \tag{4.3.47}$$

$$\frac{H_y^{n+1}(i+1/2,j)-H_y^n(i+1/2,j)}{\Delta t}=\frac{1}{\sqrt{\varepsilon_0\mu_0}}\left(\frac{E_z^{n+1/2}(i+1,j)-E_z^{n+1/2}(i+1,j)}{\Delta x}\right) \tag{4.3.48}$$

In Fig. 4.9, 4.10 and 4.11 we depicted the traveling of a Gaussian pulse initiated at the center of the problem space and travels outward.

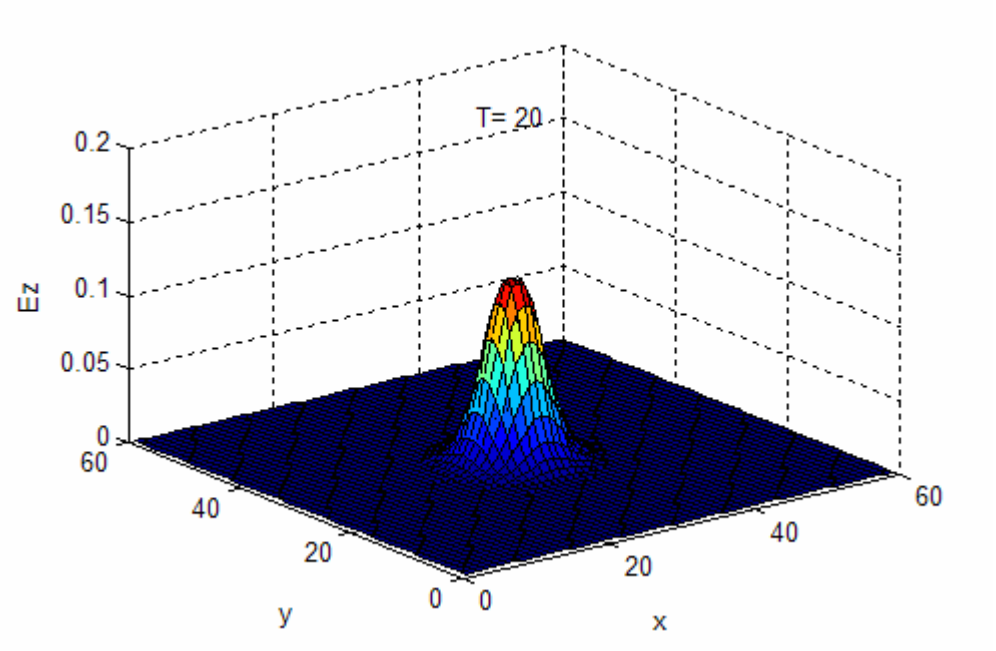

Figure 4.9 Simulation of a Gaussian pulse originates at the center of the problem space at T=20.

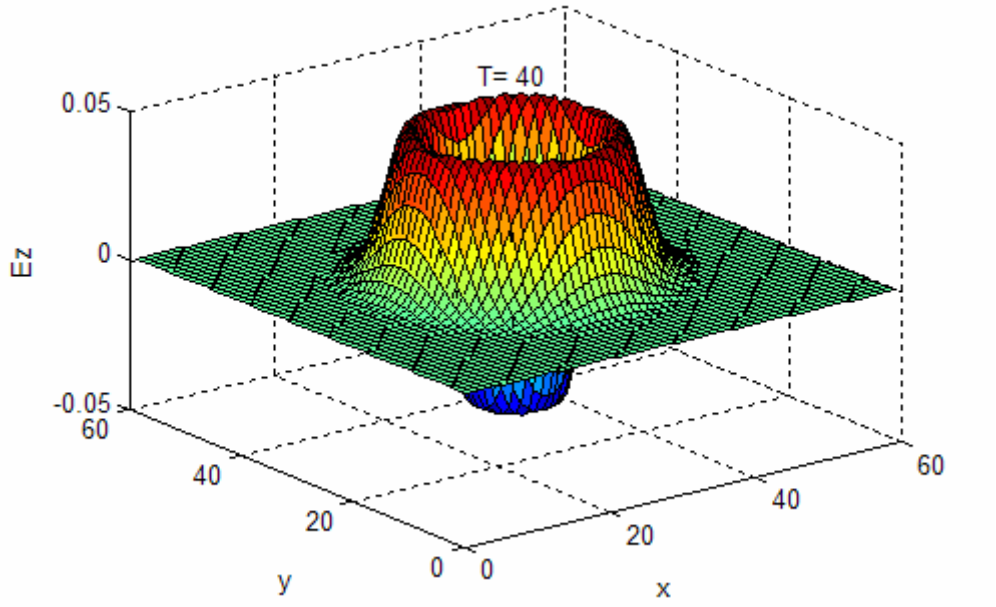

Figure 4.10 Simulation of a Gaussian pulse originates at the center of the problem space at T=40.

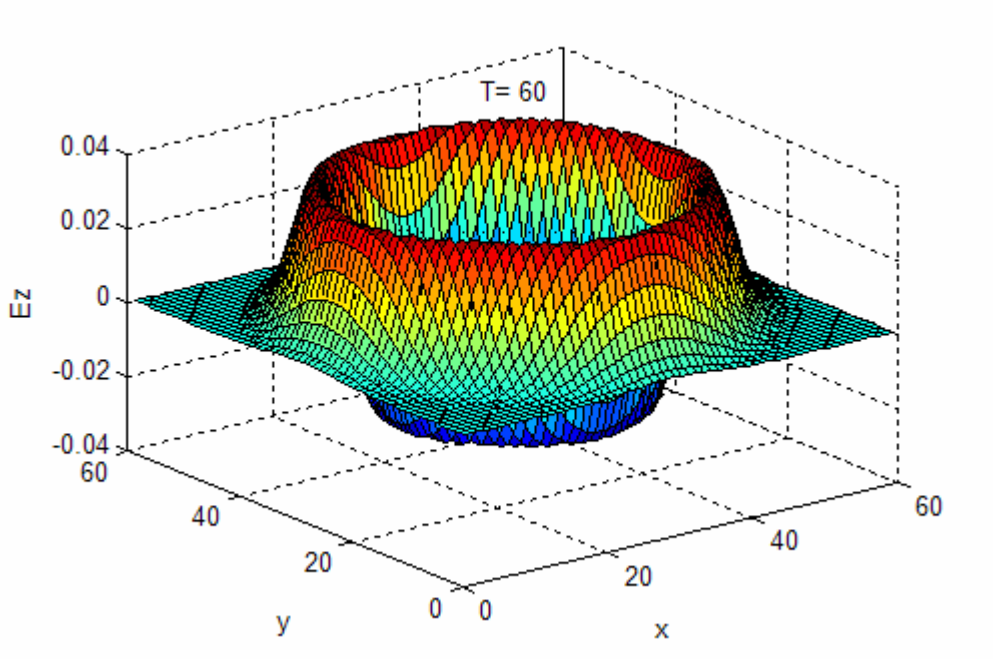

Figure 4.11 Simulation of a Gaussian pulse originates at the center of the problem space at T=60.

4.3.7 Absorbing Boundary Conditions for Two-Dimensional FDTD Analysis

We have mentioned the absorbing boundary conditions (ABCs) in the section for one dimensional approach. If we do not use absorbing boundary conditions, unpredictable reflections would be generated that would go back inward. There would be no way to determine which is the real wave and which is the reflected junk. Because of this ABCs have been a necessary part for FDTD applications.

Perfectly matched layer (PML) is one of the most efficient ABCs (Berenger, 1994). The main idea of this approach that a wave is propagating in medium A and it impinges upon medium B, and the reflection value Γ is defined by the intrinsic impedances of the two media which are determined by the dielectric constants ε and permeabilities μ of the two media

$$\Gamma = \frac{\eta_A - \eta_B}{\eta_A + \eta_B} \tag{4.3.49}$$

$$\eta = \sqrt{\frac{\mu}{\varepsilon}} \tag{4.3.50}$$

If μ changed with ε and η remined a constant, Γ would be zero and no reflection occur. But propagation will continue in the new medium.

Now we will examine everything with the Fourier Domain in time. For this reason, d/dt will be $j\omega$. But the spatial derivatives are not affected with this change.

$$j\omega D_z = c_0\left(\frac{\partial H_y}{\partial x} - \frac{\partial H_x}{\partial y}\right) \tag{4.3.51a}$$

$$D_z(\omega) = \varepsilon_r^*(\omega)E_z(\omega) \tag{4.3.51b}$$

$$j\omega H_x = -c_0\frac{\partial E_z}{\partial y} \tag{4.3.51c}$$

$$j\omega H_y = c_0\frac{\partial E_z}{\partial x} \tag{4.3.51d}$$

As seen, ε and μ are removed from the spatial derivatives in Eqs. (4.3.51a) and (4.3.51b). Instead of them, we will use fictitious dielectric constant and permeability ε_{Fz}^*, μ_{Fx}^*, μ_{Fy}^* (Sullivan, 1996).

$$j\omega D_z\ \varepsilon_{Fz}^*(x)\ \varepsilon_{Fz}^*(y) = c_0\left(\frac{\partial H_y}{\partial x} - \frac{\partial H_x}{\partial y}\right) \tag{4.3.52a}$$

$$D_z(\omega) = \varepsilon_r^*(\omega)\cdot E_z(\omega) \tag{4.3.52b}$$

$$j\omega H_x\ \mu_{Fx}^*(x)\ \mu_{Fx}^*(y) = -c_0\frac{\partial E_z}{\partial y} \tag{4.3.52c}$$

$$j\omega H_y\ \mu_{Fy}^*(x)\ \mu_{Fy}^*(y) = c_0\frac{\partial E_z}{\partial x} \tag{4.3.52d}$$

There are two conditions to constitute a PML: first one is that the PML has to get constant impedance from the background medium.

$$\eta_0 = \eta_m = \sqrt{\frac{\mu_{Fx}^*}{\varepsilon_{Fx}^*}} = 1 \tag{4.3.53}$$

In our calculation, the impedance will be 1, because of the normalized units. And second one is that the relative dielectric constant and relative permeability must be the inverse to the other directions in the direction perpendicular to the boundary.

$$\varepsilon_{Fx}^{*} = \frac{1}{\varepsilon_{Fy}^{*}} \tag{4.3.54a}$$

$$\mu_{Fx}^{*} = \frac{1}{\mu_{Fy}^{*}} \tag{4.3.54b}$$

Each of these is assumed as a complex form

$$\varepsilon_{Fm}^{*} = \varepsilon_{Fm} + \frac{\sigma_{Dm}}{j\omega\varepsilon_0} \tag{4.3.55a}$$

$$\mu_{Fm}^{*} = \mu_{Fm} + \frac{\sigma_{Hm}}{j\omega\mu_0} \tag{4.3.55b}$$

The following section of parameter satisfies Eqs. (4.3.54a) and (4.3.54b) (Sullivan, 1996):

$$\varepsilon_{Fm} = \mu_{Fm} + 1 \tag{4.3.56a}$$

$$\frac{\sigma_{Dm}}{\varepsilon_0} = \frac{\sigma_{Hm}}{\mu_0} = \frac{\sigma_D}{\varepsilon_0}$$

(4.3.56b)

By adding the Eq. (4.3.56) into Eq. (4.3.55), Eq. (4.3.53) will be

$$\eta_0 = \eta_m = \sqrt{\frac{\mu_{Fx}^{*}}{\varepsilon_{Fx}^{*}}} = \sqrt{\frac{1+\sigma(x)/\,j\omega\varepsilon_0}{1+\sigma(x)/\,j\omega\varepsilon_0}} = 1$$

If σ increases, D_z and H_y in Eqs. (4.3.52a), (4.3.52c), and (4.3.52d) will be attenuated.

We start by implementing a PML only in the X direction. For this reason, we have to take into consideration only the x dependent variables of ε_F^{*} and μ_F^{*}.

$$j\omega D_z \;\varepsilon_{Fz}^{*}(x) = c_0\left(\frac{\partial H_y}{\partial x} - \frac{\partial H_x}{\partial y}\right)$$

$$j\omega H_x \;\mu_{Fx}^{*}(x)) = -c_0\frac{\partial E_z}{\partial y}$$

$$j\omega H_y \, \mu^*_{Fy}(x) = c_0 \frac{\partial E_z}{\partial x}$$

and by using the values of Eq. (4.3.56):

$$j\omega\left(1+\frac{\sigma_{D(x)}}{j\omega\varepsilon_0}\right)D_z = c_0\left(\frac{\partial H_y}{\partial x}-\frac{\partial H_x}{\partial y}\right) \tag{4.3.57a}$$

$$j\omega\left(1+\frac{\sigma_{D(x)}}{j\omega\varepsilon_0}\right)^{-1} H_x = -c_0\frac{\partial E_z}{\partial y} \tag{4.3.57b}$$

$$j\omega\left(1+\frac{\sigma_{D(x)}}{j\omega\varepsilon_0}\right) H_y = c_0\frac{\partial E_z}{\partial x} \tag{4.3.57c}$$

Firstly, we have to observe the left side of Eq. (4.3.57) to put that equation into FDTD formulation.

$$j\omega\left(1+\frac{\sigma_{D(x)}}{j\omega\varepsilon_0}\right)D_z = j\omega D_z + \frac{\sigma_{D(x)}}{\varepsilon_0}D_z$$

Moving to the time domain, and then taking the finite difference approximations, Thus,

$$\frac{\partial D_z}{\partial t}+\frac{\sigma_{D(i)}}{\varepsilon_0}D_z \cong \frac{D_z^{n+1/2}(i,j)-D_z^{n-1/2}(i,j)}{\Delta t}+\frac{\sigma_{D(i)}}{\varepsilon_0}\frac{D_z^{n+1/2}(i,j)-D_z^{n-1/2}(i,j)}{2}$$
$$= D_z^{n+1/2}(i,j)\frac{1}{\Delta t}\left[1+\frac{\sigma_{D(i)}\cdot\Delta t}{2\cdot\varepsilon_0}\right]-D_z^{n-1/2}(i,j)\frac{1}{\Delta t}\left[1-\frac{\sigma_{D(i)}\cdot\Delta t}{2\cdot\varepsilon_0}\right]$$

If we add this into Eq.(4.3.57a) along with the spatial derivatives, we get

$$D_z^{n+1/2}(i,j) = Bi3(i)D_z^{n-1/2}(i,j)$$
$$+0.5\,(Bi2(i)\left[H_y^n(i+1/2,j)-H_y^n(i-1/2,j)-H_x^n(i,j+1/2)-H_x^n(i,j-1/2)\right]), \tag{4.3.58}$$

By using the following equation again

$$\frac{\Delta t}{\Delta x} = c_0\frac{\Delta x/(2c_0)}{\Delta x} = \frac{1}{2}$$

The new parameters are given by

$$Bi2(i) = \frac{1}{1+\sigma_D(i)(\Delta t/(2\varepsilon_0))} \tag{4.3.59a}$$

$$Bi3(i) = \frac{1-\sigma_D(i)(\Delta t/(2\varepsilon_0))}{1+\sigma_D(i)(\Delta t/(2\varepsilon_0))} \tag{4.3.59b}$$

Eq. (4.3.57c) gives

$$\begin{aligned} H_y^{n+1}(i+1/2, j) = {} & Ai3(i+1/2)H_y^n(i+1/2, j) \\ & + 0.5\ (Ai2(i+1/2)\left[E_z^{n+1/2}(i+1, j) - E_z^{n+1/2}(i, j)\right]), \end{aligned} \tag{4.3.60}$$

where

$$Ai2(i+1/2) = \frac{1}{1+\sigma_D(i+1/2)(\Delta t/(2\varepsilon_0))} \tag{4.3.61a}$$

$$Ai3(i+1/2) = \frac{1-\sigma_D(i+1/2)(\Delta t/(2\varepsilon_0))}{1+\sigma_D(i+1/2)(\Delta t/(2\varepsilon_0))} \tag{4.3.61b}$$

The spatial derivative for Eq. (4.3.57b) will be written as

$$\frac{\partial E_z}{\partial y} \cong \frac{E_z^{n+1/2}(i, j+1) - E_z^{n+1/2}(i, j)}{\Delta x} = -\frac{\nabla \times E}{\Delta x}$$

Implementing this into an FDTD formulation becomes

$$\frac{H_x^{n+1}(i, j+1/2) - H_x^n(i, j+1/2)}{\Delta x} = -c_0\left[-\frac{\nabla \times E}{\Delta x} - \frac{\sigma_D(x)}{\varepsilon_0}\Delta t\sum_{n=0}^{T}\frac{\nabla \times E}{\Delta x}\right]$$

Finally, we get

$$\begin{aligned} H_x^{n+1}(i, j+1/2) &= H_x^n(i, j+1/2) + \frac{c_0\Delta t}{\Delta x}\nabla \times E \\ &\quad - \frac{\Delta t c_0}{\Delta x} - \frac{\sigma_D(x)\Delta t}{\varepsilon_0} I_{Hx}^{n+1/2}(i, j+1/2) \\ &= H_x^n(i, j+1/2) + \frac{c_0\Delta t}{\Delta x}\nabla \times E \\ &\quad + \frac{\sigma_D(x)\Delta t}{2\varepsilon_0} I_{Hx}^{n+1/2}(i, j+1/2) \end{aligned}$$

Eq. (4.3.57b) is implemented as the following series of equations:

$$\nabla \times E = \left[E_z^{n+1/2}(i, j) - E_z^{n+1/2}(i, j+1) \right] \tag{4.3.62a}$$

$$I_{Hx}^{n+1/2}(i, j+1/2) = I_{Hx}^{n-1/2}(i, j+1/2) + \nabla \times E \tag{4.3.62b}$$

$$\begin{aligned} H_x^{n+1}(i, j+1/2) = H_x^n(i, j+1/2) + 0.5\ (\nabla \times E) \\ + Ai1(i)\ I_{Hx}^{n+1/2}(i, j+1/2) \end{aligned} \tag{4.3.62c}$$

with

$$Ai1(i) = \frac{\sigma_D(i)\Delta t}{2\varepsilon_0} \tag{4.3.63}$$

In calculating the parameters A and B, it is not necessary to actually vary conductivities. Then we calculate the auxilary parameter,

$$xn = \frac{\sigma \Delta t}{2\varepsilon_0}$$

that increases as it goes into the PML. The A and B parameters are then calculated:

$$xn(i) = 0.333 * \left(\frac{i}{l\_pml} \right)^3 \qquad i = 1, 2, ..., l\_pml \tag{4.3.64}$$

$$Ai1(i) = xn(i) \tag{4.3.65a}$$

$$Bi2(i) = \frac{1}{1 + xn(i)} \tag{4.3.65b}$$

$$Bi3(i) = \frac{1 - xn(i)}{1 + xn(i)} \tag{4.3.65c}$$

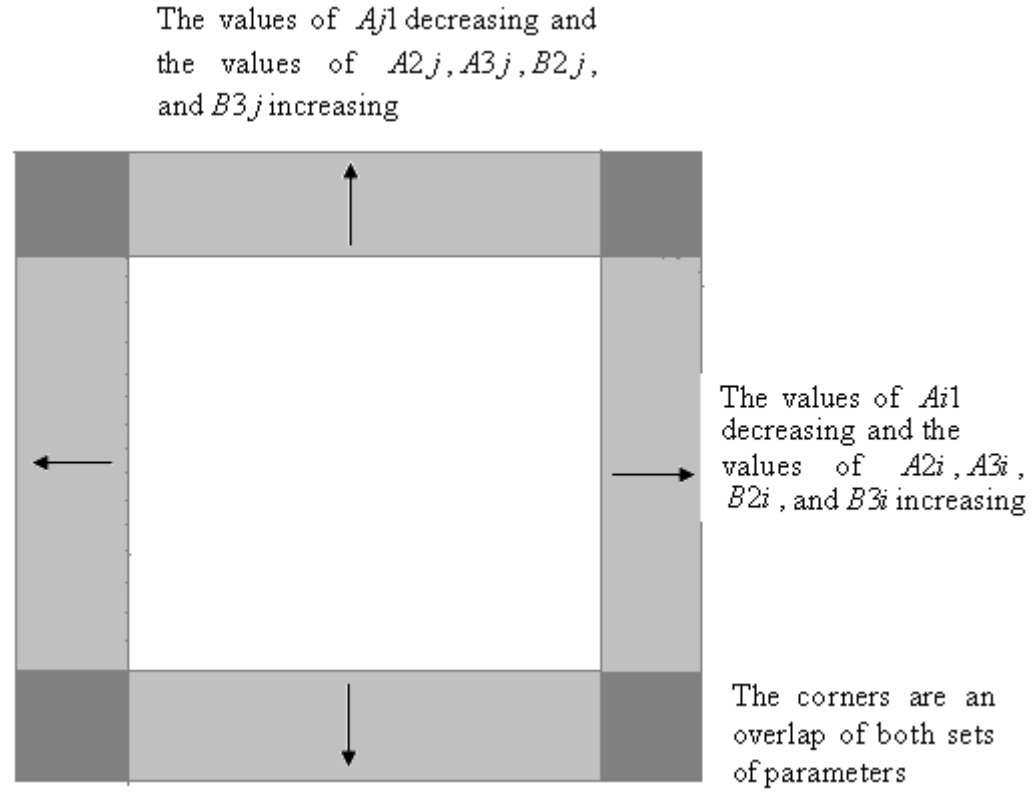

Figure 4.12 The Perfectly Matched Layer (PML) technique.

So Instead of Eq. (4.3.57) we can use

$$j\omega\left(1+\frac{\sigma_{D(x)}}{j\omega\varepsilon_0}\right)\left(1+\frac{\sigma_{D(y)}}{j\omega\varepsilon_0}\right)D_z = c_0\left(\frac{\partial H_y}{\partial x}-\frac{\partial H_x}{\partial y}\right) \tag{4.3.66a}$$

$$j\omega\left(1+\frac{\sigma_{D(x)}}{j\omega\varepsilon_0}\right)^{-1}\left(1+\frac{\sigma_{D(y)}}{j\omega\varepsilon_0}\right)H_x = c_0\left(-\frac{\partial E_z}{\partial y}\right) \tag{4.3.66b}$$

$$j\omega\left(1+\frac{\sigma_{D(x)}}{j\omega\varepsilon_0}\right)\left(1+\frac{\sigma_{D(y)}}{j\omega\varepsilon_0}\right)^{-1}H_y = c_0\left(\frac{\partial E_z}{\partial x}\right) \tag{4.3.66c}$$

Using the same procedure as before, the following replaces Eq. (4.3.58)

$$D_z^{n+1/2}(i,j) = Bi3(i)\;Bj3(j)\;D_z^{n-1/2}(i) + Bi2(i)\;Bj2(j)\;(0.5)\begin{bmatrix} H_y^n(i+1/2,j)-H_y^n(i-1/2,j) \\ -H_x^n(i,j+1/2)-H_x^n(i,j-1/2)\end{bmatrix}$$

In the Y direction, H_y will require an implementation similar to the one used for H_x in the X direction giving

$$\nabla \times E = \left[E_z^{n+1/2}(i+1, j) - E_z^{n+1/2}(i, j) \right] \tag{4.3.67a}$$

$$I_{Hy}^{n+1/2}(i+1/2, j) = I_{Hy}^{n-1/2}(i+1/2, j) + \nabla \times E \tag{4.3.67b}$$

$$\begin{aligned} H_y^{n+1}(i+1/2, j) = {} & Ai3(i+1/2)\, H_y^n(i+1/2, j) \\ & - 0.5\, (Ai2(i+1/2)(\nabla \times E)) + Aj1(j)\, I_{Hy}^{n+1/2}(i+1/2, j) \end{aligned} \tag{4.3.67c}$$

Finally, the H_x in the direction becomes

$$\nabla \times E = \left[E_z^{n+1/2}(i, j) - E_z^{n+1/2}(i, j+1) \right] \tag{4.3.68a}$$

$$I_{Hx}^{n+1/2}(i, j+1/2) = I_{Hx}^{n-1/2}(i, j+1/2) + \nabla \times E$$

$$\begin{aligned} H_x^{n+1}(i, j+1/2) = {} & Aj3(j+1/2)\, H_x^n(i, j+1/2) \\ & - 0.5\, (Aj2(j+1/2)(\nabla \times E)) + Ai1(i) I_{Hx}^{n+1/2}(i, j+1/2) \end{aligned} \tag{4.3.68c}$$

4.3.8 Analysis of SAR distribution and Bio-Heat Equation

The temperature distribution in the tissue, is given by the solution of Pennes bioheat equation:

$$\rho c \frac{\partial}{\partial t} T = \nabla \cdot k \nabla T + w_b c_b (T_a - T) + q_m + q_e \tag{4.3.69}$$

where T is the temperature elevation (°C), ρ is the physical density of the tissue ($\mathrm{kg/m^3}$), c is the specific heat ($\mathrm{J/kg/°C}$), k is the thermal conductivity ($\mathrm{W/m/°C}$), w_b is the tissue volumetric perfusion rate ($\mathrm{kg/m^3/s}$), c_b is the specific heat of blood ($\mathrm{J/kg/°C}$), T_a is the average temperature elevation of the arteries (°C), q_e is the mechanism for modeling the electromagnetic power deposition ($\mathrm{W/m^3}$), and is the mechanism for modeling physiological heat generation ($\mathrm{W/m^3}$).

To develop, from the BHTE, a parametric model involving finitely many unknowns, the time derivative is first discretized using a forward finite difference (Kovalski and Jin, 2004)

$$T\left[k+1\right]=T\left[k\right]+\frac{\Delta t}{\rho c}\left(k\nabla^2 T\left[k\right]+\omega_b c_b\left(T_a-T\left[k\right]\right)+q_m\right)$$

(4.3.70)

where $T\left[k\right]$ is used to denote the spatial dependence of the entire temperature field at some discrete time $k\Delta t$. By using forward difference

$$f_i^{'}=\frac{f_{i+1}-f_i}{h}$$

and replacing the spatial derivatives with central finite differences further yields

$$\begin{aligned}T\left[i,j,k+1\right]=T\left[i,j,k\right]&\left(1-\frac{4\Delta t}{\rho c\Delta x^2}-\omega_b c_b\right)+\frac{\Delta t}{\rho c\Delta x^2}\\&\times\left(T\left[i+1,j,k\right]+T\left[i-1,j,k\right]\right.\\&\quad\left.+T\left[i,j+1,k\right]+T\left[i,j-1,k\right]\right)\\&+\frac{\Delta t}{\rho c}\left(\omega_b c_b T_a+q_e+q_m\right)\end{aligned}\qquad(4.3.71)$$

$$q_m=\mathrm{SAR}=\frac{\sigma}{2}\left|E\right|^2\ \text{ and }\ q_e=0\qquad(4.3.72)$$

where $T\left[i,j,k\right]$ is now used to denote the temperature at a single point in space indexed by i,j on a uniform grid with separation Δx at a discrete time $k\Delta t$. The Specific Absorption Rate (SAR) is defined as

$$\mathrm{SAR}=\frac{\sigma}{2}\left|E\right|^2.$$

4.3.9 Simulation Results for Two-Dimensional FDTD Analysis

Firstly we investigated the effect of PML for 2D TM formulation. According to Berenger PML techniques, the computational area is surrounded by PML. The electromagnetic energy is absorbed rapidly in these layers so that we can set perfect conductor at the outmost. This can be also understood as that the interior area is

matched to perfect conductor by the PML. Fig. 4.13 and Fig. 4.14 show the effect of the boundary, where the wave is bounced back by the perfect conductor boundary and added to the outgoing wave.

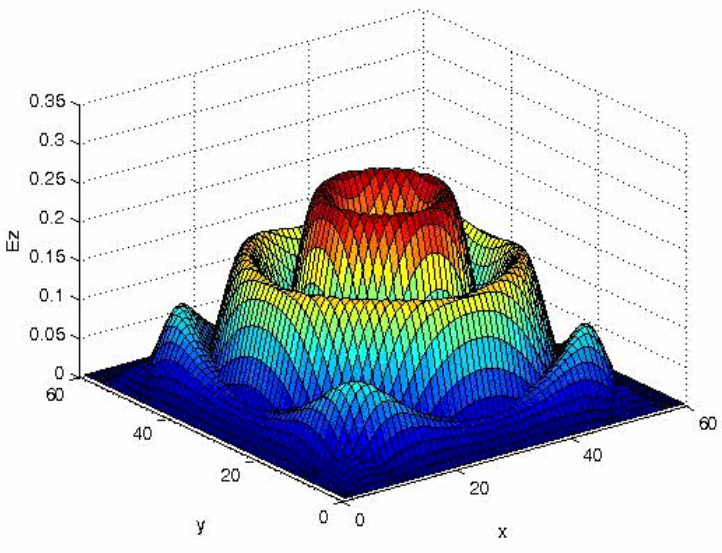

Figure 4.13 A Gaussian Pulse Radiate from the center reaching the PML boundary

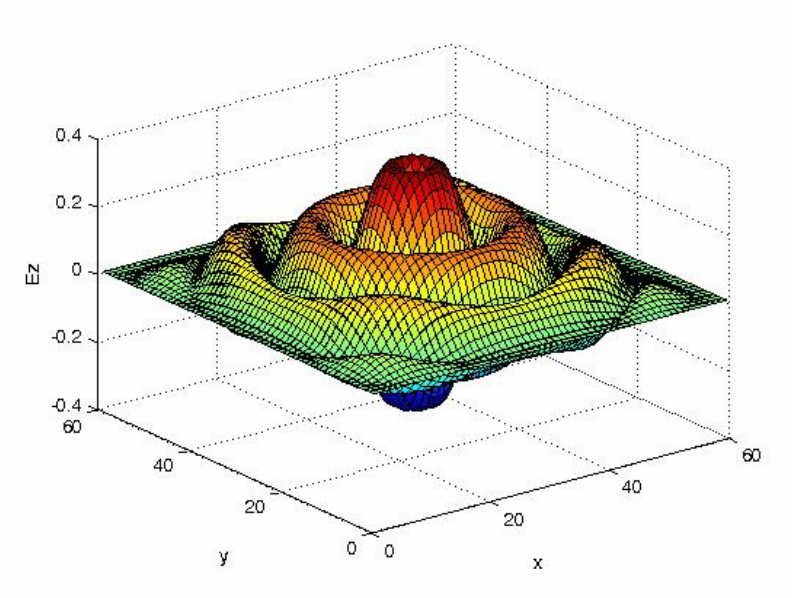

Figure 4.14 The Sinusoidal pulse generated at center being absorbed by PML boundary

Before computing FDTD calculation, we need to illustrate a FDTD region which is formed by dielectric properties of region. Our first FDTD configuration is originated from 0 to 60 in both x and y direction. This FDTD space, which is shown in Fig. 4.15, is formed by adjusting as fat and bladder tissues respectively. The electric field and SAR

distribution of this space are computed and simulated at different time steps. We formed different practises by applying different frequency and source position. In this respect we labeled these applications as cases and numbered them in turn in order.

Figure 4.15 The graphical representation of our FDTD configuration.

In Case 1, which is our first configuration, we applied a sinusoidal pulse that is initiated at 700 MHz with a source positioned on point x=35, y=45. Electric field distributions, which are simulated at time steps 100, 250 and 500, are shown in Fig. 4.16, Fig. 4.17, and Fig. 4.18.

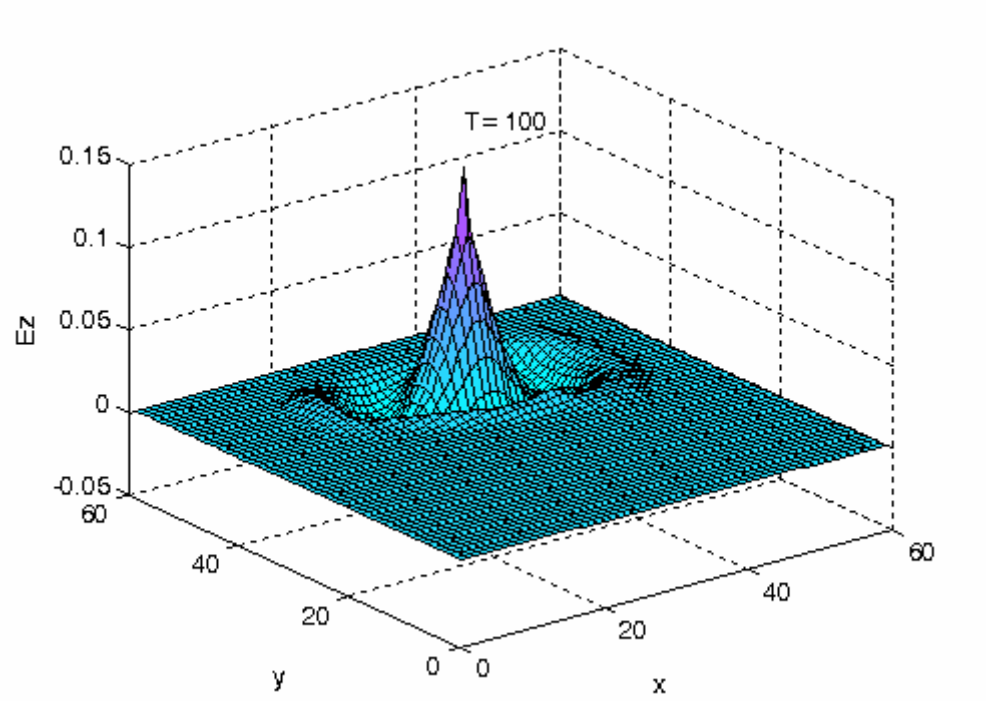

Figure 4.16 The Electric field distribution for Case 1 when time step is 100 (T=100).

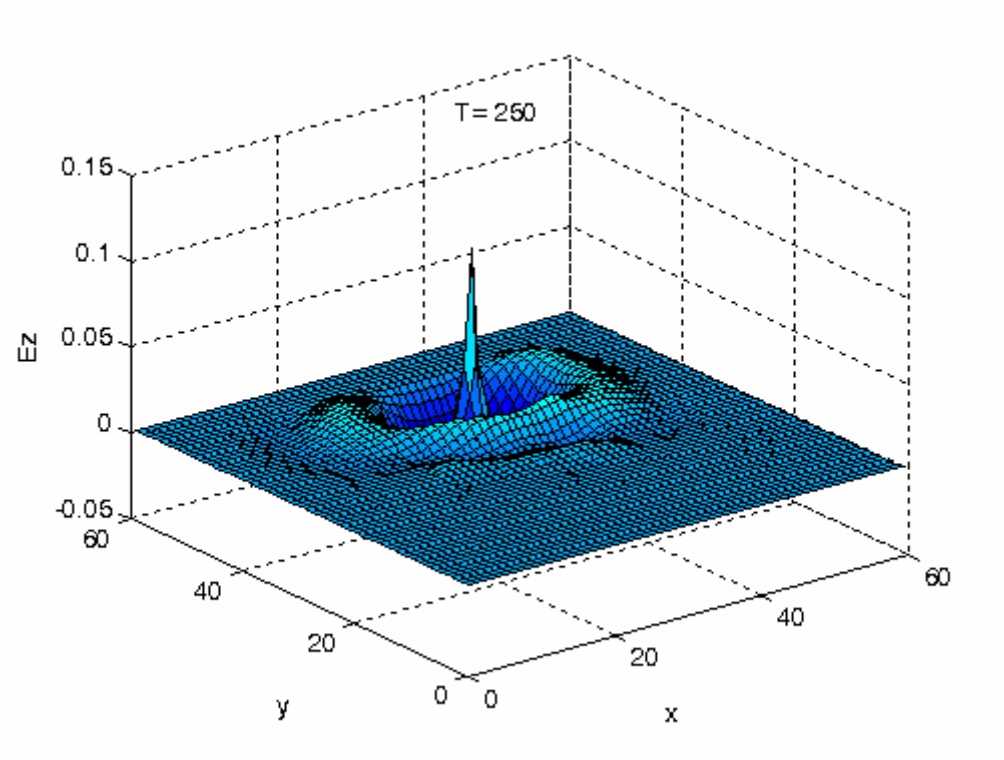

Figure 4.17 The Electric Field Distribution for Case 1 when time step is 250 (T=250).

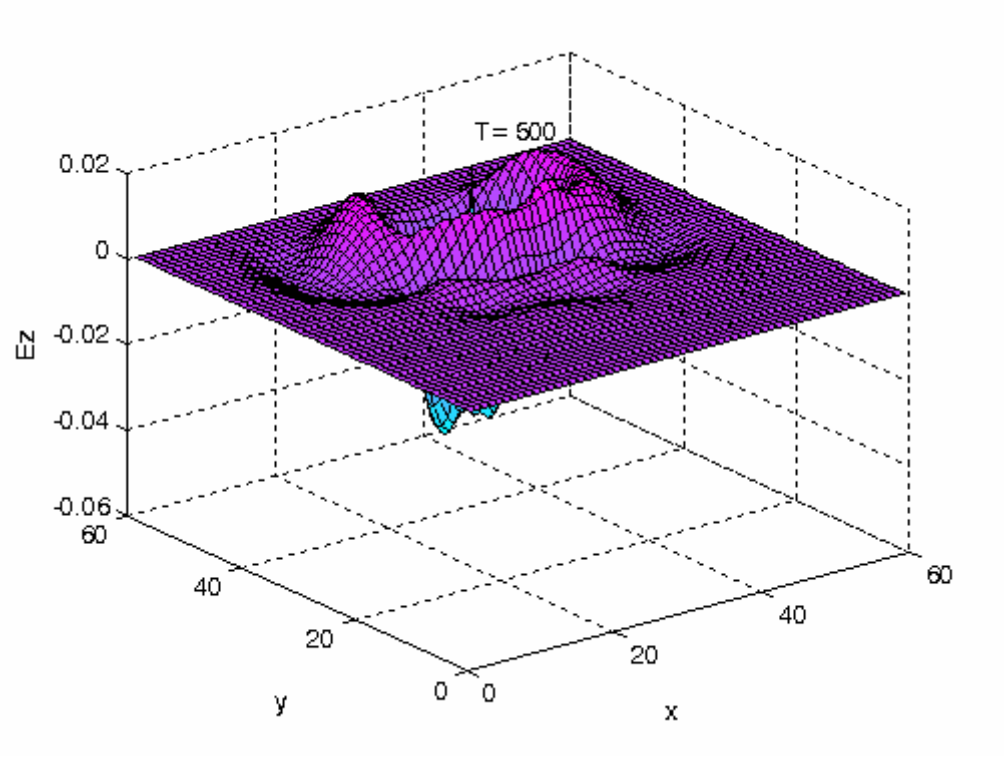

Figure 4.18 The Electric Field Distribution for Case 1 when time step is 500 (T=500).

Again according to Case 1, we applied a sinusoidal pulse that is initiated at 700 MHz with a source positioned on point x=35, y=45. SAR results, which are simulated at time steps 100, 250, and 500 are show in Fig. 4.19, Fig. 4.20 and Fig. 4.21.

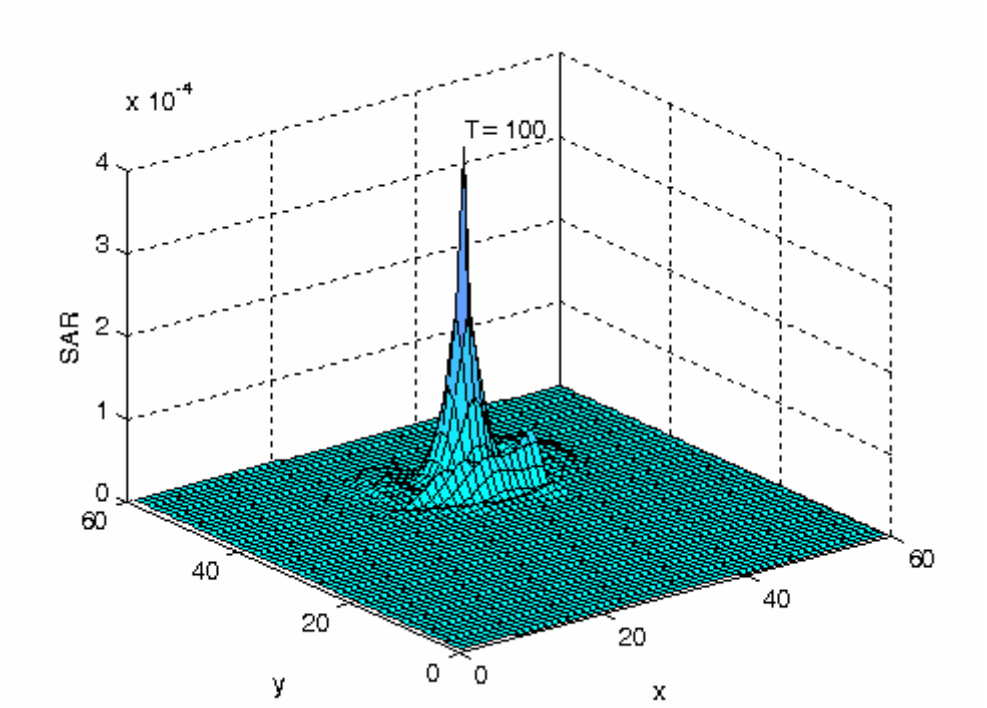

Figure 4.19 The SAR distribution for Case 1 when time step is 100 (T=100).

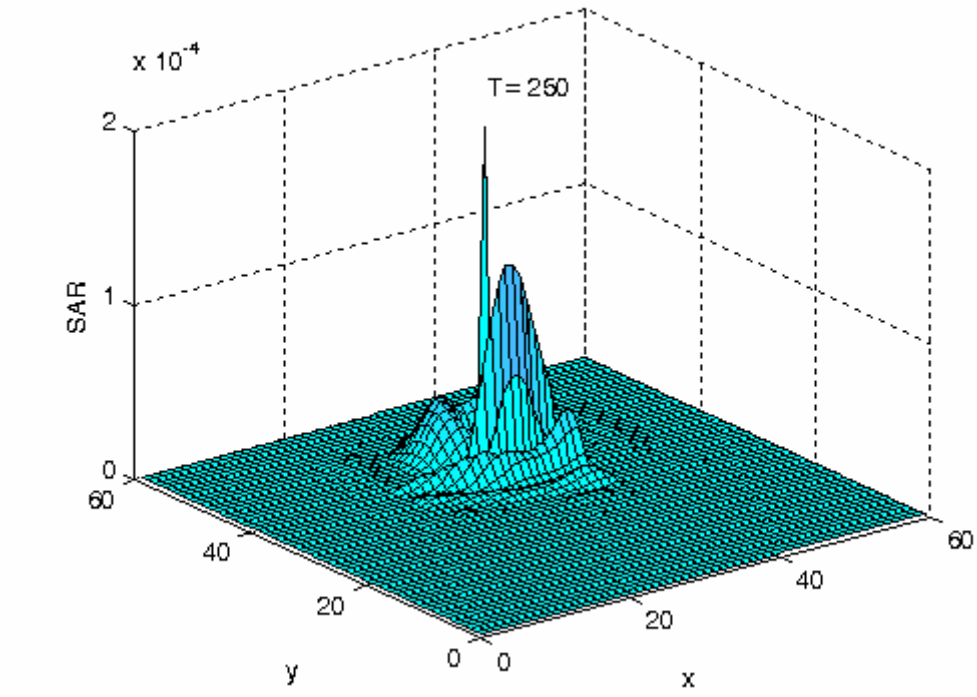

Figure 4.20 The SAR distribution for Case 1 when time step is 250 (T=250).

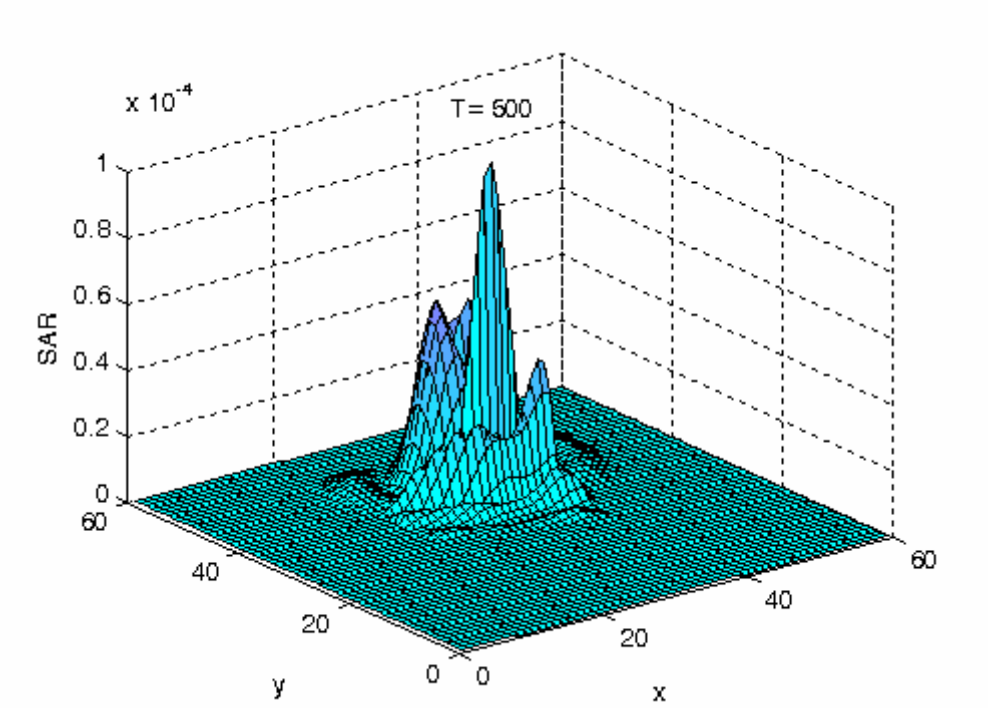

Figure 4.21 The SAR distribution for Case 1 when time step is 500 (T=500).

In Case 2, Gaussian pulse is initiated at at 700 MHz. and the source is positioned on point x=35, y=45. Electric field distributions, which are simulated at time steps 100, 250 and 500, are shown in Fig. 4.22, Fig. 4.23, and Fig. 4.24.

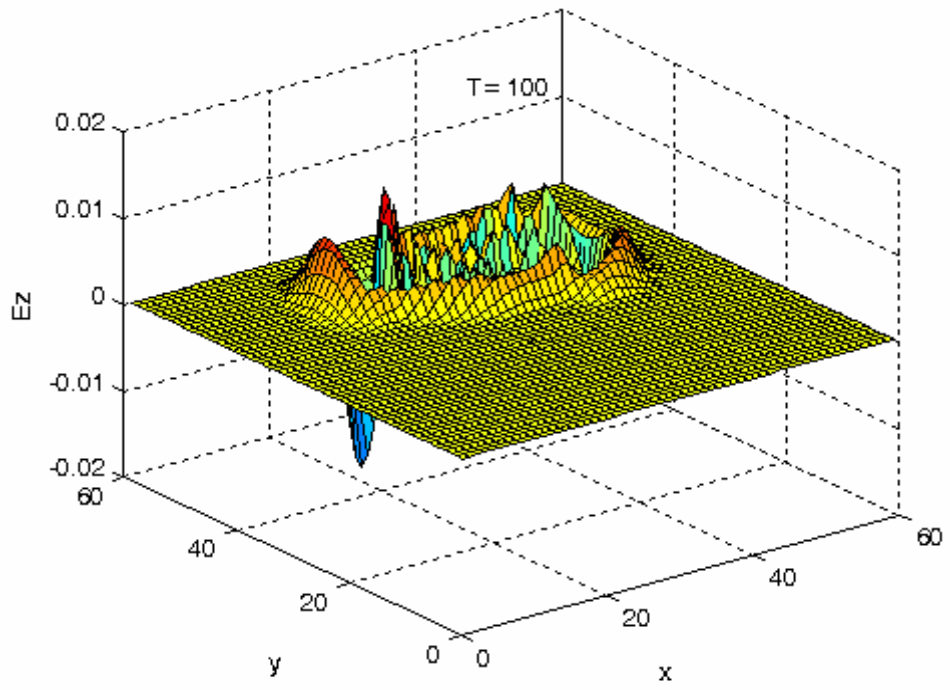

Figure 4.22 The Electric field distribution for Case 2 when time step is 100 (T=100).

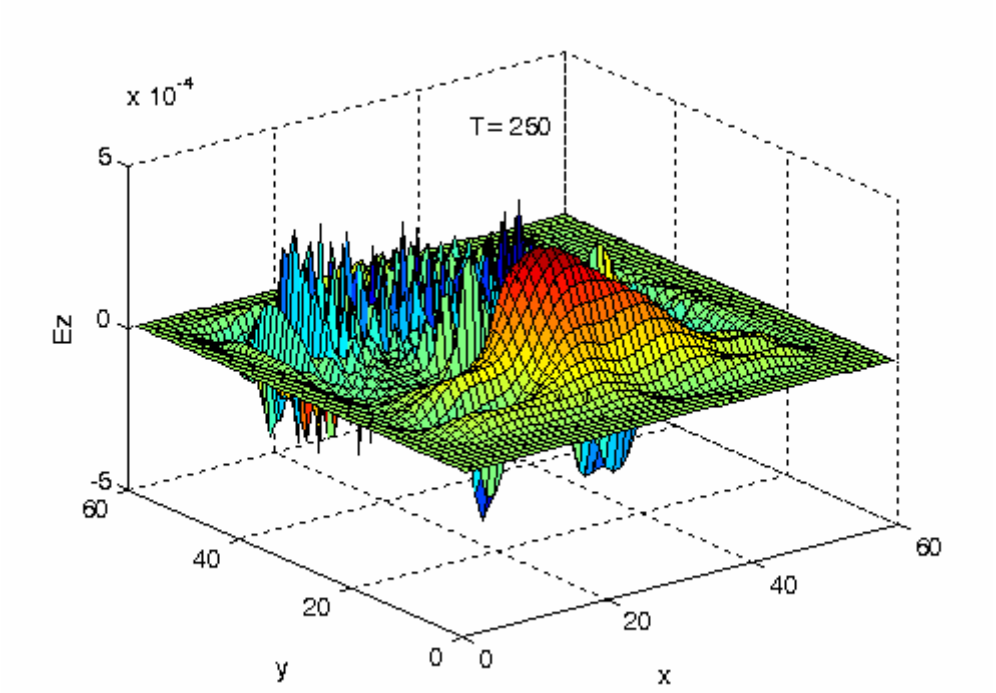

Figure 4.23 The Electric field distribution for Case 2 when time step is 250 (T=250).

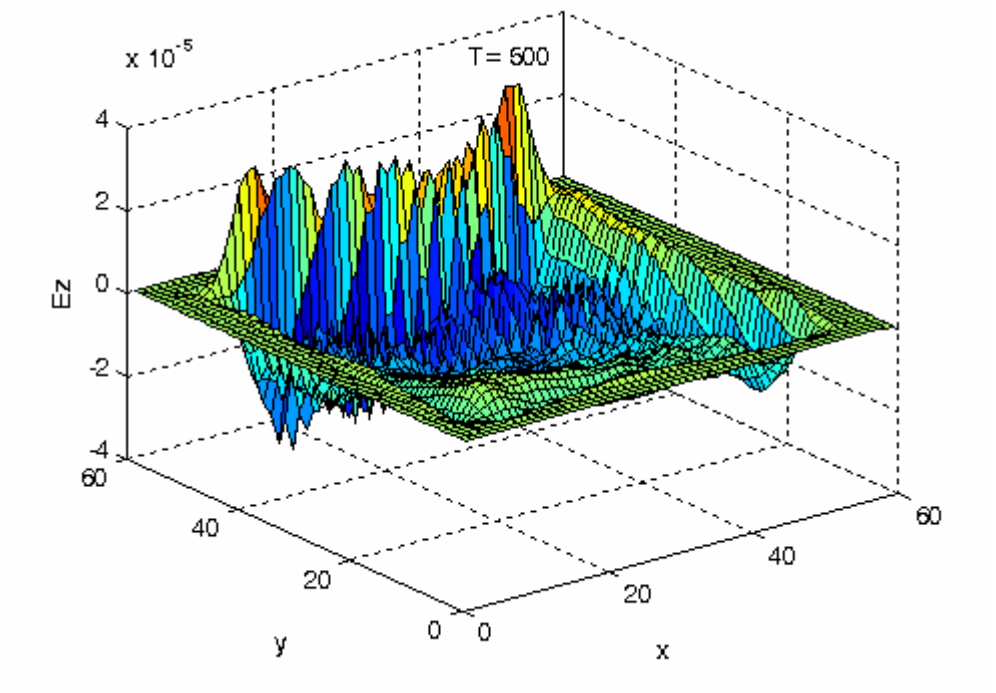

Figure 4.24 The Electric field distribution for Case 2 when time step is 500 (T=500).

In Case 2, a Gaussian pulse is initiated at at 700 MHz and the source is positioned on point x=35, y=45. SAR distributions, which are simulated at time steps 100, 250 and 500, are shown in Fig. 4.25, Fig. 4.26, and Fig. 4.27.

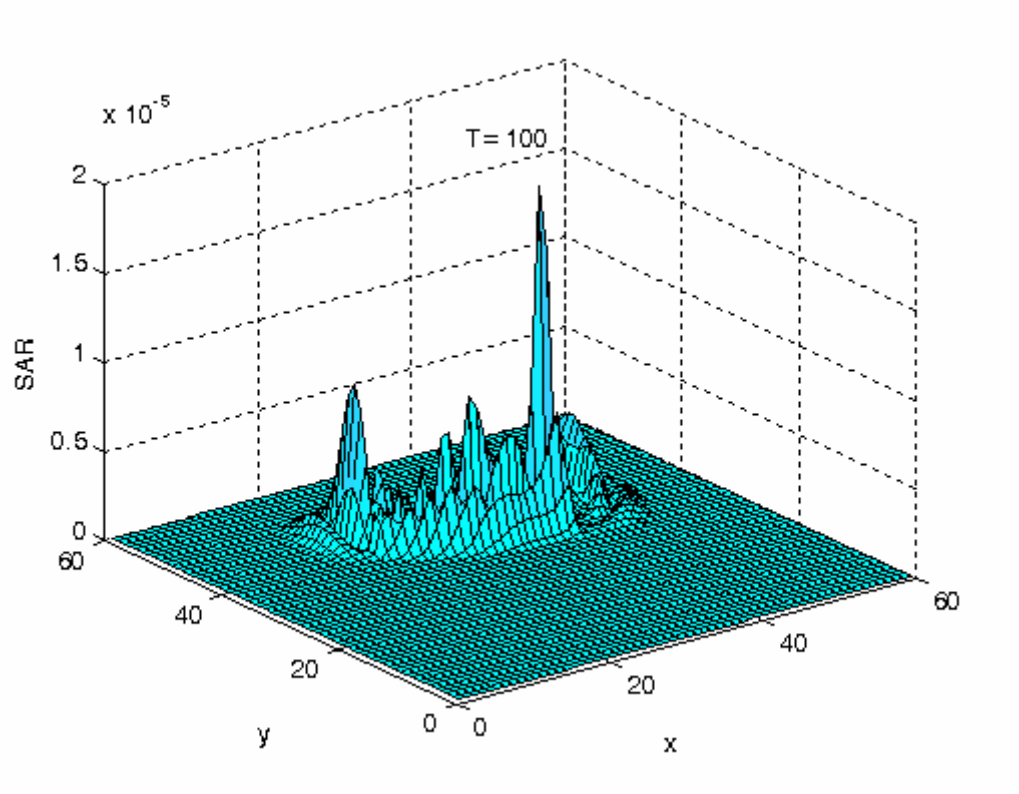

Figure 4.25 The SAR distribution for Case 2 when time step is 100 (T=100).

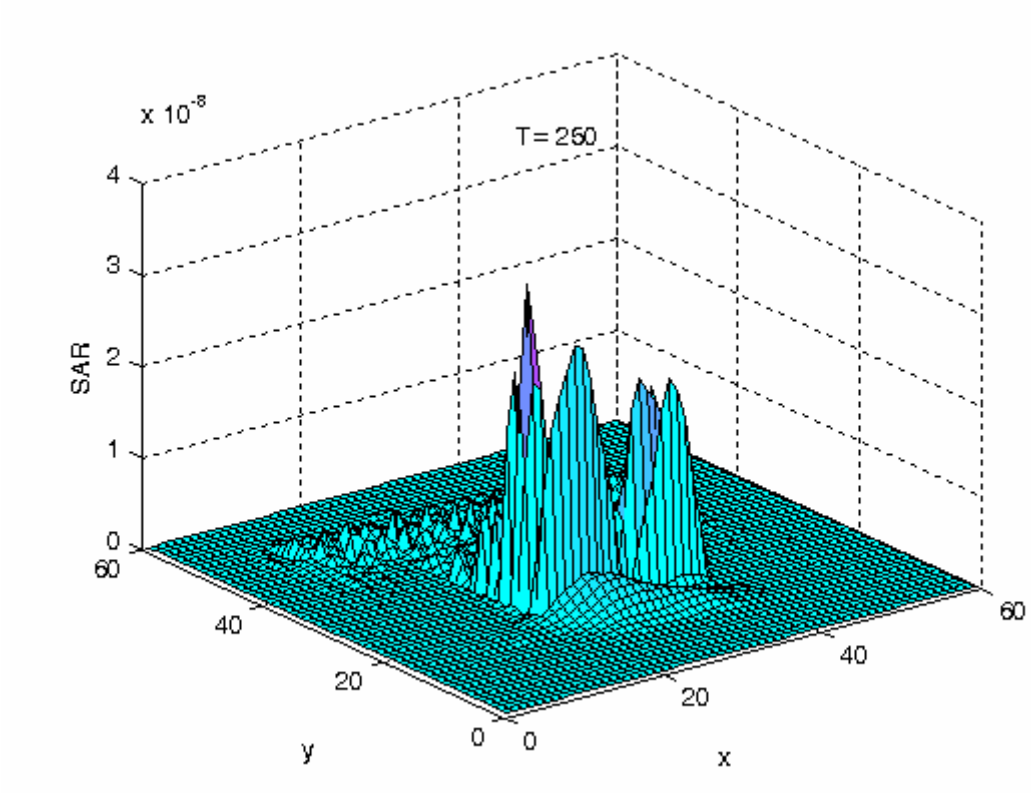

Figure 4.26 The SAR distribution for Case 2 when time step is 250 (T=250).

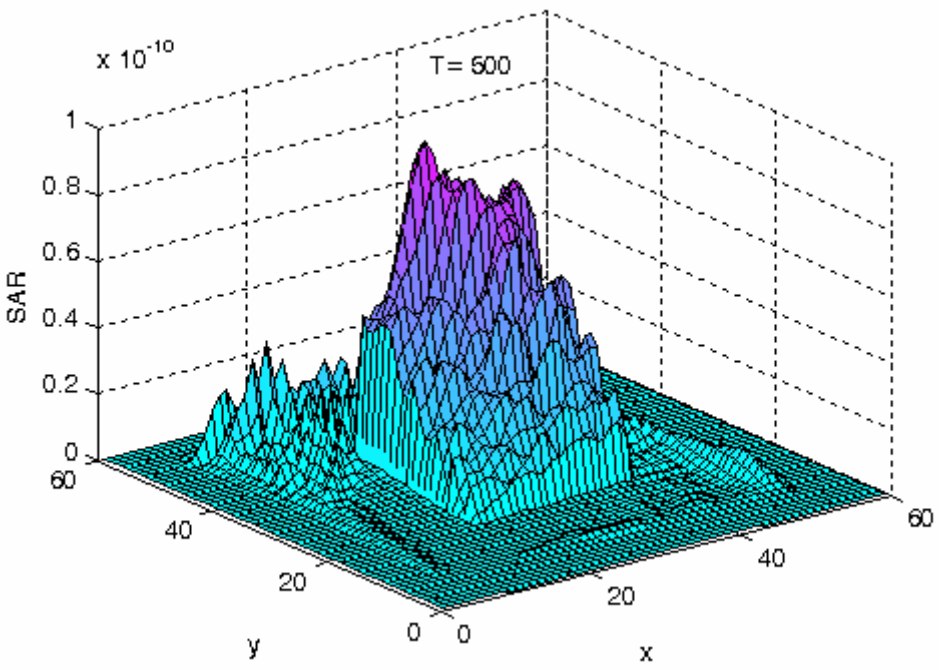

Figure 4.27 The SAR distribution for Case 2 when time step is 500 (T=500).

Our second FDTD configuration is originated from 0 to 60 in both x and y direction, which is shown in Fig. 4.28, and is formed by adjusting according to dielectric properties of free space and breast fat respectively. The electric field and SAR distribution of this configuration are computed and simulated at different time steps.

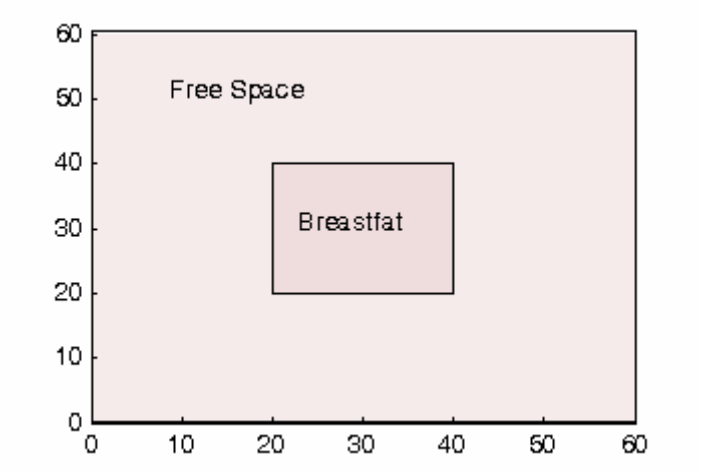

Figure 4.28 The graphical representation of our second FDTD configuration.

In Case 3, we applied a sinusoidal pulse that is initiated at 900 MHz for second configuration. And source is positioned on the point x=45, y=35. Electric field distributions, which are simulated at time steps 250, 750, 1000 and 1500, are shown in Fig. 4.29, Fig. 4.30, Fig. 4.31, and Fig. 4.32.

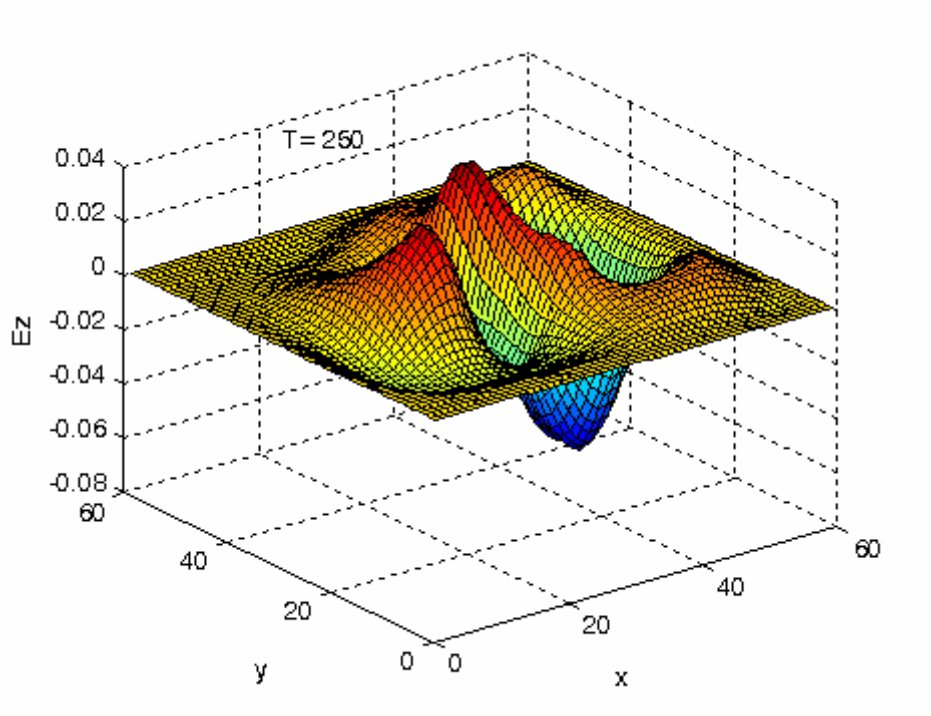

Figure 4.29 The Electric field distribution for Case 3 when time step is 250 (T=250).

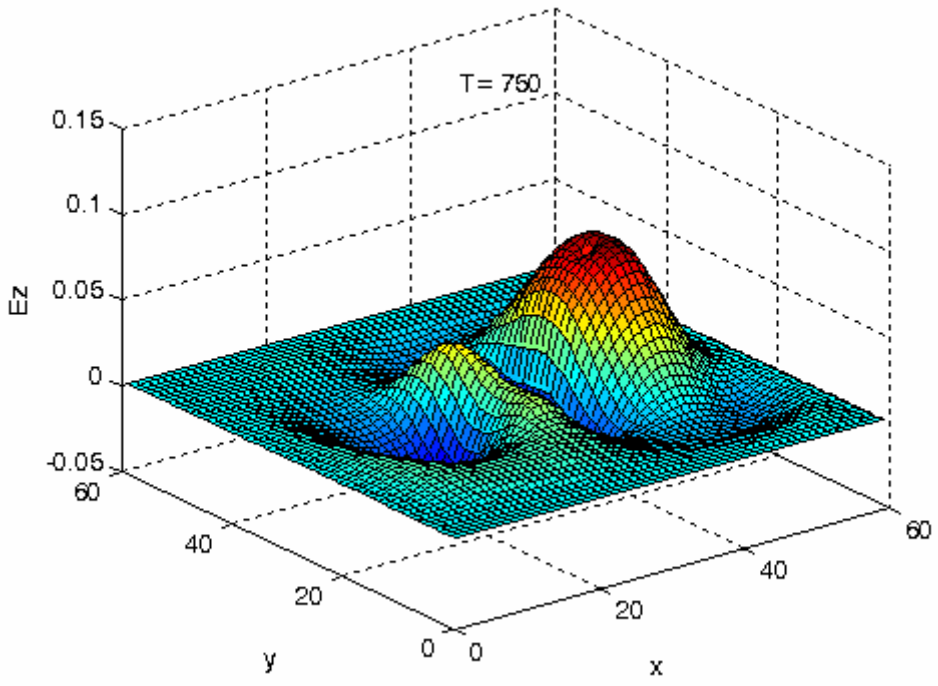

Figure 4.30 The Electric field distribution for Case 3 when time step is 750 (T=750).

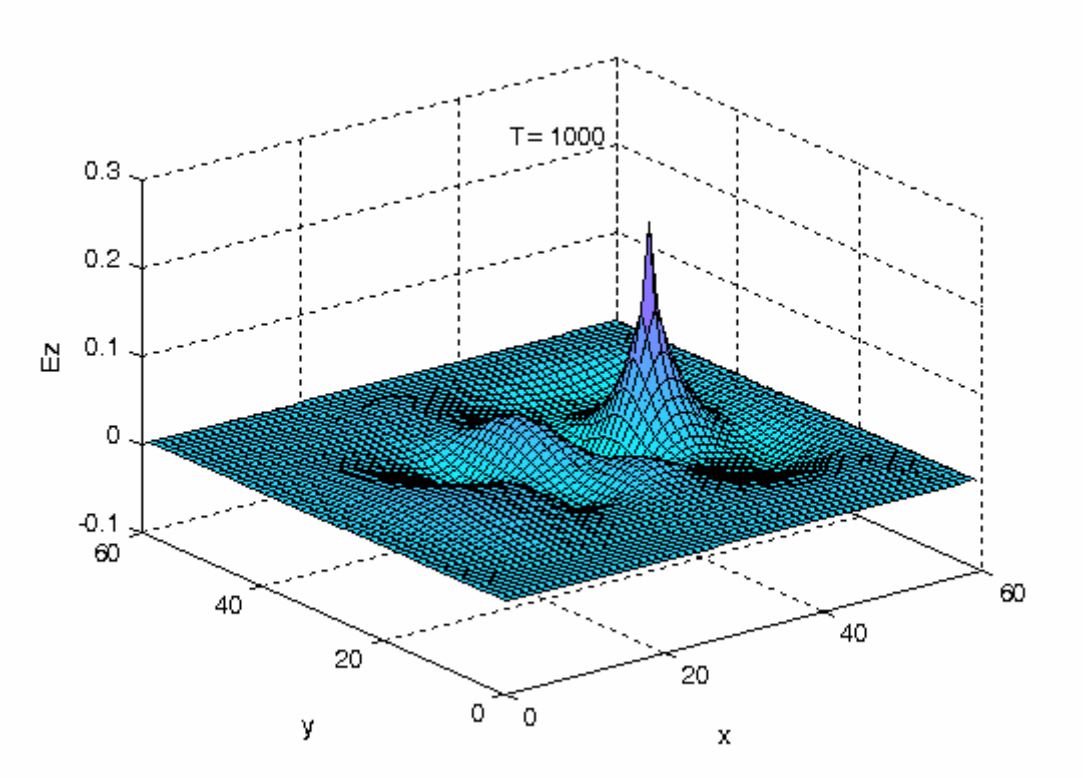

Figure 4.31 The Electric field distribution for Case 3 when time step is 1000 (T=1000).

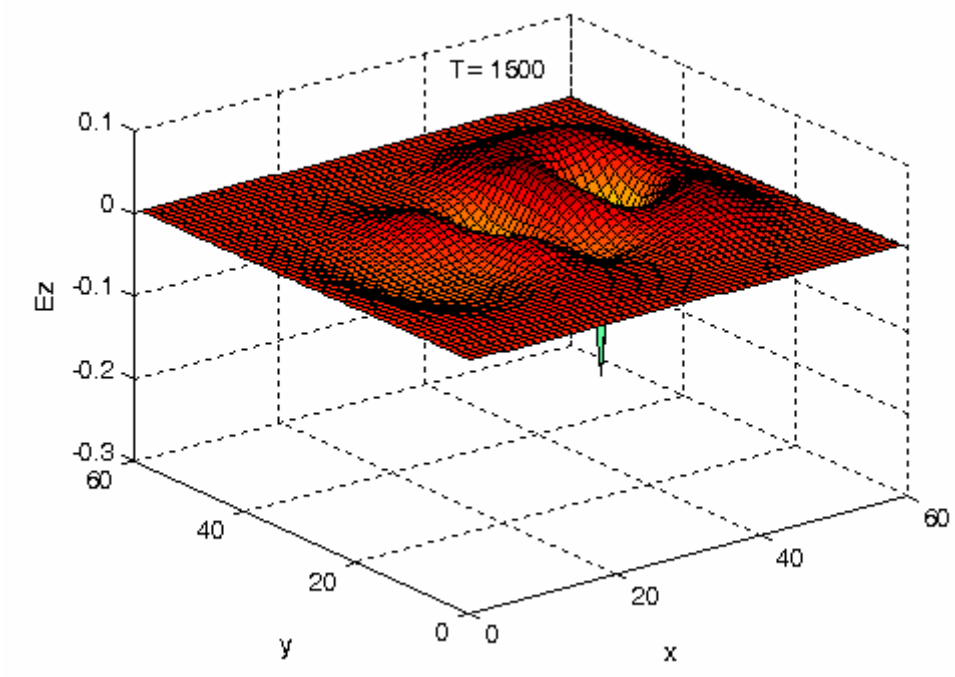

Figure 4.32 The Electric field distribution for Case 3 when time step is 1500 (T=1500).

Due to Case 3 conditions of second configuration, we applied a sinusoidal pulse that is initiated at 900 MHz. And source is positioned on the point x=45, y=35. SAR results, which are simulated at time steps 250, 750, 1000 and 1500 are shown in Fig. 4.33, Fig. 4.34, Fig. 4.35 and Fig. 4.36.

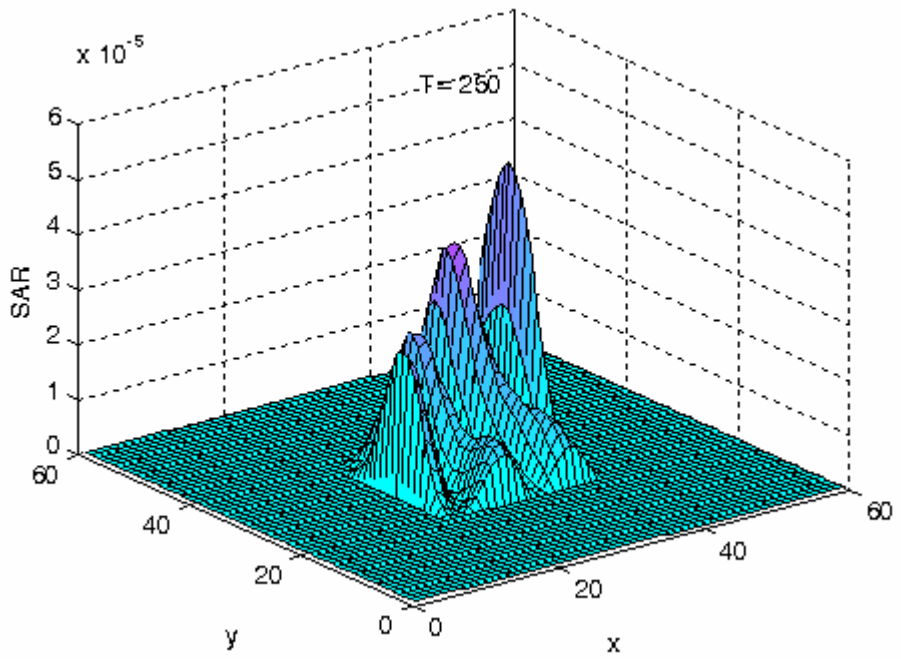

Figure 4.33 The SAR distribution for Case 3 when time step is 250 (T=250).

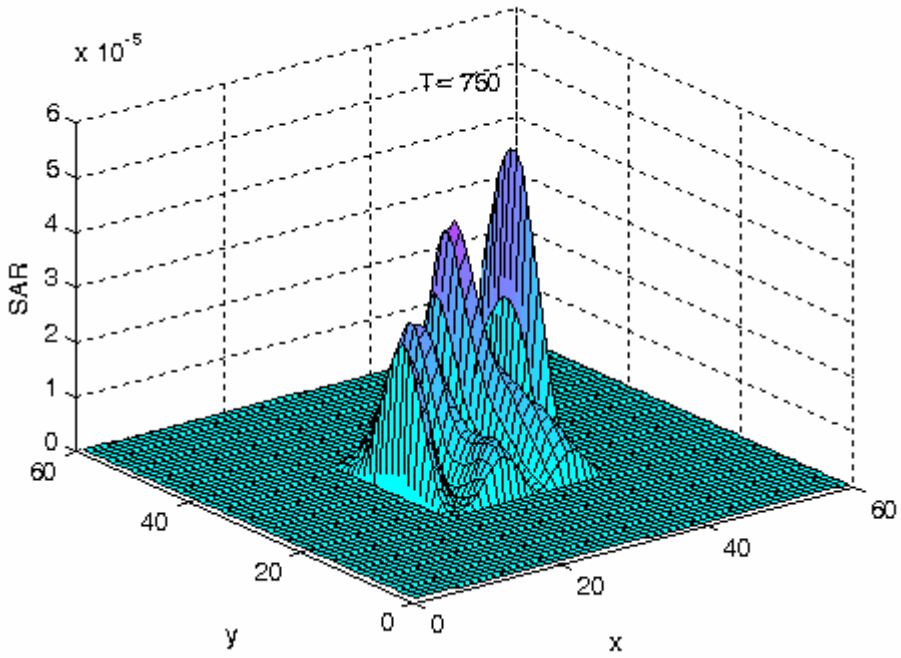

Figure 4.34 The SAR distribution for Case 3 when time step is 750 (T=750).

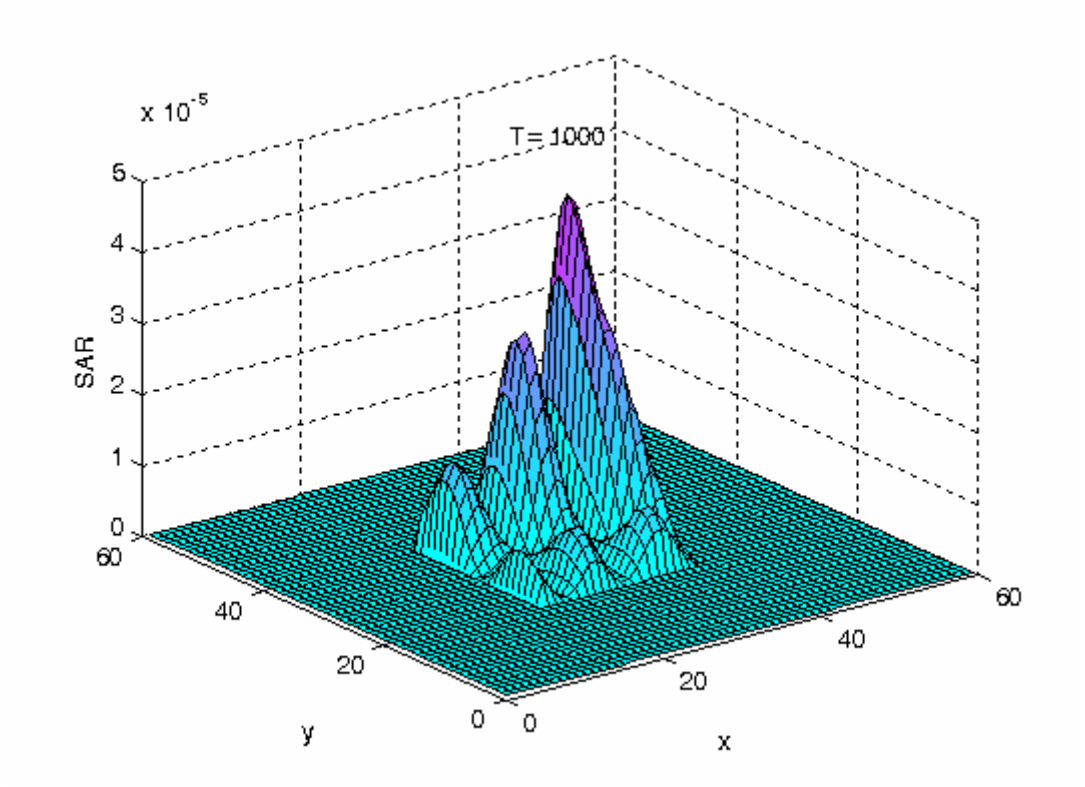

Figure 4.35 The SAR distribution for Case 3 when time step is 1000 (T=1000).

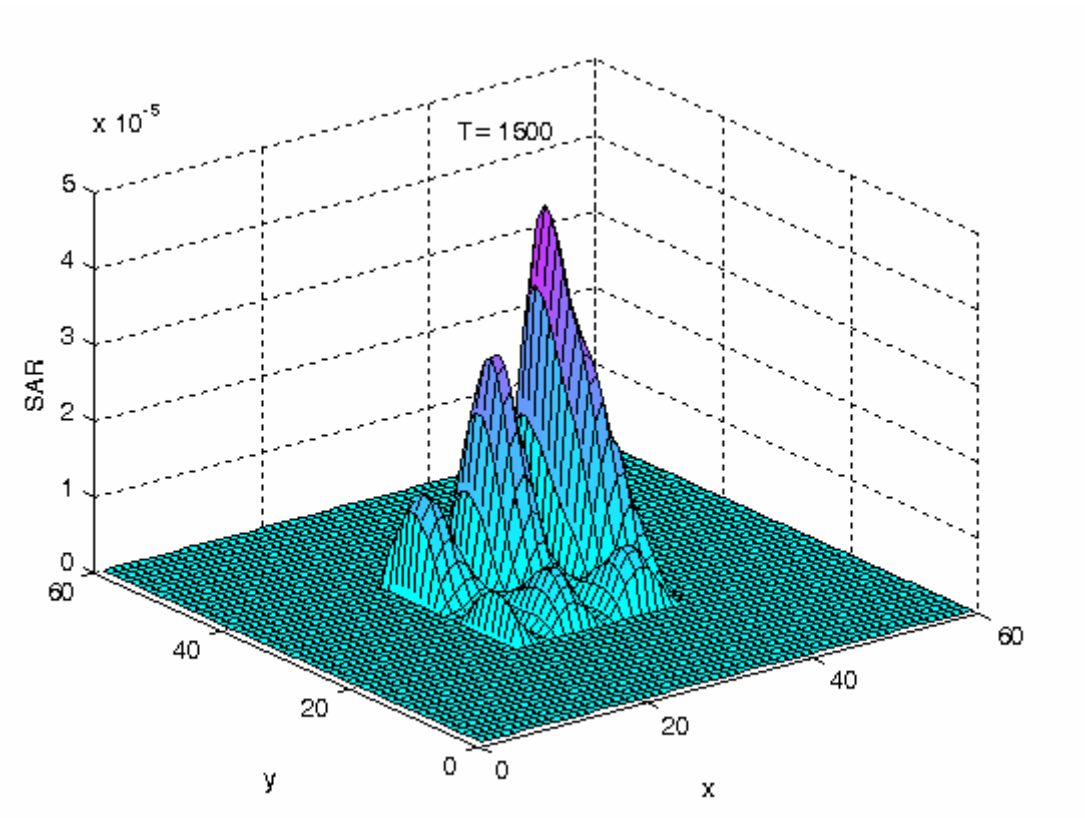

Figure 4.36 The SAR distribution for Case 3 when time step is 1500 (T=1500).

CHAPTER 5

CONCLUSIONS

This chapter concludes the thesis by considering all the other chapters, and summarizing the outcomes that we have revealed. The content of this chapter is presented in several forms. First, it reviews a few of the highlights from. Second, a discussion of lessons learned is presented. And the last, some suggestions for the future research are discussed. And finally, a brief summary is presented for the main idea.

5.1 THESIS HIGHLIGHTS

In chapter 1, an introduction is presented to the central topics of this thesis. The main objective of this chapter is to clarify the aim of the thesis by giving general information about central topics. First, Cancer is introduced briefly. The causes, general effects, risks and the potential role in human life of cancer are discussed. The main treatment options are mentioned briefly.

In chapter 2, Radiation therapy is presented to enlighten the way for hyperthermia treatment system. Because hyperthermia is revealed to be an alternative or additional technique for radiation therapy. In this respect, radiation therapy is one of the most important parts of this thesis. All formations for radiation therapy are introduced in this section. To understand radiation therapy clearly, it is needed to get knowledge about nature of radiation penetrating. The theory of radiation, which constitutes the configuration of radiation therapy, is described in this section.

In chapter 3, a literature survey is presented about main topic of this thesis which is hyperthermia in cancer treatment. This chapter considers the basis of hyperthermia in cancer therapy.

Chapter 4, covers the computations, numerical results, simulations and their interpretations which are revealed by this thesis. Important topics associated with FDTD analysis are first introduced. Practical issues associated with the actual use of the FDTD method are discussed as well. The Yee Cell is introduced along with a description of its implications. One and two dimensional FDTD computations and simulations are presented in this chapter. The determination of Absorbing Boundary Conditions (ABC) is formed. The results are compared and discussed. The SAR distribution for different conditions are observed. And finally, the Bio-Heat transfer equation is solved by using finite difference method. And so the temperature changes are determined, and simulated by using SAR values into Bio-Heat transfer equation.

The appendices contained in this thesis must not be overlooked. Appendix A provides a glossary for the scientific words, terms, expressions. And the programming codes for one and two dimensional FDTD, which are written by Fortran Programming, are presented in Appendix B.

5.2 LESSONS LEARNED

This section discusses a few of the gains that were revealed while studying this thesis. Cancer research has very deep area. There are many scientific research, which relates to different fields.

Hyperthermia is a very effective approach for cancer therapy as an alternative tehcnique. I deduced that FDTD is an effective and easy way to simulate electromagnetic (EM) wave propagation. I recognized the advantage of Berenger PML ABC while programming two dimensional FDTD .

5.3 SUGGESTIONS FOR FUTURE STUDIES

This thesis is an introductory study for electromagnetic hyperthermia. That is why, it is open to new developments. For example the devolopment of a three dimensional simulation with realistic computational models which imply a complicated

discretization procedure is a challenge for future work. Further, in order to increase the local temperature only in cancer tissues the choice and the arrangement of the source should be investigated.

5.4 SUMMARY

In this thesis, we firstly tried to get into the hyperthermia treatment system extensively. Secondly, the required researches and studies are materialized. In order to calculate the temperature change caused by electromagnetic hyperthermia we need to calculate the induced electromagnetic field distribution through the computational model. The deposited electromagnetic power in the modeled cells is our input for the calculation of the temperature distribution by solving of bio-heat equation. It is needed to solve Bio-Heat transfer equation to observe the temperature changes in cancer region. The electric fields in human tissues (models) are simulated by using two dimensional FDTD computational schemes. After that we have calculated SAR distributions. Finally we have added these SAR values into Bio-Heat transfer equation. And the temperature change is simulated with this process.

The work conducted in this research is the first step toward the modeling of real time patient specific hyperthermia treatment. This computational scheme and written code will be very useful to make a second step toward the final goal. The first step in the future work will include a finer modeling of the (cancer) tissues. This includes sophisticated discretization schemes. Further the choice of source(s) and their configuration is an important step in order to obtain a local temperature increase in only cancer tissues.

REFERENCES

Abitbol, A. A., James G. Schwade, Alan A. Lewin, Charles F. Gottlieb, Mark J. Hagmann, and Taudeusz M. Babij, "Hyperthermia: A potential useful adjunct to radiation therapy", *IEEE Engineering in Medicine &Biplogy Society 10th Annual International Conference*, 1988.

Ahnesjö, A. and M. M. Aspradakis, "Dose calculations for external photon beams in radiotherapy", *Physics In Medicine And Biology*, Vol. 44, pp. R99–R155, July 1999.

American Society for Therapeutic Radiology (ASTRO), *Radiation therapy for cancer*, 2004.
http://www.radonc.ucla.edu/images/ASTRO/ASTRO_RT_cancer_brochure.pdf

Arangarasan, R., S. Kim and S. Orcun, "Dynamic Volume Rendering for Intensity Modulated Radiation Therapy (IMRT) Treatment", *Proceedings of the IEEE Visualization,* October 23-28 2005, Minneapolis, MN, USA (VIS'05).

Artacho Terrer, J. M., M. A Nasarre Benedé., E. Bernués del Río, and S. Cruz Llanas, "A Feasible Application of Constrained optimization in the IMRT System", *IEEE Transactıons on Biomedical Engineering,* Vol. 54, No. 3, pp. 370-379, March 2007.

Babincová, M., P. Sourivong, D. Leszczynska and P. Babinec, "Blood-specific whole-body electromagnetic hyperthermia", *Medical Hypotheses*, Vol. 55, No. 6, pp. 459–460, November 1999.

Berenger, J. B., "A perfectly matched layer for the absorption of electromagnetic waves", *J. Comput. Phys.*, Vol. 114, pp. 185-200, 1994.

Brahme, A., "Development of Radiation Therapy Optimization", *Acta Oncologica*, Vol. 39, No. 5, pp. 579–595, April 2000.

Bucci, M. Kara, Alison Bevan, and Mack Roach, "Advances in Radiation Therapy: Conventional to 3D, to IMRT, to 4D, and Beyond ", *American Cancer Soceity on Cancer Journal for Clinicals* , Vol. 55, pp.117–134. 2005.

Calvagna, M., *Radiation therapy for cancer treatment*, EBSCO 2007.
http://healthlibrary.epnet.com/

Canadian Cancer Society (CCS), Systemic radiation therapy, 2006.

http://www.cancer.ca/

Censor, Y., "Mathematical aspects of radiation therapy treatment planning: Continuous inversion versus full discretization and optimization versus feasibility", in C. Borgers and F. Natterer (Editors), *Computational Radiology and Imaging: Therapy and Diagnosis*, , The IMA Volumes in Mathematics and its Applications, Vol. 110, pp. 101-112, Springer-Verlag, New York, USA, 1999.

Chou, Chung-Kwang, "Application of Electromagnetic Energy in Cancer Treatment", IEEE Transactions on Instrumentation and Measurement, Vol. 31, No. 4. December 1988.

Clark, B. G. and Michael R. McKenzie, " Radiation techniques for the 21st century", *JAMC*, Vol. 161, No. 10, p. 1292, November 1999.

Converse, M., Essex J. Bond, et al. "A Computational Study of Ultra-Wideband Versus Narrowband Microwave Hyperthermia for Breast Cancer Treatment", *IEEE Transactions On Microwave Theory And Techniques*, Vol. 54, No. 5, pp. 2169-2180, May 2006.

Coosa Valley Technical College (CVTC), *History of Radiation Therapy*, 2007. http://test.cvtcollege.org/Ac_Programs/radtherapy/history.html

Cukier, Daniel. *Coping with Chemotherapy and Radiation Therapy.* McGraw-Hill Companies, Blacklick, OH, USA, 2005.

Deuflhard, P., M. Seebass et al., "Hyperthermia Treatment Planning in Clinical Cancer Therapy: Modelling, Simulation, and Visualization", 15th IMACS World Congress, Berlin-Dahlem, June 1997.

Dunscombe, P. B., C. Cetas Tomas, et al. Hyperthermia Treatment Planning, AAPM Report No. 27, August 1989.

Ehrgott, M. and M. Burjony, "Radiation Therapy Planning by Multicriteria Optimization", *Proceedings of the 36th Annual Conference of the Operational Research Society of New Zealand*, pp. 244-253, 2001.

Enderling, H., Alexander R.A. Anderson, Mark A.J. Chaplain, Alastair J. Munro, and Jayant S. Vaidya, " Mathematical modelling of radiotherapy strategies for early breast cancer", *Journal of Theoretical Biology*, Vol. 241, pp. 158–171, November 2005.

Entine, G., M.R. Squillante, R. Hahn, L.J. Cirignano, W. McGann, and P.J. Biggs, "High Contrast, CdTe Portal Scanner for Radiation Therapy", *IEEE Transactions on Nuclear Scıence*, Vol. 39, No. 5, pp. 1480-1484, October 1992.

Haas, 0. C. L., K. J. Bumham, J. A. Mills," Hybrid Optimisation Technique for Radiotherapy Treatment Planning", *International Conference on Control Applications*, Trieste, 1-4 September 1998, pp. 368-372, IEEE, Italy, 1998.

Hamza-Lup, F. G., L. Davis, and Omar A. Zeidan, "Web–based 3D Planning Tool for Radiation Therapy Treatment", *Association for Computing Machinery (ACM)*, Columbia, Maryland, 18–.21 April 2006, pp. 159-162, ACM 2006.

Hildebrandt, B., P. Wust, O. Ahlers, A. Diein, G. Sreenivasa, T. Kerner, R. Felix, H. Riess, "The cellular and molecular basis of hyperthermia", Critical Reviews in Oncology/Hematology, Vol. 43, pp. 33-56, 2002.

Holder, A. and Bill Salter, *Tutorials on Emerging Methodologies and Applications in Operations Research*, Springer New York, 2005.

Imaginis, *History of radiation therapy*, August 2006.
http://www.imaginis.com/radiotherapy/radio_history.asp

Jordan, A., R. Scholz, P. Wust, H. Fähling and R. Felix, "Magnetic fluid hyperthermia (MFH): Cancer treatment with AC magnetic field induced excitation of biocompatible superparamagnetic nanoparticles", *Journal of Magnetism and Magnetic Materials*, Vol. 201, pp. 413-419, 1999.

Kalet, Ira J., and Mary M. Austin-Seymour, "The Use of Medical Images in Planning and Delivery of Radiation Therapy", *Journal of the American Medical Informatics Association*, Vol. 4, No. 5, pp. 327-339, Sep / Oct 1997.

Kowalski, Marc E., and Jian-Ming Jin, "Model-Based Optimization of Phased Arrays for Electromagnetic Hyperthermia", *IEEE Transactions on Microwave Theory and Techniques*, Vol. 52, No. 8, pp. 1964-1977, August 2004.

Lodwick, W., F. Newman, and A. Neumaier, "Optimization Under Uncertainity: Methods and Applications in Radiation", *IEEE International Fuzzy Systems Conference*, pp. 1219-1222, IEEE 2001.

Mayo Clinic, *Radiation therapy,* 2007.
http://www.mayoclinic.com/health/radiation-therapy/CA00031

National Cancer Institute Fact Sheet 6.7, *Cancer: Questions and Answers*, 6/6/2005.
http://www.cancer.gov/cancertopics/factsheet/Sites-Types/general

National Cancer Institute Fact Sheet 7.1, *Radiation Therapy for Cancer: Questions and Answers*, August 2004.
http://www.cancer.gov/cancertopics/factsheet/Therapy/radiation

National Cancer Institute Fact Sheet 7.3, *Hyperthermia in Cancer Treatment: Questions and Answers*, 2004.
http://www.cancer.gov/cancertopics/factsheet/Therapy/hyperthermia

Nielsen, O.S., M. Horsman, J. Overgaard, "A future for hyperthermia in cancer treatment?" *European Journal of Cancer*, 37, pp.1587-1589, 2001.

Nondestructive Testing (NDT) Resource Center, *Physics of Radiography*, 2007. http://www.ndt-ed.org/EducationResources/CommunityCollege/Radiography/cc_rad index.htm

Palo Alto Medical Foundation (PAMF), *Three-Dimensional Conformal Therapy*, 2004. http://www.pamf.org/radonc/tech/3d.html

Peters, L. J. and Lizbeth M. Kenny, "Radiation oncology ", *MJA*, Vol. 176, pp. 37, July 2002.

Prutchi, D., John L. Prince, and Lawrence J. Stotts, "X- and Gamma-Ray Hardness of Floating-Gate EEPROM Technology as Applied to Implantable Medical Devices", *IEEE Transactions on Components And Packaging Technology*, Vol. 22, No. 3, pp. 390-398, September 1999.

Shepard, D. M., Michael C. Ferris, Gustavo H. Olivera and T. Rockwell Mackie, "Optimizing the Delivery of Radiation Therapy to Cancer Patients", *Society for Industrial and Applied Mathematics (SIAM Review)*, Vol. 41, No. 4, pp. 721–744, October 1999.

Stewart, J. and D. E. Davison,"Dose Control in Radiotherapy Cancer Treatment: Improving Dose Coverage with Estimation and Feedback", *Proceedings of the 2006 American Control Conference*, Vol. FrA18.3, pp. 4806-4811, Minneapolis, Minnesota, USA, June 14-16, 2006.

Strohbehn, J. W., and B. Douple Evan," Hyperthermia and Cancer Therapy: A Review of Biomedical Engineering Contributions and Challenges", *IEEE Transactions on Biomedical Engineering*, Vol. BME-31, No. 12, December 1984.

Sullivan, Dennis M., "Exceeding the Courant Condition with the FDTD Method", *IEEE Microwave and Guided Wave Letters*, Vol. 6, No. 8, pp. 289-291, August 1996

The National Cancer Institute (NCI) booklet, *Radiation Therapy and You: A Guide to Self-Help During Cancer Treatment*, NIH Publication No. 03-2227, revised October 1998.

Wu, Q., D. Djajaputra, M. Lauterbach, Y. Wu and R. Mohan, "A fast dose calculation method based on table lookup for IMRT optimization", *Physics In Medicine And Biology*, Vol. 48, pp. N159–N166, June 2003.

Wust, P., B. Hildebrandt, G. Sreenivasa et al., "Hyperthermia in combined treatment of cancer", *The Lancet Oncology*, Vol. 3, pp. 487–497, 2002.

Yang, X., J. Du, Y. Liu, "Advances in Hyperthermia Technology", *IEEE Engineering in Medicine and Biology 27th Annual Conference*, Shanghai, China, September 1-4, 2005, pp. 6766-6769.

Yee, K. S., “Numerical solution of initial boundary value problems involving Maxwell’s equations in isotropic media,” *IEEE Trans. Antennas Propagat.*, Vol. AP-14, pp. 302–307, May 1966.

APPENDIX A

GLOSSARY

Adjuvant therapy: Treatment added to the primary treatment to enhance the effectiveness of the primary treatment. Radiation therapy often is used as an adjuvant to surgery.

Blood: The familiar red fluid in the body that contains white and red blood cells, platelets, proteins, and other elements.

Blood pressure: The blood pressure is the pressure of the blood within the arteries.

Brachytherapy: Internal radiation therapy using an implant of radioactive material placed directly into or near the tumor; also called "internal radiation therapy."

Cancer: A term for diseases in which abnormal cells divide without control. Cancer cells can invade nearby tissues and can spread through the bloodstream and lymphatic system to other parts of the body.

Chemotherapy: Treatment with anticancer drugs.

CT (computed tomography) scan: An x-ray procedure that uses a computer to produce a series of detailed pictures of a cross-section of the body; also called a CAT scan.

Electron beam: A stream of electrons (small negatively charged particles found in atoms) that can be used for radiation therapy.

External radiation: The use of radiation from a machine located outside of the body to aim high-energy rays at cancer cells.

Gamma knife: Radiation therapy in which high energy rays are aimed at a brain tumor from many angles in a single treatment session.

Gamma rays: High-energy rays that come from a radioactive source such as cobalt-60.

Implant: A radioactive source in a small holder that is placed in the body in or near a cancer.

Internal radiation: Radiation therapy that uses the technique of placing a radioactive source in or near a cancer.

Interstitial radiation: A radioactive source (implant) placed directly into the cancerous tissue such as the head and neck region or the breast.

Intraoperative radiation: External radiation treatment given during surgery to deliver a large dose of radiation to the tumor bed and surrounding tissue; also called IORT.

Invasive: It refers to a tumor that invades healthy tissues; also called diffuse or infiltrating.

Linear accelerator: A machine that creates high-energy radiation to treat cancers, using electricity to form a stream of fast-moving subatomic particles; also called 'mega-voltage (MeV) linear accelerator' or a "linac."

Oncologist: A doctor who specializes in treating cancer.

Physical therapist: A health professional trained in the use of treatments such as exercise and massage.

Proton: A small, positively charged particle of matter found in the atoms of all elements. Streams of protons generated by special equipment can be used for radiation treatment.

Radiation: Energy carried by waves or a stream of particles.

Radiation nurse: A nurse who specializes in caring for people who are undergoing radiation therapy.

Radiation oncologist: A doctor who specializes in treating cancer with radiation.

Radiation physicist: The person who makes sure that the radiation machine delivers the right amount of radiation to the treatment site. In consultation with the radiation oncologist, the physicist also determines the treatment schedule that will have the best chance of killing the most cancer cells.

Radiation therapist: The person who runs the equipment that delivers the radiation.

Radiation therapy: Treatment with high-energy rays (such as x-rays) to kill cancer cells.

Radioactive: Capable of emitting high-energy rays or particles.

Radiologist: A doctor with special training in creating and interpreting pictures of areas inside the body. The pictures are produced with x-rays, sound waves, or other types of energy.

Symptom: Any subjective evidence of disease.

Tumor: An abnormal mass of excess tissue that results from excessive cell division.

X-rays: High-energy radiation that is used in low doses to diagnose disease and in high doses to treat cancer.

Vital: Necessary to maintain life.

APPENDIX B

PROGRAMMING CODES

ONE-DIMENSIONAL FDTD

```
!*****************************************************
! This module initilize all dumy arguments!
*****************************************************
MODULE gl_data
IMPLICIT NONE
SAVE
INTEGER*4,PARAMETER :: NC=200
INTEGER*4,PARAMETER :: Nsteps=40
REAL*8, PARAMETER :: c0=299792458, pi=3.1415926536D0
REAL*8, PARAMETER :: f=1500.0D6 !frequency
REAL*8, PARAMETER :: lambda0 = c0/f
REAL*8, PARAMETER :: omg=2.0D0*pi*f
REAL*8, PARAMETER :: eps0=8.8541878D-12   ! [F/m]
REAL*8, PARAMETER :: mu= 4.0D0*pi*1.0D-7 ! [H/m]
REAL*8, PARAMETER :: k0=2.0D0*pi/lambda0
END MODULE gl_data


PROGRAM FDTD_oneD
USE gl_data
IMPLICIT NONE
REAL*8:: T,t0,spread,pulse
INTEGER*4:: n,k,kc,ke
INTEGER*4:: k_begin  !start point for dielectric media
REAL*8:: Ex(0:NC),Hy(0:NC)
REAL*8:: ca(0:NC), cb(0:NC)         !constants of E field
REAL*8:: epsR, sigma          !dielectric constant and conductivity
REAL*8::ex_lb1,ex_lb2,ex_hb1,ex_hb2  !dummy arguments for boundary
cond.
REAL*8:: ddx,dt,cnst

OPEN(UNIT=20,FILE="D:\EM_work\FDTD\EHfield.m")

ke=200
```

```
kc=ke/2
t0=40.0D0
spread=12.0D0
T=0.0D0

DO k=1,ke
                Ex(k)=0.0D0
                Hy(k)=0.0D0
END DO

ddx=0.01D0 !set the cell size to 1 cm
dt=ddx/(2*c0) !Calculate the time step

k_begin=100
epsR=4.0D0
sigma=0.05
cnst=dt*sigma/(2.0D0*eps0*epsR)

!Initialization to free space
DO k=1,ke
                ca(k)=1.0D0
                cb(k)=0.5D0
END DO

!Initialization to lossy medium
        DO k=k_begin,ke
                ca(k)=(1.0D0-cnst)/(1.0D0+cnst)
                cb(k)=0.5D0/(epsR*(1.0D0+cnst))
                !cb(k)=0.5D0/epsR
END DO

WRITE(20,*) "fields = ["

DO n=1,Nsteps
        T=T+1
                DO k=1,ke
                !Calculate Ex
                Ex(k)=ca(k)*Ex(k)+cb(k)*(Hy(k-1)-Hy(k))
                END DO

                !Put a Gaussian pulse in the middle
                !pulse=EXP(-0.5D0*(((t0-T)/spread)**2))
                !_____________________________________

                !Put a sinusoidal pulse in the middle
                pulse=SIN(2*pi*f*dt*T)

                Ex(20)=Ex(20)+pulse
                !Ex(kc+20)=pulse
```

```
                !Ex(kc)=Ex(kc)+pulse

                !Apply Absorbing Boundary conditions
                !_____________________________________________
                !Apply at low boundary
                Ex(0)=ex_lb2
                ex_lb2=ex_lb1
                ex_lb1=Ex(1)

                !Apply at high boundary
                Ex(ke-1)=ex_hb2
                ex_hb2=ex_hb1
                ex_hb1=Ex(ke-2)

                DO k=0,ke-1
                !Calculate Hy
                Hy(k)=Hy(k)+0.5D0*(Ex(k)-Ex(k+1))
                END DO

!PRINT*,T
END DO

DO k=1,ke
                WRITE(20,*) k,Ex(k),Hy(k)
END DO

WRITE(20,*) "]"
WRITE(20,*) "figure;plot(fields(:,1),fields(:,2))"
WRITE(20,*) "xlabel('k')"
WRITE(20,*) "ylabel('Ex')"

END PROGRAM
```

TWO-DIMENSIONAL FDTD

```
PROGRAM fdtd_twoD
 USE gl_data
 IMPLICIT NONE
 REAL*8:: T,t0,spread,pulse
 INTEGER*4:: i,j,n,k,kc,ke,ic,jc,a,b,m,l
 INTEGER*4:: npml
 INTEGER*4:: i_begin  !start point for dielectric media
 REAL*8:: Dz(0:NC,0:NC),Ez(0:NC,0:NC),Hx(0:NC,0:NC),Hy(0:NC,0:NC)
 REAL*8:: ca(0:NC,0:NC), cb(0:NC,0:NC),SAR(0:NC,0:NC) !constants of E field
 REAL*8:: gx1(0:NC), gx2(0:NC), gy1(0:NC), gy2(0:NC)
 REAL*8:: fx1(0:NC), fx2(0:NC), fx3(0:NC),Iz(0:NC,0:NC)
 REAL*8:: fy1(0:NC), fy2(0:NC), fy3(0:NC)
 REAL*8:: ihx(0:NC,0:NC), ihy(0:NC,0:NC)
 REAL*8:: epsR1,sigma1,epsR2,sigma2,sigma0 !dielectric / conductivity const
 REAL*8::ex_lb1,ex_lb2,ex_hb1,ex_hb2   !dummy arguments for boundary cond.
 REAL*8:: ddx,dt,cnst1_1,cnst1_2,cnst2_1,cnst2_2
 REAL*8:: xn,xxn,xnum,xd,curl_e

 OPEN(UNIT=20,FILE="EHfield.m")
 OPEN(UNIT=21,FILE="SAR_value.m")

 !ke=Nx
 ic=45
 jc=35
 !a=35
 !b=42
 !m=42
 !l=25
 t0=20.0D0
 spread=6.0D0
 T=0.0D0

 ddx=0.01D0 !set the cell size to 1 cm
 dt=ddx/(2*c0) !Calculate the time step

 i_begin=30

 !sigma0=0.0D0

 !medium 1 for skindry
 epsR1=1.0D0
 sigma1=0.0D0
 cnst1_1=1/(epsR1+(dt*sigma1/eps0))
 cnst1_2=dt*sigma1/eps0
```

```
!medium 2 for breastfat
epsR2=5.4244D0
sigma2=0.048964D0
cnst2_1=1/(epsR2+(dt*sigma2/eps0))
cnst2_2=dt*sigma2/eps0

npml=16 !Number of perfectly matched layer points

!Initialization of fields
DO i=0,Nx-1
        DO j=0,Ny-1
        Dz(i,j)=0.0D0
        Ez(i,j)=0.0D0
        Hx(i,j)=0.0D0
        Hy(i,j)=0.0D0
        Iz(i,j)=0.0D0
        ihx(i,j)=0.0D0
        ihy(i,j)=0.0D0
        ca(i,j)=1.0D0
        END DO
END DO
!Calculate the PML parameters
DO i=0,Nx-1
        gx1(i)=1.0D0
        gx2(i)=1.0D0
        fx1(i)=0.0D0
        fx2(i)=1.0D0
        fx3(i)=1.0D0
END DO
DO j=0,Ny-1
        gy1(j)=1D0
        gy2(j)=1D0
        fy1(j)=0D0
        fy2(j)=1D0
        fy3(j)=1D0
END DO
DO i=0,npml-1
        xnum=npml-i
        xd=npml
        xxn=xnum/xd
        xn=0.333D0*(xxn)**3
        gx1(i)=1D0/(1D0+xn)
        gx1(Nx-1-i)=1D0/(1D0+xn)
        gx2(i)=(1D0-xn)/(1D0+xn)
        gx2(Nx-i-1)=(1D0-xn)/(1D0+xn)

        xxn=(xnum-0.5D0)/xd
        xn=0.25D0*(xxn)**3
```

```
        fx1(i)=xn
        fx1(Nx-2-i)=xn
        fx2(i)=1D0/(1D0+xn)
        fx3(Nx-2-i)=1D0/(1D0+xn)
        fx3(i)=(1D0-xn)/(1D0+xn)
        fx3(Nx-2-i)=(1D0-xn)/(1D0+xn)
END DO

DO j=0,npml-1
        xnum=npml-j
        xd=npml
        xxn=xnum/xd
        xn=0.333D0*(xxn)**3
        gy1(j)=1D0/(1D0+xn)
        gy1(Ny-1-j)=1D0/(1D0+xn)
        gy2(j)=(1D0-xn)/(1D0+xn)
        gy2(Ny-j-1)=(1D0-xn)/(1D0+xn)

        xxn=(xnum-0.5D0)/xd
        xn=0.25D0*(xxn)**3

        fy1(j)=xn
        fy1(Ny-2-j)=xn
        fy2(j)=1D0/(1D0+xn)
        fy3(Ny-2-j)=1D0/(1D0+xn)
        fy3(j)=(1D0-xn)/(1D0+xn)
        fy3(Ny-2-j)=(1D0-xn)/(1D0+xn)
END DO
!Initialization to free space
!DO i=1,Nx
!       DO j=1,Ny
!       ca(i,j)=1.0D0
!       cb(i,j)=0.0D0
!       END DO
!END DO

!Initialization to lossy medium1
DO i=1,Nx
DO j=1,Ny
        ca(i,j)=cnst1_1 !for lossy dielectric
        cb(i,j)=cnst1_2 !for lossy dielectric
        !cb(k)=0.5D0/epsR !for free space to dielectric without loss
        END DO
END DO

!Initialization to lossy medium2
DO i=20,40
        DO j=20,40
        ca(i,j)=cnst2_1 !for lossy dielectric
```

```
        cb(i,j)=cnst2_2 !for lossy dielectric
        !cb(k)=0.5D0/epsR !for free space to dielectric without loss
        END DO
END DO

WRITE(20,*) "Ez = ["
WRITE(21,*) "SAR_q = ["

DO n=1,Nsteps
        T=T+1
        DO i=1,Nx-1
                DO j=1,Ny-1
        !Calculate Dz
        Dz(i,j)=gx2(i)*gy2(j)*Dz(i,j)+0.5D0*gx1(i)*gy1(j)*
  &               (Hy(i,j)-Hy(i-1,j)-Hx(i,j)+Hx(i,j-1))
                END DO
        END DO

        !Put a Gaussian pulse in the middle
        !pulse=EXP(-0.5D0*(((t0-T)/spread)**2))
        !_____________________________________

        !Put a sinusoidal pulse in the middle

        pulse=SIN(2*pi*f*dt*T)

        Dz(jc,ic)=Dz(jc,ic)+pulse
        !Dz(a,b)=Dz(a,b)+pulse
        !Dz(m,l)=Dz(k,l)+pulse

        !Calculate the Ez field
        DO i=0,Nx-1
                DO j=0,Ny-1
                Ez(i,j)=ca(i,j)*(Dz(i,j)-Iz(i,j))
                Iz(i,j)=Iz(i,j)+cb(i,j)*Ez(i,j)
                END DO
        END DO

        !Calculate the SAR field
        DO i=0,Nx-1
                DO j=0,Ny-1
                SAR(i,j)=(sigma1/2D0)*(ABS(Ez(i,j)))**2
                END DO
        END DO
        !DO i=10,50
        !       DO j=10,50
        !       SAR(i,j)=(sigma1/2D0)*(ABS(Ez(i,j)))**2
        !       END DO
        !END DO
```

```
        DO i=20,40
                DO j=20,40
                SAR(i,j)=(sigma2/2D0)*(ABS(Ez(i,j)))**2
                END DO
        END DO

        !Set the Ez edges to zero, as part of the PML
        !_____________________________________________

        DO i=0,Nx-2
        Ez(i,0)=0D0
        Ez(i,Ny-1)=0D0
        END DO

        DO j=1,Ny-2
        Ez(0,j)=0D0
        Ez(Nx-1,j)=0D0
        END DO

        !Calculate the Hx field
        DO i=0,Nx-1
                DO j=0,Ny-2
                curl_e=Ez(i,j)-Ez(i,j+1)
                ihx(i,j)=ihx(i,j)+fx1(i)*curl_e
                Hx(i,j)=fy3(j)*Hx(i,j)+0.5D0*fy2(j)*(curl_e+ihx(i,j))
                END DO
        END DO

        !Calculate the Hy field
        DO i=0,Nx-2
                DO j=0,Ny-2
                curl_e=Ez(i+1,j)-Ez(i,j)
                ihy(i,j)=ihy(i,j)+fy1(j)*curl_e
                Hy(i,j)=fx3(i)*Hy(i,j)+0.5D0*fx2(i)*(curl_e+ihy(i,j))
                END DO
        END DO

END DO

DO i=1,Nx
        DO j=1,Ny
        WRITE(20,*) i,j,Ez(i,j)
        WRITE(21,*) i,j,SAR(i,j)
        END DO
END DO

WRITE(20,*) "];"

WRITE(20,*)"Nx=",Nx
```

```
WRITE(20,*)"k=1;for i=1:Nx;for j=1:Nx;E(i,j)=Ez(k,3);k=k+1;end;end;"
WRITE(20,*)"figure;surf(E)"
WRITE(20,*) "xlabel('x')"
WRITE(20,*) "ylabel('y')"
WRITE(20,*) "zlabel('Ez')"

WRITE(20,*)"T=",T

WRITE(20,*) "annotation('textbox','String',['T= ',num2str(T)],..."
WRITE(20,*)"'LineStyle','none','HorizontalAlignment','center',..."
WRITE(20,*) "'Position',[0.4339 0.7999 0.1607 0.05722]);"

WRITE(21,*) "];"

WRITE(21,*)"Nx=",Nx

WRITE(21,*)"k=1;for i=1:Nx;for j=1:Nx;
  &                    SAR(i,j)=SAR_q(k,3);k=k+1;end;end;"
WRITE(21,*)"figure;surfc(SAR)"
WRITE(21,*) "xlabel('x')"
WRITE(21,*) "ylabel('y')"
WRITE(21,*) "zlabel('SAR')"

WRITE(21,*)"T=",T

WRITE(21,*) "annotation('textbox','String',['T= ',num2str(T)],..."
WRITE(21,*)"'LineStyle','none','HorizontalAlignment','center',..."
WRITE(21,*) "'Position',[0.4339 0.7999 0.1607 0.05722]);"
END PROGRAM
```